

The Effect of a Layered Airspace Concept on Conflict Probability and Capacity

M.A.P. Tra

Master of Science Thesis

The Effect of a Layered Airspace Concept on Conflict Probability and Capacity

MASTER OF SCIENCE THESIS

For the degree of Master of Science in Air Traffic Management,
Airports and Safety at Delft University of Technology

M.A.P. Tra

August 26, 2016



Copyright © M.A.P. Tra
All rights reserved.

DELFT UNIVERSITY OF TECHNOLOGY
DEPARTMENT OF
CONTROL AND OPERATIONS

The undersigned hereby certify that they have read and recommend to the Faculty of
Aerospace Engineering for acceptance a thesis entitled

THE EFFECT OF A LAYERED AIRSPACE CONCEPT ON CONFLICT PROBABILITY
AND CAPACITY

by

M.A.P. TRA

in partial fulfillment of the requirements for the degree of

MASTER OF SCIENCE AIR TRAFFIC MANAGEMENT, AIRPORTS AND SAFETY

Dated: August 26, 2016

Supervisor(s):

Prof. dr. ir . J. M. Hoekstra

Dr. ir. J. Ellerbroek

E. Sunil M.Sc.

Reader(s):

Ir. P.C. Roling

Acknowledgements

I would first like to thank my daily supervisor Emmanuel Sunil for his expert advice. The door to his office was always open, resulting in valuable discussions during the writing of this thesis. Furthermore I would also like to acknowledge the roles of prof. dr. ir. Jacco. M. Hoekstra and dr. ir. Joost Ellerbroek for their much appreciated input to this thesis work.

Finally, I want to express my gratitude to my parents and my friends, for supporting and encouraging me throughout my years of study. You greatly contributed to this accomplishment, thank you.

Delft, University of Technology
August 26, 2016

M.A.P. Tra

Table of Contents

Acknowledgements	i
List of Figures	vii
List of Tables	xiii
List of Symbols	xv
Thesis Outline	xvii
I Scientific Paper	1
II Preliminary Thesis Report	23
1 Introduction	25
1-1 Air Traffic Demand vs. Capacity	25
1-2 Distributed Air Traffic Management	26
1-3 Thesis Objective and Research Questions	28
1-4 Research Approach	29
1-5 Outline of the Report	31
2 Literature Review	33
2-1 Airspace Structure	33
2-1-1 Current Airspace Structure	34
2-1-2 Full Mix / Free Flight	35
2-1-3 Layers	35

2-1-4	Tubes	36
2-1-5	Concepts that will be evaluated in the Thesis assignment	37
2-2	Conflict Probability and Random Variable models	37
2-2-1	Application of Random Variable Models to Predict Airspace Capacity	38
2-2-2	Centralized vs. Decentralized Conflict Probability	40
2-2-3	2D-model for Theoretical Conflict Probability	41
2-2-4	Verification of the 2D-model	44
2-3	Airspace Capacity	48
2-3-1	Safety	48
2-3-2	Stability	48
2-3-3	Efficiency	51
3	Conflict Modelling in 3D	53
3-1	3D-model for Theoretical Conflict Probability	53
3-2	Level vs. Level Aircraft	56
3-3	Climbing/Descending vs. Climbing/Descending Aircraft	56
3-4	Climbing/Descending vs. Level Aircraft	56
3-5	Overview of Conflict Estimation for Layers and Full Mix	57
4	Experiment Design	59
4-1	Simulation environment: BlueSky	59
4-1-1	Implementation of Layers Concept	60
4-1-2	Airborne Separation Assurance System	61
4-2	Traffic Scenario	61
4-2-1	Test Region	61
4-2-2	Experiment Time	65
4-2-3	Traffic Demand	66
4-3	Independent Variables	66
4-4	Dependent Variables	67
4-5	Hypotheses	67
5	Conclusion/Summary	69
III	Appendices	71
A	Validation of Conflict Probability Model using Two-dimensional Simulations	73

B	Graphs of Thesis Results for All Airspace Concepts	77
B-1	Validation of Conflict Probability Model	77
B-2	Effect of Airspace Design on Capacity	81
B-2-1	Safety	81
B-2-2	Stability	85
B-2-3	Efficiency	87
B-3	Miscellaneous	95
B-3-1	Density Distribution in Experiment Area	95
B-3-2	Average Conflict Angle	97
B-3-3	Ratio of Cruising Aircraft	99
C	Simulation Scenarios Generation	101
C-1	Airport Generation	102
C-2	Origin-Destination Pairs Generation	104
C-3	Scenario Generation	105
C-4	Scenario Writing	107
	Bibliography	117

List of Figures

1-1	Example of the highly structured airways in the current ATM system [1]	26
1-2	Long Term ATM Forecast by Eurocontrol [2]	26
1-3	Number of conflicts (with conflict resolution) for different airspace concepts and traffic demand levels [3]	27
1-4	A layered airspace concept: using altitude rules as a priori separation method . .	28
1-5	Domino Effect Parameter (DEP) for different airspace concepts and traffic demand levels; The DEP is inversely related to the stability of a system [4, 3]	28
1-6	Effect of traffic demand on system efficiency for different airspace concepts; The efficiency is measured through the average work done to complete a flight [3] . .	28
1-7	Road map of the research approach used during the Preliminary Thesis and Main Thesis	30
1-8	Relating concept parameters to capacity	30
2-1	Example of the highly structured ATM system, indicating the division of the airspace in different FIR's [5]	34
2-2	Schematic representation of the unstructured Full Mix concept (B) compared with the current centralized ATM system (A) [6]	35
2-3	Schematic overview of the Layers concept, with 45° heading range per flight level	36
2-4	Example of airspace structure in the Tubes concept [3]	37
2-5	Conflict counts for structured and great-circle routes [7]	38
2-6	Relation between number of aircraft and expected number of conflicts for an ATCo (ground) and pilot (air). A conflict probability of 1.9e-4 is used to generate this example.	41
2-7	The area searched for conflicts; using a linear extrapolation of the flight path based on the speed, V , and the look-ahead time, t	41
2-8	Relation between heading difference and relative velocity	42
2-9	Probability distribution for the absolute heading difference between two uniform distributed random variables [8]	43

2-10	Effect of separation distance on expected number of conflicts. A conflict probability of $1.9e-4$ and $9.5e-5$ are used for D_{sep} and $\frac{D_{sep}}{2}$, respectively.	44
2-11	Effect of heading limitations on expected number of conflicts. A conflict probability of $1.9e-4$ is used for the 360° heading band, and scaled accordingly for the other heading bands.	44
2-12	Simulations with a randomly selected separation distance: theoretical (blue) and results of simulations (red)	45
2-13	Simulations with a randomly selected separation distance: theoretical (blue) and average of simulations (red)	45
2-14	Simulations for the look-ahead time : theoretical (blue) and results of simulations (red)	46
2-15	Simulations for the look-ahead time: theoretical (blue) and average of simulations (red)	46
2-16	Simulations with a randomly selected speed: theoretical (blue) and results of simulations (red)	47
2-17	Simulations with a randomly selected speed: theoretical (blue) and average of simulations (red)	47
2-18	Simulations for the heading range: theoretical (blue) and results of simulations (red)	47
2-19	Simulations for the heading range: theoretical (blue) and average of simulations (red)	47
2-20	Visualization of the Domino Effect Parameter [7]	49
2-21	Effect of separation distance on expected number of conflicts. A conflict probability of $1.9e-4$, and k of 3 are used for the standard horizontal separation of 5 nm, and scaled accordingly for $\frac{D_{sep}}{2}$	50
2-22	Effect of heading limitations on expected number of conflicts. A conflict probability of $1.9e-4$, and k of 3 are used for the 360° heading band, and scaled accordingly for the other heading bands	50
3-1	The side-view on the volume searched for conflicts; using a linear extrapolation of the flight path based on the speed, vertical speed, separation criteria and the look-ahead time	54
3-2	Graphical representation of the side-view of the simplified volume searched by a climbing aircraft	54
3-3	The difference between the exact solution and the approximation of the volume searched by aircraft, for a vertical speed up to 8,000 ft/min	55
4-1	Graphical representation of δ , the deviation between the heading of the initially defined route and the required heading to fly to the active waypoint	61
4-2	Flight path using the regular waypoint selection	61
4-3	Flight path with adjusted waypoint selection	61
4-4	Flow Chart for trajectory recovery logic, used in case of a conflict between two aircraft	62
4-5	Example of circular test region with origins and destinations at cruise altitude	63
4-6	Example of square test region with origins and destinations of the ground	63
4-7	Simplified visualization of different phases of flight	65

4-8	Size of the test region compared with the size of France	65
A-1	Model validation with a heading range of 360 degrees.	74
A-2	Model validation with a heading range of 180 degrees.	74
A-3	Model validation with a heading range of 90 degrees.	75
A-4	Model validation with a heading range of 45 degrees.	75
B-1	Free Flight: model fitted at low densities with a k -value of 0.92.	77
B-2	Layers 360: model fitted at low densities with a k_1 of 1.15, k_2 of 1.65 and k_3 of 1.05.	78
B-3	Layers 180: model fitted at low densities with a k_1 of 0.99, k_2 of 1.61 and k_3 of 1.09.	78
B-4	Layers 90: model fitted at low densities with a k_1 of 0.93, k_2 of 1.34 and k_3 of 0.82.	78
B-5	Layers 45: model fitted at low densities with a k_1 of 0.93, k_2 of 1.12 and k_3 of 0.64.	78
B-6	Variation in vertical speed for the Free Flight concept: model fitted at low densities with a k value of 1.07.	78
B-7	Variation in vertical speed for the Layers 45 concept: model fitted at low densities with a k_1 of 1.01, k_2 of 1.23 and k_3 of 1.48.	78
B-8	Variation in speed settings for the Layers 45 concept: A uniform speed distribution between 450 kts and 550 kts. Model fitted at low densities with a k_1 of 0.99, k_2 of 1.24 and k_3 of 0.94.	79
B-9	Comparison of all concepts: all conflict types.	79
B-10	Comparison of all concepts: cruise - cruise conflicts.	79
B-11	Comparison of all concepts: cruise - climbing/descending conflicts.	79
B-12	Comparison of all concepts: climbing/descending - climbing/descending conflicts.	79
B-13	Free Flight: Total number of conflicts during the experiment time. Simulation results fitted to the model $f(x) = -4.3e^{-6} \cdot x^5 + 2.9e^{-4} \cdot x^4 + 7.6e^{-2} \cdot x^3 + 5.9e^{-1} \cdot x^2 + 9.7 \cdot x - 17.1$, where x is the number of aircraft.	81
B-14	Layers 360: Total number of conflicts during the experiment time. Simulation results fitted to the model $f(x) = -1.6e^{-7} \cdot x^5 + 1.8e^{-4} \cdot x^4 - 8.7e^{-3} \cdot x^3 + 1.6 \cdot x^2 - 5.3 \cdot x + 15.4$, where x is the number of aircraft.	81
B-15	Layers 180: Total number of conflicts during the experiment time. Simulation results fitted to the model $f(x) = -2.3e^{-6} \cdot x^5 + 6.6e^{-4} \cdot x^4 - 4.2e^{-2} \cdot x^3 + 2.1e \cdot x^2 - 10.3 \cdot x + 24.0$, where x is the number of aircraft.	81
B-16	Layers 90: Total number of conflicts during the experiment time. Simulation results fitted to the model $f(x) = -3.8e^{-7} \cdot x^5 + 1.9e^{-4} \cdot x^4 - 1.2e^{-2} \cdot x^3 + 1.1 \cdot x^2 - 4.2 \cdot x + 10.49$, where x is the number of aircraft.	82
B-17	Layers 45: Total number of conflicts during the experiment time.	82
B-18	Free Flight with secondary priority settings: Total number of conflicts during the experiment time. Simulation results fitted to the model $f(x) = 8.7e^{-2} \cdot x^3 + 1.2 \cdot x^2 - 2.6 \cdot x + 22.1$, where x is the number of aircraft.	82
B-19	Layers 45 with secondary priority settings: Total number of conflicts during the experiment time. Simulation results fitted to the model $f(x) = 6.2e^{-3} \cdot x^3 + 6.8e^{-1} \cdot x^2 - 7.8e^{-1} \cdot x + 4.0$, where x is the number of aircraft.	82

B-20 Free Flight: Total number of intrusions during the experiment time. Simulation results fitted to the model $f(x) = 8.1e6 - 7 \cdot x^5 - 8.8e^{-5} \cdot x^4 + 3.4e^{-3} \cdot x^2 - 3.5e^{-2} \cdot x + 2.2e^{-1} \cdot x - 0.4$, where x is the number of aircraft.	83
B-21 Layers 360: Total number of intrusions during the experiment time. Simulation results fitted to the model $f(x) = 2.8e^{-7} \cdot x^5 - 4.1e^{-5} \cdot x^4 + 2.3e^{-3} \cdot x^3 - 4.4e^{-2} \cdot x^2 + 3.7e^{-1} \cdot x - 0.8$, where x is the number of aircraft.	83
B-22 Layers 180: Total number of intrusions during the experiment time. Simulation results fitted to the model $f(x) = 4.1e^{-7} \cdot x^5 - 5.8e^{-5} \cdot x^4 + 2.7e^{-3} \cdot x^3 - 3.9e^{-2} \cdot x^2 + 2.2e^{-1} \cdot x - 0.4$, where x is the number of aircraft.	83
B-23 Layers 90: Total number of intrusions during the experiment time. Simulation results fitted to the model $f(x) = -9.3e^{-8} \cdot x^5 + 2.5e^{-5} \cdot x^4 - 2.0e^{-3} \cdot x^3 + 6.2e^{-2} \cdot x^2 - 5.6e^{-1} \cdot x + 1.4$, where x is the number of aircraft.	84
B-24 Layers 45: Total number of intrusions during the experiment time. Simulation results fitted to the model $f(x) = -1.8e^{-8} \cdot x^5 + 6.0e^{-6} \cdot x^4 - 2.8e^{-4} \cdot x^3 + 5.3e^{-3} \cdot x^2 + 9.4e^{-2} \cdot x - 0.3$, where x is the number of aircraft.	84
B-25 Free Flight with secondary priority settings: Total number of intrusions during the experiment time. Simulation results fitted to the model $f(x) = 0.0008516 \cdot x^3 - 3.7e^{-2} \cdot x^2 + 7.0e^{-1} \cdot x - 2.3$, where x is the number of aircraft.	84
B-26 Layers 45 with secondary priority settings: Total number of intrusions during the experiment time. Simulation results fitted to the model $f(x) = 1.6e^{-3} \cdot x^3 - 3.1e^{-2} \cdot x^2 + 8.7e^{-1} \cdot x - 3.2$, where x is the number of aircraft.	84
B-27 Free Flight: Domino Effect Parameter, with a ρ_{max} of 81 aircraft per 10,000 nm^2	85
B-28 Layers 360: Domino Effect Parameter, with a ρ_{max} of 168 aircraft per 10,000 nm^2	85
B-29 Layers 180: Domino Effect Parameter, with a ρ_{max} of 162 aircraft per 10,000 nm^2	85
B-30 Layers 90: Domino Effect Parameter, with a ρ_{max} of 200 aircraft per 10,000 nm^2	86
B-31 Layers 45: Domino Effect Parameter, with a ρ_{max} of 215 aircraft per 10,000 nm^2	86
B-32 Free Flight with secondary priority settings: Domino Effect Parameter, with a ρ_{max} of 73 aircraft per 10,000 nm^2	86
B-33 Layers 45 with secondary priority settings: Domino Effect Parameter, with a ρ_{max} of 135 aircraft per 10,000 nm^2	86
B-34 Free Flight: The increment of the flight time for simulations with CR compared to simulations without CR. Simulation results fitted to the model $f(x) = 6.00e^{-5} \cdot x^2 + 1.0$, where x is the number of aircraft.	87
B-35 Layers 360: The increment of the flight time for simulations with CR compared to simulations without CR. Simulation results fitted to the model $f(x) = 2.47e^{-5} \cdot x^2 + 1.0$, where x is the number of aircraft.	87
B-36 Layers 180: The increment of the flight time for simulations with CR compared to simulations without CR. Simulation results fitted to the model $f(x) = 1.64e^{-5} \cdot x^2 + 1.0$, where x is the number of aircraft.	87
B-37 Layers 90: The increment of the flight time for simulations with CR compared to simulations without CR. Simulation results fitted to the model $f(x) = 1.16e^{-5} \cdot x^2 + 1.0$, where x is the number of aircraft.	88
B-38 Layers 45: The increment of the flight time for simulations with CR compared to simulations without CR. Simulation results fitted to the model $f(x) = 8.71e^{-6} \cdot x^2 + 1.0$, where x is the number of aircraft.	88

B-39 Free Flight with secondary priority settings: The increment of the flight time for simulations with CR compared to simulations without CR. Simulation results fitted to the model $f(x) = 6.46e^{-5} \cdot x^2 + 1.0$, where x is the number of aircraft.	88
B-40 Layers 45 with secondary priority settings: The increment of the flight time for simulations with CR compared to simulations without CR. Simulation results fitted to the model $f(x) = 1.32e^{-5} \cdot x^2 + 1.0$, where x is the number of aircraft.	88
B-41 Free Flight: The average flight time for simulations with and without CR.	89
B-42 Layers 360: The average flight time for simulations with and without CR.	89
B-43 Layers 180: The average flight time for simulations with and without CR.	89
B-44 Layers 90: The average flight time for simulations with and without CR.	89
B-45 Layers 45: The average flight time for simulations with and without CR.	89
B-46 Free Flight: The increment of the flight distance for simulations with CR compared to simulations without CR. Simulation results fitted to the model $f(x) = 4.94e^{-5} \cdot x^2 + 1.0$, where x is the number of aircraft.	90
B-47 Layers 360: The increment of the flight distance for simulations with CR compared to simulations without CR. Simulation results fitted to the model $f(x) = 1.93e^{-5} \cdot x^2 + 1.0$, where x is the number of aircraft.	90
B-48 Layers 180: The increment of the flight distance for simulations with CR compared to simulations without CR. Simulation results fitted to the model $f(x) = 1.30e^{-5} \cdot x^2 + 1.0$, where x is the number of aircraft.	90
B-49 Layers 90: The increment of the flight distance for simulations with CR compared to simulations without CR. Simulation results fitted to the model $f(x) = 8.83e^{-6} \cdot x^2 + 1.0$, where x is the number of aircraft.	91
B-50 Layers 45: The increment of the flight distance for simulations with CR compared to simulations without CR. Simulation results fitted to the model $f(x) = 6.67e^{-6} \cdot x^2 + 1.0$, where x is the number of aircraft.	91
B-51 Free Flight with secondary priority settings: The increment of the flight distance for simulations with CR compared to simulations without CR. Simulation results fitted to the model $f(x) = 5.34e^{-5} \cdot x^2 + 1.0$, where x is the number of aircraft.	91
B-52 Layers 45 with secondary priority settings: The increment of the flight distance for simulations with CR compared to simulations without CR. Simulation results fitted to the model $f(x) = 1.02e^{-5} \cdot x^2 + 1.0$, where x is the number of aircraft.	91
B-53 Free Flight: The average flight distance for simulations with and without CR.	92
B-54 Layers 360: The average flight distance for simulations with and without CR.	92
B-55 Layers 180: The average flight distance for simulations with and without CR.	92
B-56 Layers 90: The average flight distance for simulations with and without CR.	92
B-57 Layers 45: The average flight distance for simulations with and without CR.	92
B-58 Free Flight: Ratio of aircraft in the simulation with and without CR. Simulation results fitted to the model $f(x) = 1.45e^{-7} \cdot x^2 + 1$, where x is the number of aircraft without CR.	93
B-59 Layers 360: Ratio of aircraft in the simulation with and without CR. Simulation results fitted to the model $f(x) = 3.81e^{-8} \cdot x^2 + 1$, where x is the number of aircraft without CR.	93
B-60 Layers 180: Ratio of aircraft in the simulation with and without CR. Simulation results fitted to the model $f(x) = 2.99e^{-8} \cdot x^2 + 1$, where x is the number of aircraft without CR.	93

B-61	Layers 90: Ratio of aircraft in the simulation with and without CR. Simulation results fitted to the model $f(x) = 2.05e^{-8} \cdot x^2 + 1$, where x is the number of aircraft without CR.	94
B-62	Layers 45: Ratio of aircraft in the simulation with and without CR. Simulation results fitted to the model $f(x) = 1.36e^{-8} \cdot x^2 + 1$, where x is the number of aircraft without CR.	94
B-63	Free Flight: The average density distribution in the experiment area, with 1331 instantaneous aircraft.	95
B-64	Layers 360: The average density distribution in the experiment area, with 1331 instantaneous aircraft.	95
B-65	Layers 180: The average density distribution in the experiment area, with 1331 instantaneous aircraft.	95
B-66	Layers 90: The average density distribution in the experiment area, with 1331 instantaneous aircraft.	96
B-67	Layers 45: The average density distribution in the experiment area, with 1331 instantaneous aircraft.	96
B-68	Free Flight: The average conflict angle per simulation run. Only conflicts between cruising aircraft are considered.	97
B-69	Layers 360: The average conflict angle per simulation run. Only conflicts between cruising aircraft are considered.	97
B-70	Layers 180: The average conflict angle per simulation run. Only conflicts between cruising aircraft are considered.	97
B-71	Layers 90: The average conflict angle per simulation run. Only conflicts between cruising aircraft are considered.	98
B-72	Layers 45: The average conflict angle per simulation run. Only conflicts between cruising aircraft are considered.	98
B-73	Free Flight: The ratio of cruising aircraft in the experiment area during the simulations.	99
B-74	Layers 360: The ratio of cruising aircraft in the experiment area during the simulations.	99
B-75	Layers 180: The ratio of cruising aircraft in the experiment area during the simulations.	99
B-76	Layers 90: The ratio of cruising aircraft in the experiment area during the simulations.	100
B-77	Layers 45: The ratio of cruising aircraft in the experiment area during the simulations.	100
C-1	Graphic overview of the interaction between the four different modules in the scenario generation.	101

List of Tables

2-1	Overview of discrete random variable models [9, 10]	39
2-2	Setting for simulations regarding the horizontal separation requirements	45
2-3	Setting for simulations regarding the look-ahead time	45
2-4	Setting for simulations regarding the speed	46
2-5	Setting for simulations regarding the heading range	47
4-1	The independent variables of the experiment	67
4-2	The dependent variables of the experiment	67
A-1	Explanation of the two-dimensional model	74
A-2	Model parameters for validation simulations of two-dimensional scenarios	74
B-1	Instantaneous Conflict Probability, p_2 (filtered on t_{cpa}	80
B-2	Overview of the average instantaneous number of conflicts [filtered / non-filtered], for simulations without conflict resolution. Filtering is based on t_{cpa} , as discussed in the scientific paper.	80

List of Symbols

Abbreviations

<i>ASAS</i>	Airborne Separation Assurance System
<i>ATC</i>	Air Traffic Control
<i>ATCo</i>	Air Traffic Controller
<i>ATCU</i>	Air Traffic Control Unit
<i>ATM</i>	Air Traffic Management
<i>C/D</i>	Climbing or Descending
<i>CD&R</i>	Conflict Detection and Resolution
<i>DEP</i>	Domino Effect Parameter
<i>FIR</i>	Flight Information Region
<i>FMS</i>	Flight Management System
<i>LoS</i>	Loss of Separation
<i>SESAR</i>	Single European Sky ATM Research
<i>TBO</i>	Trajectory-Based Operations
<i>VFR</i>	Visual Flight Rules

Greek Symbols

α	Heading range per altitude band
δ	The difference between the required heading to the active waypoint and the heading of the initially defined route
γ	Flight path angle
ρ_{ac}	Aircraft density
ρ_{max}	Aircraft density at which the airspace is saturated

Latin Symbols

A	Area
D	Average distance travelled by aircraft
D_{sep}	Required horizontal separation distance

E	Expected number of conflicts
E_{nr}	Number of conflicts, without conflict resolution
E_{wr}	Number of conflicts, with CD&R active
h_{sep}	Required vertical separation distance
hdg	Heading
k	Constant model parameter, which includes both the average amount of extra path distance flown as a result of conflict resolution and the effective extra path distance searched for conflicts per conflict resolution
L	Number of layers in an airspace
N	Number of aircraft
p	Conflict probability
p_0	Parameter used to match the theoretical model with empirical data
r_c	Conflict rate
s	Displacement vector of an aircraft
T	Thrust vector of an aircraft
t	Time interval used to count conflicts
V	Aircraft velocity
V'	Relative velocity
V_H	Horizontal speed
v_s	Vertical speed
V_0	Total airspace volume
V_{CD}	Volume searched by climbing/descending aircraft
V_{level}	Volume searched by cruising aircraft
W	Work done by aircraft

Thesis Outline

This report contains the work performed in fulfillment of the Master of Science thesis, part of the requirements for the degree of Master of Science. The report is divided into three parts:

- I Scientific Paper: Paper describing the research objective, methodology, results and discussion.
- II Preliminary Report: Report containing thesis objectives, literature study and a proposal for the simulation design.
- III Appendices: Supplementary documents regarding the simulation results and description of the software.

Part I

Scientific Paper

The Effect of a Layered Airspace Concept on Conflict Probability and Capacity

Martijn Tra*, Emmanuel Sunil†, Joost Ellerbroek‡, Jacco Hoekstra§
Delft University of Technology, Delft, The Netherlands

I. Introduction

Abstract - Introducing a decentralized air traffic management system could potentially increase the capacity of en-route airspace. Previous research in this field shows that a layered airspace might have benefits compared to an unstructured airspace, but the exact extent of the benefits are unknown. This research compares four layered airspace concepts, with a variation in heading range per layer, to assess the effect on capacity using fast-time simulations. First, a theoretical model is presented and validated to predict the number of conflicts in a three-dimensional airspace. When performing a model fit to the simulation results at low densities, it can be used to accurately predict the number of conflicts at high densities. Secondly, the influence on capacity of layered airspace concepts is determined based on safety, stability and efficiency. The results show that the safety is the most limiting performance metric, due to a steep increase in the number of conflicts and intrusions for an increase in traffic density. A priori separation of traffic using a layered airspace positively influences the performance compared to an unstructured airspace. Comparing the different layered airspace concepts, a clear improvement in capacity is observed for a decreasing heading range per layer.

Since the early days of aviation, all over the world, a highly centralized Air Traffic Management (ATM) system has been used to control aircraft. With an expected growth in air traffic demand, it is debated that the centralized ATM system might be approaching its saturation level [1, 2]. Introducing a fundamentally new airspace structure could potentially increase the capacity of en-route airspace by implementing a decentralized system [3, 4, 5, 6]. A decentralized system may require innovative safety management techniques due to the new dimension in conflict handling. But when the equipment in the cockpit is equally reliable as the equipment on the ground, a decentralized system could potentially increase safety and efficiency, and thereby increase airspace capacity by several orders of magnitude compared to the current ATM system [3].

Most research performed on new airspace concepts, however, is of a qualitative nature, especially when an attempt is made to compare different concepts. The Metropolis project [7] is one of the first research projects to distinguish qualitative differences between multiple airspace concepts. The results of that research showed that a distribution of traffic over the complete airspace is the key in dealing with extremely high traffic densities and minimizing the occurrence of conflicts. The two concepts that utilize this property best and showed the most promising results were the Free Flight and Layers concepts [7].

The Free Flight concept, using the direct routing philosophy, has been the topic of research in many studies that considered the capacity of ATM systems [3, 4, 5, 6]. In this concept, no constraints are imposed on the traffic and aircraft can determine their own flight paths; there are no restrictions in longitudinal or lateral position, altitude and speed. The original concept for Free Flight is described in the report of the RTCA Free Flight Task Force. The design philosophy is that a decentralized system increases the flexibility for the airlines, while also improving the level of safety [8].

Where the Free Flight concept is completely unstructured, the Layers concept uses segmentation of the airspace into altitude bands. Per altitude band, also referred to as a layer, the allowed headings are limited. These rules could enhance the intrinsic safety of the airspace [9] as they can be interpreted as predefined vertical separation, while maintaining part of the direct routing philosophy. This leaves the freedom for aircraft to select their longitudinal and lateral position and speed.

While the Metropolis results indicated that implementing a layered structure can improve capacity [7], the extent of the capacity benefit is unknown. The Metropolis research was only focused on comparing one specific implementation of decentralized airspace concepts to analyze the degree of structuring needed to maximize capacity. To create a more in depth and generalized understanding of the influence of a layered airspace design on capacity, this research aims to compare different implementations of the Layers concept. The Free Flight airspace concept will be used as a benchmark during this research.

The effect of the layered airspace on capacity is analyzed using the effect of variation in traffic demand on the safety, stability and efficiency metrics. For the safety metrics, an analytical approach to predict the effect of a layered airspace is available. The conflict probability between aircraft can be used as a measure for the ability of an airspace concept to prevent a conflict, and therefore an indication for safety. The effect of airspace parameters, such as the average true airspeed and separation criteria, on safety can be modeled by a probabilistic model. This model gives insight into the relation between the number of aircraft in the airspace and the expected number of conflicts [3, 10, 11].

The main limitation of the model presented in literature, is that it can only be applied to a two-dimensional airspace; the effect of alti-

Nomenclature

α	=	heading range per altitude band
γ	=	flight path angle
ρ	=	traffic density
A	=	area
d_{sep_h}	=	horizontal separation distance
d_{sep_v}	=	vertical separation distance
E	=	expected number of instantaneous conflicts
hdg	=	heading
\hat{I}	=	normalized intrusion severity
k	=	constant model parameter
L	=	number of layers in an airspace
n_{cfl}	=	number of conflicts
n_{int}	=	number of intrusions
N	=	number of aircraft
p_2	=	instantaneous conflict probability
$p_{2_{layer}}$	=	instantaneous conflict probability for one layer in the airspace
S_1	=	set of all conflicts without conflict resolution
S_2	=	set of all conflicts with conflict resolution
t	=	time interval used to count conflicts
t_{cpa}	=	time to closest point of approach
t_{inconf}	=	time to first moment of intrusion
v	=	aircraft velocity
v_{rel}	=	relative velocity between two aircraft
V	=	volume

*B.Sc. Control and Simulation, Faculty of Aerospace Engineering, m.a.p.tra@student.tudelft.nl

†PhD Candidate, Control and Simulation, Faculty of Aerospace Engineering

‡Assistant Professor, Control and Simulation, Faculty of Aerospace Engineering

§Professor, Control and Simulation, Faculty of Aerospace Engineering

tude is not included. In this paper, first the conflict probability model is extended for application in a three-dimensional airspace and fast-time simulations are used to validate the theoretical relations. The validated theoretical model is used to gain more insight in the effect of en-route airspace design on intrinsic safety, including the effect of climbing/descending aircraft.

Second, the effect of a layered airspace on the capacity is considered, by assessing the impact of the heading range per layer on the safety, stability and efficiency metrics using fast-time simulations. This can be used to gain insight in the effect of a variation on heading range per layer on the airspace capacity, and the secondary effects that might occur with decreasing the heading range per layer.

This paper is structured as follows. The implementation of the Layers concept is discussed in Section II. In Section III the theoretical relations between the conflict probability and airspace parameters are presented. The theoretical relations to determine capacity using the safety, stability and efficiency are presented in Section IV. In Section V the design of the simulation experiment to validate the theoretical relations is elaborated on. The results of the simulations are described and discussed in Section VI and VII, respectively. Finally, the conclusions are presented in Section VIII.

II. Implementation of the Layers Concept

For the implementation of the Layers concept, segmentation of the decentralized en-route airspace in altitude bands is used. The segmentation in the Layers concept is described using ‘height rules’. These rules describe at which altitude an aircraft should fly during cruise, based on the specific heading of the aircraft. This leaves the freedom for aircraft to select their longitudinal and lateral position and speed. Climbing and descending aircraft are exempted from the rules and can violate them in order to reach their cruise altitude or destination. In Figure 1 an example of a segmented airspace is visualized, and in this example the heading range per layer, α , is 45 degrees. The heading range prescribes the allowed headings for cruising aircraft to fly in that layer, see Figure 2. A set of layers can be defined as the number of layers required to include all possible headings; from 0 degrees to 360 degrees. In the example presented in Figure 1, one set of layers is used. When multiple set of layers are available, the total flight distance is used to determine in which set of layers the aircraft should fly; for a relatively short flight distance, a set of layers at a low altitude is selected. And for a relatively long flight distance, a set of layers at a high altitude is selected.

To analyze the theoretical effect of a layered airspace on the safety of an airspace concept, one can look at the expected number of conflicts at a given moment in time. The relationship between the expected number of conflicts and the number of aircraft in the airspace can be described using a binomial random variable model, see Equation 1 [3]:

$$E = \frac{N(N-1)}{2} \cdot p_2 \quad (1)$$

where E represents the expected number of instantaneous conflicts, N the number of instantaneous aircraft in the airspace and p_2 the probability that any two aircraft have a conflict at a given moment in time.

Set of Layers	315° to 360°	FL 127
	270° to 315°	FL 116
	225° to 270°	FL 105
	180° to 225°	FL 94
	135° to 180°	FL 83
	90° to 135°	FL 72
	45° to 90°	FL 61
	0° to 45°	FL 50

Figure 1. Schematic overview of the Layers concept that indicates the Flight Levels (FL) of the layers. This example is created with a 45° heading range per layer.

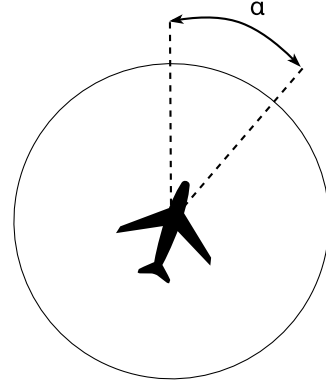


Figure 2. The heading range for a layer is defined by α , in this example 45 degrees. A combination of layers ensures the 360 degrees availability of headings.

As described by Hoekstra *et al.* [11], the two effects that can be observed by implementing a layered airspace are a *spreading effect* and a *sorting effect*. Those will be discussed in Section II.A and Section II.B, respectively. Finally, the specific Layers implementation that is used in this research is described in Section II.C.

A. Spreading over Altitude

The first effect that can be observed by implementing a layered structure, is the *spreading effect*. Segmentation of the airspace in altitude bands affects the possible combinations of aircraft pairs in the conflict probability model. The number of layers in the airspace is defined by the variable L , and the assumption is made that the traffic is evenly distributed over all layers.

Per layer, the expected number of instantaneous conflicts is defined by Equation 2, where the subscript *layer* indicates that the variables are for one specific layer.

$$E_{layer} = \frac{N_{layer}(N_{layer}-1)}{2} \cdot p_{2_{layer}} \quad (2)$$

The expected number of conflicts for the complete airspace can be defined as a summation over all layers, see Equation 3.

$$E = \sum_{layer=1}^L \frac{N_{layer}(N_{layer}-1)}{2} \cdot p_{2_{layer}} \quad (3)$$

Using the assumption that the traffic is distributed evenly over all layers, the conflict probability per layer, $p_{2_{layer}}$, is equal for all layers. Therefore this can be generalized to the conflict probability p_2 . Performing the summation over all layers results in Equation 4 for the estimation of the total number of instantaneous conflicts in the complete airspace.

$$E = \frac{N(\frac{N}{L}-1)}{2} \cdot p_2 \quad (4)$$

B. Sorting based on Heading

The second effect due to a layered airspace is the *sorting effect*, by limiting the allowed heading range within a layer. The limitation in heading range per layer results in a lower relative velocity between cruising aircraft, and is therefore expected to enhance safety. A linear dependency between the relative velocity and the conflict probability is found [11]:

$$p_2 \sim v_{rel} \quad (5)$$

The relative velocity between aircraft is a function of the true airspeed and the absolute heading difference between two aircraft, as visualized in Figure 3, and can be described using Equation 6. It is assumed that both aircraft have the same true airspeed and fly in the same layer.

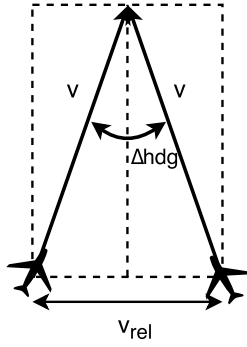


Figure 3. Relation between heading difference and the relative velocity.

$$v_{rel}(|\Delta hdg|) = 2 \cdot v \cdot \sin\left(\frac{|\Delta hdg|}{2}\right) \quad (6)$$

The relation for the relative velocity between aircraft, as described by Equation 6, is a simplification that is valid for conflicting aircraft, but not for all situations of non-conflicting aircraft, for example diverging aircraft. Since only conflicting aircraft are of interest for the conflict probability model, this simplification can be used.

When using a segmented airspace, the heading range of a layer, α , represents the maximum heading difference between two aircraft. Assuming that the headings of all aircraft in a layer are uniformly distributed within the heading range, the probability density function for the heading difference between any two aircraft becomes a triangular distribution, see Figure 4, and can be described by Equation 7.

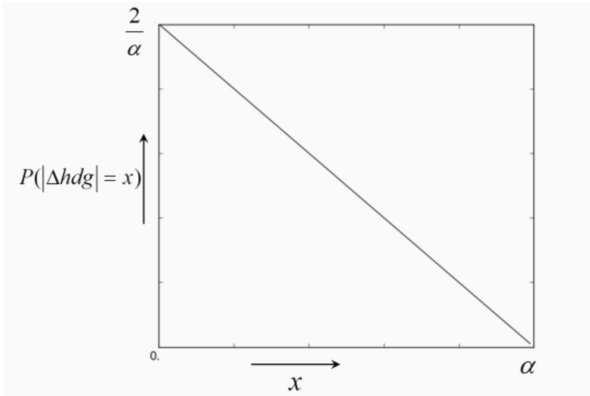


Figure 4. The probability density function for the absolute heading difference of two uniformly distributed random headings between 0 and α [11].

$$P(|\Delta hdg|) = \frac{2}{\alpha^2} (\alpha - x) \quad (7)$$

The effect of the average relative velocity on the conflict probability at any given moment in time, p_2 , can be calculated by integrating the product of relative velocity as function of the heading difference with the probability density function for the relative heading, see Equation 8.

$$p_2 \sim \int_0^\alpha P(|\Delta hdg| = x) \cdot v_{rel}(|\Delta hdg| = x) dx \quad (8)$$

Performing this integration results in the relation between the estimated number of conflicts, E , and the heading range of the layers, α , as presented in Equation 9 [11]. A constant k is included to account for other airspace parameters that influence the conflict probability.

$$E = \frac{N(N-1)}{2} \cdot k \cdot \frac{2\pi}{\alpha} \left(1 - \frac{2}{\alpha} \sin \frac{\alpha}{2}\right) \quad (9)$$

Using Equation 9, one can predict the effect of a layered airspace on the number of instantaneous conflicts. In Table 1, the theoretical

effect of a variation in heading range, α , is presented and the effect of a reduced relative velocity is clear: a reduction in α is expected to significantly reduce the number of conflicts.

Table 1. Theoretical effect of a change in heading range per layer on the number of conflicts, using $L = 1$ [11].

Heading Range, α (deg)	Conflict Reduction
360	0%
180	27%
90	60%
45	80%
22.5	90%
10	95%

C. Implemented concepts

The implementation of height rules to define the airspace can be used in many different ways, for example semicircular, quadrantal and spiral rules [9, 12, 13, 14, 15]. The variation in the Layer concepts that are tested in this research, is the result of a different heading range per layer. Details regarding the implementation of the Layers concept for this research will be presented next.

A total number of eight layers are used for cruising aircraft in this research, with altitudes as defined in Figure 1.

- The first concept that can be defined is the Layers 360; based on flight distance, the aircraft are uniformly distributed over the layers. There is no segmentation based on heading in the Layers 360 concept.
- Secondly, the Layers 180 concept is introduced; the headings are divided over two layers with a heading range of 180 degrees, resulting in four sets of layers. The aircraft are uniformly distributed, based on flight distance, between the sets of layers.
- For the Layers 90 concept, the headings are divided over four layers, with a 90 degrees heading range per layer. This results in two sets of layers, again with a uniform distribution of aircraft based on flight distance.
- The use of eight layers results in a minimal heading range per layer of 45 degrees, the Layers 45 concept. Aircraft are assigned to a specific layer, based on their heading.

An important practical reason to use the Layers concept with a minimum of 45 degrees heading range per layer is the difference in altitude between the top and bottom layer; this distance doubles when an extra set of eight layers is introduced to reduce α to 22.5 degrees, and thereby increases significantly. Additionally, a theoretical reason to use a minimum heading range of 45 degrees can be explained using Table 1; the net effect of reducing α from 45 degrees to 22.5 degrees becomes small.

III. Theoretical Relations for Conflict Probability

As mentioned in Section II, the expected number of *instantaneous* conflicts is an indication for the safety performance of an airspace concept. By obtaining a theoretical relation between airspace parameters and the expected number of instantaneous conflicts, one can estimate the effect of a change in these parameters. In Section III.A the relation between airspace parameters and conflict probability for a two-dimensional airspace will be elaborated on. Based on literature, the conflict probability, p_2 , can be defined as a function of the area searched by aircraft for conflicts [10] and the allowed heading range in the airspace [11]. Next, in Section III.B these theoretical relations will be extended for application in a three-dimensional airspace. This section is concluded with an overview of the theoretical relations of conflict probability for the Free Flight and the Layers concepts.

A. Two-Dimensional Airspace

A two-dimensional airspace is defined in the horizontal plane. In this horizontal plane, the area searched for conflicts by an aircraft is related to the conflict probability between aircraft. For this relationship, Jardin [10] describes that this area can be approximated as a function of the horizontal separation distance, d_{seph} , the velocity, v , the time spent searching for conflicts at a given time instant (the look-ahead time), t , and the total area of the airspace, A , see Equation 10 and Equation 11. The geometric relation between these parameters and the area searched for conflicts is visualized in Figure 5.

$$p_2 \sim \frac{\Delta A}{A} \quad (10)$$

$$p_2 \sim \frac{2 \cdot d_{seph} \cdot v \cdot t}{A} \quad (11)$$

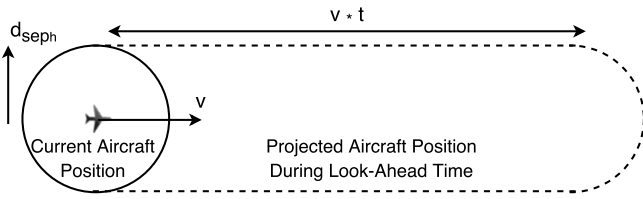


Figure 5. Top-view of the area searched for conflicts by an aircraft, using the horizontal separation distance (d_{seph}), the speed (v) and the look-ahead time (t).

Hoekstra *et al.* [11] extended this relation by including the effect of layered airspace design parameters on conflict probability. In that paper it is described that the conflict probability can also be related to the average relative velocity between aircraft. It is assumed that the conflict probability relates proportional to the relative velocity between two aircraft v_{rel} . The relative velocity between aircraft can be directly related to allowed range of heading in the airspace, as explained in Section II.B, resulting in the relation as presented in Equation 12 [11]:

$$p_2 \sim \frac{2\pi}{\alpha} \left(1 - \frac{2}{\alpha} \sin \frac{\alpha}{2}\right) \quad (12)$$

where α is the heading range of a layer. Combining equations 1, 11 and 12 results in the following equation for the number of instantaneous conflicts in a two-dimensional airspace:

$$E = \frac{N(\frac{N}{L} - 1)}{2} \cdot k \cdot \frac{2 \cdot d_{seph} \cdot v \cdot t}{A} \cdot \frac{2\pi}{\alpha} \left(1 - \frac{2}{\alpha} \sin \frac{\alpha}{2}\right) \quad (13)$$

where k is included to account for other parameters that influence the conflict probability. The value for k is determined by fitting the conflict probability model in a least-squares sense with simulation results. A value for k of 1.0 is desired, since this means that the model is able to predict the instantaneous number of conflicts accurately. When k is less than 1.0, the model is over-predicting the conflicts and when k is greater than 1.0, the model is under-estimating the number of conflicts. A validation of the model using two-dimensional simulations can be found in Appendix A of the report.

B. Three-Dimensional Airspace

When a three-dimensional airspace is considered, climbing and descending aircraft will affect the total number of conflicts within that airspace. In literature, the conflict probability is only described for two-dimensional scenarios, as discussed in Section III.A. In this section, the model described in literature is extended such that it can be applied to three-dimensional scenarios.

When considering a three-dimensional airspace, the area searched by an aircraft for conflicts becomes a volume. The relation between the volume searched and the instantaneous conflict probability can be defined by Equation 14.

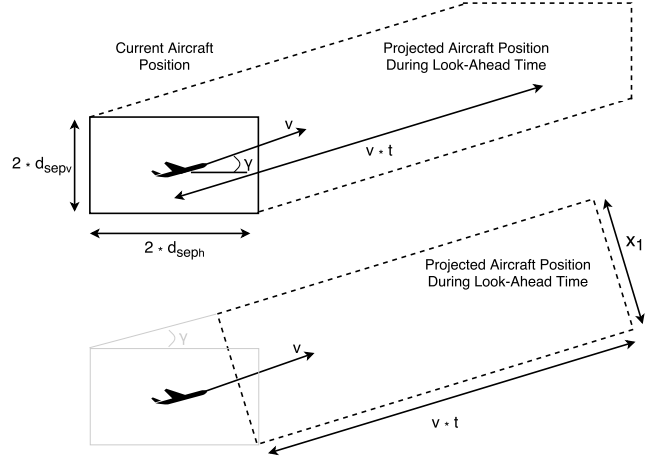


Figure 6. Side-view of the volume searched by an aircraft in a three-dimensional airspace. The top figure indicates the dependency on the airspace parameters, and the bottom figure represents the simplification using $v \cdot t \gg d_{seph}$.

$$p \sim \frac{\Delta V}{V} \quad (14)$$

where ΔV is the volume searched by an aircraft at a particular time instant, and V is the total volume of the airspace considered. A side-view of the volume searched, ΔV , is visualized in Figure 6.

Comparable to the two-dimensional situation, the volume searched can be described using the following parameters; the horizontal separation distance, d_{seph} , the velocity, v , the time interval used, t , and additionally to the two-dimensional derivation, the vertical separation distance, d_{sepv} , and the flight path angle. The flight path angle, indicated in Figure 6 with γ , can be described using the horizontal and vertical speed, as presented in Equation 15.

$$\gamma = \tan^{-1} \left(\frac{v_v}{v_h} \right) \quad (15)$$

Since $v \cdot t \gg d_{seph}$, the volume can be simplified, and the simplified side-view is presented in Figure 6. The distance x_1 depends on the flight path angle and the separation minima, d_{seph} and d_{sepv} , and is defined using Equation 16.

$$x_1 = 2 \cdot d_{seph} \cdot \sin(\gamma) + 2 \cdot d_{sepv} \cdot \cos(\gamma) \quad (16)$$

Since the vertical speed, v_v , is usually small compared with the horizontal velocity, v_h , the flight path angle will also be small. For small angles of the flight path, the assumptions in Equation 17 and Equation 18 can be used to simplify the model.

$$2 \cdot d_{seph} \cdot \sin(\gamma) = 2 \cdot d_{seph} \cdot \gamma \quad (17)$$

$$2 \cdot d_{sepv} \cdot \cos(\gamma) = 2 \cdot d_{sepv} \quad (18)$$

Using these approximations, the area searched by aircraft for conflicts can be simplified to Equation 19.

$$\Delta V = [2 \cdot d_{seph} \cdot |\gamma| + 2 \cdot d_{sepv}] \cdot 2 \cdot d_{seph} \cdot v \cdot t \quad (19)$$

For vertical speeds up to 6,000 ft/min, the difference in volume searched between the exact solution and the approximation is presented in Figure 7, using the parameters described in Table 2. It can be concluded that for climbing speeds of average aircraft, of around 2,000 ft/min, the simplifications are a good approximation.

Combining equations 14 and 19 results in the following relation for the conflict probability:

$$p \sim \left(\frac{[2 \cdot d_{seph} \cdot |\gamma| + 2 \cdot d_{sepv}] \cdot 2 \cdot d_{seph} \cdot v \cdot t}{V} \right) \quad (20)$$

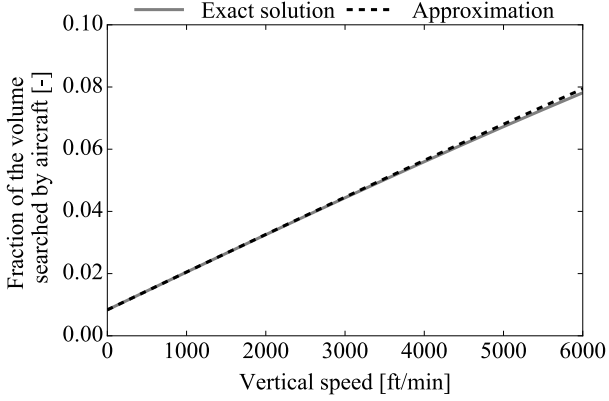


Figure 7. The difference between the exact solution and the approximation of the volume searched by aircraft, for a vertical speed up to 6,000 ft/min.

Table 2. Parameters used to assess difference between the exact solution and the approximation for the volume searched for conflicts.

Model Parameter	Value	Unit
d_{sep_h}	5.0	nm
d_{sep_v}	1000.0	ft
v	400.0	fts
t	300.0	s
V	$10.0 \cdot 10^3 \times 8,000$	$nm^2 \times ft$

For the application of this theoretical relation to different airspace concepts, one has to carefully consider whether the assumptions used for the derivation are still valid. In this particular case, the assumption that the conflict probability between any two aircraft in the airspace is equal for all aircraft needs to be reconsidered. In case of an airspace using the Free Flight concept, one does not actively influence the conflict probability between any two aircraft, and therefore the *spreading effect* does not occur. The theoretical relation will be presented in Section III.B.1.

When one uses a priori means of separation between aircraft, like the Layers concept, the assumption that any two aircraft can meet each other does not hold due to the *spreading effect*. A method to account for this is splitting the estimation for the total number of conflicts in three types: cruising versus cruising, climbing/descending versus climbing/descending (C/D versus C/D) and mixed (cruising versus C/D). The resulting theoretical relationship between the number of conflicts and the number of aircraft for the Layers concept can be found in Section III.B.2.

1. Free Flight

For the Free Flight concept, there is no effect of a priori vertical separation ($L=1$) and no limitation in heading range on the conflict probability. Therefore there is no differentiation required of the conflict probability between cruising and climbing/descending aircraft. The average volume searched by aircraft can be used to estimate the number of conflicts. This results in Equation 21, where $|\gamma|_{avg}$ is the average of the absolute climb angles of all aircraft in the airspace.

$$E_{total} = \frac{N(N-1)}{2} \cdot k \cdot f(|\gamma|_{avg}) \quad (21)$$

where:

$$f(|\gamma|_{avg}) = \left(\frac{[2 \cdot d_{sep_h} \cdot |\gamma|_{avg} + 2 \cdot d_{sep_v}] \cdot 2 \cdot d_{sep_h} \cdot v \cdot t}{V} \right) \quad (22)$$

2. Layers

The estimation of the total number of conflicts for a three-dimensional airspace, using the Layers concept, requires a distinction between the three classes as discussed in the beginning of this chapter. The parameter L is introduced because the number of layers becomes important in estimating the number of conflicts. It is assumed that the number of cruising aircraft is uniformly distributed over the available layers, and that the heading of aircraft in a particular layer are also uniformly distributed. The estimated number of conflicts is a summation of the three different classes of conflicts as presented in Equation 23.

$$E_{total} = \frac{N_{cruise} \left(\frac{N_{cruise}}{L} - 1 \right)}{2} \cdot k_1 \cdot \left(\frac{2 \cdot d_{sep_h} \cdot v \cdot t}{A} \right) \cdot g(\alpha) + N_{CD} \cdot N_{cruise} \cdot k_2 \cdot f(|\gamma|_{avg}) + \frac{N_{CD}(N_{CD}-1)}{2} \cdot k_3 \cdot f(|\gamma|) \quad (23)$$

where:

$$g(\alpha) = \frac{2\pi}{\alpha} \left(1 - \frac{2}{\alpha} \sin \frac{\alpha}{2} \right) \quad (24)$$

$$f(\gamma) = \left(\frac{[2 \cdot d_{sep_h} \cdot |\gamma| + 2 \cdot d_{sep_v}] \cdot 2 \cdot d_{sep_h} \cdot v \cdot t}{V} \right) \quad (25)$$

In Equation 23, $|\gamma|$ is the absolute climb angle of climbing/descending aircraft and $|\gamma|_{avg}$ is the average of the absolute climb angles of all aircraft in the airspace. Note that the possible conflicts between cruising and climbing/descending aircraft are combinations between different sets of aircraft. Therefore a different equation is used in Equation 23 to describe the number of possible conflicting aircraft pairs between cruising and climbing/descending aircraft. For the three conflict types, the model can be fitted to the simulation data, resulting in three k -values; k_1 for cruising versus cruising conflicts, k_2 for cruising versus climbing/descending conflicts and k_3 for climbing/descending versus climbing/descending conflicts.

IV. Determining Airspace Capacity Limits from Simulations

The capacity of an airspace can be assessed using multiple performance metrics; safety, stability and efficiency. These metrics give a good indication of the saturation level of the airspace; an airspace has reached its capacity when one of these metrics diverges to infinity, as expressed using Equation 26.

$$\rho_{capacity} = \min \left(\rho_{sa}, \rho_{st}, \rho_{ef} \left| \begin{array}{l} \lim_{\rho \rightarrow \rho_{sa}} \frac{\delta sa}{\rho} = \infty \\ \lim_{\rho \rightarrow \rho_{st}} \frac{\delta st}{\rho} = \infty \\ \lim_{\rho \rightarrow \rho_{ef}} \frac{\delta ef}{\rho} = \infty \end{array} \right. \right) \quad (26)$$

where ρ is the theoretical maximum density and *sa*, *st* en *ef* abbreviations for safety, stability and efficiency, respectively. In Section IV.A, it is explained how the safety metric can be measured and how it limits the capacity. The stability of a system can be expressed using the Domino Effect Parameter (DEP), as is explained in Section IV.B. Finally, in Section IV.C the efficiency metric is discussed.

A. Safety

When considering the capacity of airspace, safety is of utmost importance. It can be related to the ability of an airspace concept to prevent a Loss of Separation (LoS). A Loss of Separation is defined as an intrusion of the protected zone of an aircraft. The protected zone is described by the horizontal and vertical separation criteria. Safety can be analyzed by considering the number of conflicts, a predicted LoS, and the number of intrusions, the actual LoS. If the application of a new height rule results in a reduced conflict and intrusion count, then it can be said that this new rule is intrinsically safer than the old rule [9].

Considering the safety of an airspace concept, Jardin describes that a high number of conflicts and a steep rate of growth of conflicts is an indication that the airspace is nearing saturation[10]. In this paper, the same method is used to determine the capacity based on the number of conflicts as well as the number of intrusions.

A second method to assess the safety is using the Intrusion Prevention Rate (IPR). This method considers the number of conflicts that are successfully avoided. Equation 27 is used to calculate the IPR [7].

$$IPR = \frac{n_{cfl} - n_{int}}{n_{cfl}} \quad (27)$$

where n_{cfl} represents the total number of conflicts, and n_{int} the total number of intrusions, or Loss of Separations.

Besides considering the total number of intrusions and the intrusion prevention rate, it is important to look at the intrusion severity. Note that intrusions are not directly resulting in collisions. The severity of an intrusion is determined by the degree of penetration of the protected zone of an aircraft and can be computed using Equation 28 [7].

$$\hat{I}_{sev} = \max \left[\min \left(\hat{I}_H(t), \hat{I}_V(t) \right) \right] \quad (28)$$

where \hat{I}_{sev} is the normalized intrusion severity, \hat{I}_H is the normalized intrusion severity in the horizontal plane, and \hat{I}_V is the normalized intrusion severity in the vertical plane. The intrusion severity is measured at the moment of most severe intrusion, for a particular LoS.

B. Stability

The stability of an airspace concept can be inversely related to the Domino Effect Parameter, a parameter that describes the number of secondary conflicts per primary conflict. Secondary conflicts are conflicts that occur while resolving a conflict, and primary conflicts are conflicts that are detected when an aircraft is not solving any other conflict. The DEP can be defined by Equation 29 [16] and is visualized using Figure 8. When the value for the DEP is greater than zero, conflict resolution results in a destabilization. For a value less than zero, solving conflicts would result in a stabilizing effect, and therefore a lower total number of conflicts.

$$DEP = \left(\frac{S_2}{S_1} - 1 \right) \quad (29)$$

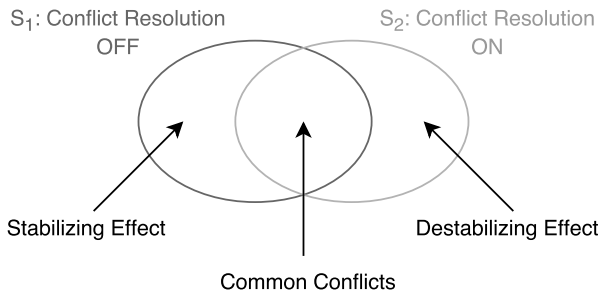


Figure 8. Domino Effect Parameter: visualization of the difference in the number of conflicts with and without resolution maneuvers.

Jardin [10] suggests a theoretical model to predict the number of secondary conflicts per primary conflict. For the derivation of this model, it is assumed that the conflict rate, the average number of conflicts per unit distance, is constant whether or not conflict resolution is applied. This results in the model presented in Equation 30.

$$DEP = \left(\frac{\rho_{ac}}{\rho_{max} - \rho_{ac}} \right) \quad (30)$$

where ρ_{ac} is the average density of aircraft in the airspace, and ρ_{max} is a measure for the theoretical maximum capacity. To assess the capacity due to stability limitations, the theoretical model described in this section can be matched with empirical data to yield a value for ρ_{max} .

C. Efficiency

The third performance metric that will be considered is the efficiency of the aircraft. The efficiency can be analyzed using the average flight distance and flight time of aircraft to complete their flight. This metric shows the result of conflict resolutions as well as concept dependent in-efficiency on the flight compared to the preferred trajectory.

Comparable with assessing the safety of an airspace concept, a steep rate of growth of the distance or time to complete a flight would suggest that the airspace is nearing saturation.

V. Simulation Experiment Design

The effect of the heading range per altitude band in the Layers concept will be tested and compared with the Free Flight concept using data obtained from large-scale, fast-time simulation experiments. The simulations have the following goals:

1. To validate the conflict probability model.
2. To determine the influence of the heading range per layer on the performance for the Layers concept.

First in Section V.A, the simulation environment, BlueSky, will be discussed. This includes a short explanation regarding the software, the implementation of the concepts and the airborne separation assurance system. The independent and dependent variables are discussed in Section V.B and Section V.C, respectively. The traffic scenarios, including the test region, simulation time and traffic demand, are discussed in Section V.D. The simulation procedure is discussed in Section V.E. Finally, the hypotheses are presented in Section V.F.

A. Simulation Development

1. Simulation Platform

BlueSky is an open-source tool for performing research on Air Traffic Management and Air Traffic Flows. It can be used to simulate, analyze and visualize air traffic on a global scale. It is developed in the programming language Python in combination with a user-friendly interface. BlueSky is capable of simulating hundreds of aircraft at the same time and traffic scenarios can easily be created and introduced using the command stack of BlueSky, including a time stamp. The traffic script language is compatible with the NLR Traffic Manager TMX [17].

2. Concept Implementation

The airspace concepts are implemented by making use of the trajectory planning functions of BlueSky. The Free Flight concept, as well as the Layers concept, uses a direct horizontal route. For the Free Flight concept, this is combined with an altitude selection based on the distance between origin and destination. Since the length of the routes are uniformly distributed³, this also ensures a uniform vertical distribution of traffic, in combination with a fuel efficient altitude. For the Layers concept, the altitude is selected based on the bearing to the destination and the matching altitude from a predefined list. When multiple sets of layers are available, the distance between origin and destination determines the choice of the correct set; for a longer distance, a layers set with a higher altitude is selected.

The route of an aircraft is defined by the origin, destination and a cruise altitude. Since the Free Flight concept lacks structure, trajectory recovery after a conflict is solely based on the location of the destination. After performing a resolution maneuver, a new heading is selected that results in a direct route to the destination. The Layers concept, however, does have limitations in the heading range per layer for cruising aircraft. When performing a resolution maneuver, solving the conflict has priority over following the altitude rules. After solving the conflict, a new heading is selected that will result in a direct route to the destination. A check is performed to compare the new heading with the altitude rules. If a violation of the altitude rules with more than five degrees is detected, a new cruise altitude is assigned to this aircraft. The margin of five degrees is included to avoid that aircraft,

³The scenarios are generated with a uniformly distributed length between 240 nm and 450 nm.

on the boundary of the heading range in a layer, need to switch layers after every conflict resolution maneuver.

3. Airborne Separation Assurance System

The Airborne Separation Assurance System (ASAS) used in the simulations consists of a Conflict Detection (CD) module and a Conflict Resolution (CR) module. After performing initial simulations, the necessity for a Conflict Probe (CP) module became clear. All three modules will shortly be elaborated on next.

Conflict Detection

The conflict detection, as implemented in BlueSky, is based on linear extrapolation of the aircraft states over a pre-defined look-ahead time of five minutes. When conflicts are resolved with this look-ahead time, the heading changes and vertical speed changes are relatively small, minimizing the effect on the route to the destination.

Conflicts are detected using a vertical separation of 1,000 ft and horizontal separation of five nautical miles [19]. Conflict detection is disabled at take-off to ensure that aircraft are not in conflict directly at taking off from the origin^b. After aircraft reach an altitude of 1,000 ft, the conflict detection is enabled.

Conflict Resolution

Predicted conflicts are solved using the Modified Voltage Potential (MVP) method, implemented in BlueSky as described in [20]. The limitations on conflict resolution maneuvers are implemented as described in Section V.B.2.

Vertical Conflict Probe

Next to the CD and CR modules of the airborne separation assurance system, a conflict probe module is included. After performing initial simulations, most of the intrusions that were observed occurred due to aircraft changing their state from cruising to climbing or descending. These changes in state are initiated by the Vertical Navigation (VNAV)^c functionality of BlueSky and can result in conflicts with a time-to-closest-point-of-approach (t_{cpa}) that is too small for solving the conflict. To prevent these type of conflicts, aircraft perform a conflict detection with their future state. If this results in short-term conflicts, a t_{cpa} of 60 seconds or less, the VNAV functionality is postponed until the maneuver is free of short-term conflicts as visualized in Figure 9. By postponing the maneuver, a conflict and intrusion are prevented, and to not affect the simulation results, these prevented conflicts are counted as normal conflicts.

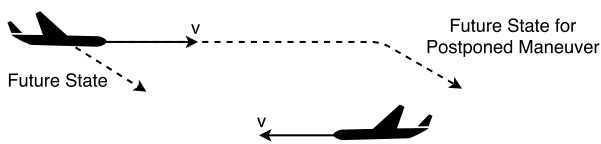


Figure 9. Conflict Probe: postponing the vertical maneuver to avoid short-term conflicts.

B. Independent Variables

This research includes two types of simulations: simulations to validate the conflict probability model and simulations to assess the effect of a layered airspace on capacity.

1. Conflict Probability Model

- *Airspace structure* was an independent factor with 5 levels: the airspace configuration could be either Free Flight, or Layers with a 360, 180, 90, or 45 degrees heading limitation, respectively.

^bThe experiment area in the vertical direction is defined from 5,000 ft to 12,700 ft. Therefore, disabling conflict resolution below 1,000 ft does not affect the results.

^cThe autopilot module in BlueSky, used for navigation in the vertical plane.

- *Traffic demand* was an independent factor with 13 levels: the traffic demand ranged from 2.0 up to 111.5 aircraft per 10,000 nm^2 , see Table 3 for a complete overview. Note that this relates to a current en-route density of approximately 21.6 aircraft per 10,000 nm^{2d} [21].
- *Climb angle* was an independent factor with 2 levels: the effect of the climb angle is analyzed by reducing the climb angle by a factor 2, from 2.8^{0e} to 1.4^0 . Simulations are conducted for the Free Flight and Layers 45 concepts, using traffic demands of 2 - 56.9 aircraft per 10,000 nm^2 without conflict resolution.
- *Speed variations* was an independent factor with 2 levels; the first setting is a constant true airspeed of 500 knots. And a second setting is used, where the aircraft have uniformly distributed speeds, with a range of the distribution of 500 knots +/- 10%. Simulations with the secondary settings are performed for the Layers 45 concept, with traffic demands of 2.0 up to 56.9 aircraft per 10,000 nm^2 .

This results in 5 (airspace structure) \times 13 (traffic demand) simulation conditions to analyze *the effect of a layered airspace on the conflict probability model*, 2 (airspace structure) \times 11 (traffic demand) \times 2 (climb angle) simulation conditions to analyze *the effect of variation in climb angle*, and 11 (traffic demand) \times 2 (speed variations) simulation conditions to analyze *the effect of variation in airspeed*. During these simulations, the conflict resolution module was not active. For each of the simulation conditions, 2 repetitions were performed.

2. Effect of Airspace Design on Capacity

- *Airspace structure* was an independent factor with 5 levels: the airspace configuration could be either Free Flight, or Layers with a 360, 180, 90, or 45 degrees heading limitation, respectively.
- *Traffic demand* was an independent factor with 13 levels: the traffic demand ranged from 2.0 up to 111.5^f aircraft per 10,000 nm^2 , see Table 3 for a complete overview. Note that this relates to a current en-route density of approximately 21.6 aircraft per 10,000 nm^2 [21].
- *Conflict Resolution* was an independent factor with 2 levels; the conflict resolution could either be on or off.
- *Priority Settings* was an independent factor with 2 levels; the conflict resolution is implemented using specific priority settings. These settings prescribe which aircraft is solving the conflict, and potential limitations for the resolution maneuver. The priority settings are discussed below. The effect of priority settings on the results is tested for the Free Flight concept and Layers concept with a 45 degrees heading range. Simulations are conducted for traffic demands of 2.0 up to 56.9 aircraft per 10,000 nm^2 .

This results in 5 (airspace structure) \times 13 (traffic demand) \times 2 (conflict resolution) simulation conditions to analyze *the effect of a layered airspace on the capacity*, and 2 (airspace structure) \times 11 (traffic demand) \times 2 (conflict resolution) \times 2 (priority settings) simulation conditions to analyze *the effect of priority rules on the results*. For each of the simulation conditions, 2 repetitions were performed.

Next, details regarding the specific implementation of the priority rules of the Free Flight concept for this research are discussed. Since the Free Flight concept builds on the lack of structure, preferably there

^dBased on an area centered on Brussels that includes five large TMAs, the positions of which are approximated to Brussels, London, Frankfurt, Paris and Amsterdam. The airspace category U is used, since it shows comparable characteristics with the simulation design.

^eA γ of 2.8^0 corresponds to a change in altitude of 3,000 ft per 10 nm.

^fBlueSky could not handle all scenarios with great number of aircraft, in combination with the conflict resolution module. These scenarios are indicated in the table with '-'

Table 3. Overview of the independent variable *traffic demand*. Simulations performed without CR (-) due to simulation limitations, and simulations performed with and without CR (+).

	Number of aircraft per 10,000 nm^2 , for complete vertical airspace												
	2.0	2.7	3.8	5.4	7.6	10.6	14.8	20.7	29.0	40.6	56.9	79.6	111.5
Free Flight	+	+	+	+	+	+	+	+	+	+	+	-	-
Layers 360	+	+	+	+	+	+	+	+	+	+	+	+	-
Layers 180	+	+	+	+	+	+	+	+	+	+	+	+	-
Layers 90	+	+	+	+	+	+	+	+	+	+	+	+	+
Layers 45	+	+	+	+	+	+	+	+	+	+	+	+	+

are no restrictions for solving conflicts. However, to guarantee the robustness of the simulations, which include Climbing and Descending aircraft (C/D), priority rules are included. The rules prescribe which aircraft solves the conflict and possible limitations in the conflict resolution maneuver. Two sets of priority rules are defined, see Table 4: the primary rules will be used for the standard simulations, and the secondary rules to test the effect of the priority rules on the performance.

Table 4. Priority rules and limitations for resolution maneuvers in Free Flight airspace

	Conflict Type	Solving Aircraft	CR Direction
Primary Settings	Cruise - Cruise	Both	Horizontal + Vertical
	Cruise - C/D	Cruise	Horizontal
	C/D - C/D	Both	Horizontal + Vertical ¹
Secondary Settings	Cruise - Cruise	Both	Horizontal + Vertical
	Cruise - C/D	Both	Horizontal + Vertical ¹
	C/D - C/D	Both	Horizontal + Vertical ¹

¹ To guarantee that aircraft climbing into the simulation airspace can enter this airspace, the resolution maneuver of an aircraft in conflict below 5000 ft is limited to horizontally only.

Comparable with the Free Flight concept, the Layers concepts uses the Airborne Separation Assurance System for safe separation between aircraft. In order to use the reduced relative velocity between aircraft, cruising aircraft should not leave their layer in the vertical direction when resolving a conflict. The limitations in solving conflicts are presented in Table 5 for simulations using the primary settings and for the simulations to test the effect of the priority rules on the performance metrics, the secondary settings.

Table 5. Priority rules and limitations for resolution maneuvers in layered airspace

	Conflict Type	Solving Aircraft	CR Direction
Primary Settings	Cruise - Cruise	Both	Horizontal
	Cruise - C/D	Cruise	Horizontal
	C/D - C/D	Both	Horizontal
Secondary Settings	Cruise - Cruise	Both	Horizontal
	Cruise - C/D	C/D	Horizontal
	C/D - C/D	Both	Horizontal

C. Dependent Variables

The dependent variables can be split in two categories; the validation of the conflict probability model and the effect of airspace design on capacity. Both will be discussed next.

1. Conflict Probability Model

The conflict probability models, as presented in Section III.B, will be validated using the *number of instantaneous conflicts* when no resolution maneuvers are applied. The conflict probability model for a layered airspace uses three different types of conflicts; cruising versus cruising, climbing/descending versus climbing/descending and mixed (cruising versus climbing/descending). Therefore, the dependent variable for the conflict probability model will use a distinction in these types of conflicts.

2. Effect of Airspace Design on Capacity

Three performance metrics will be used to quantitatively compare the different airspace concepts: safety, stability and efficiency. An explanation of the different metrics can be found in Section IV and a short overview of the dependent variables that are used to for these metrics is presented next.

- **Safety:** The safety metric will be assessed using the *number of conflicts/intrusions*, *intrusion prevention rate* and the *intrusion severity*.
- **Stability:** The difference in number of conflicts between not performing CR and with CR, expressed using the *domino effect parameter*, is used to assess the stability of an airspace concept.
- **Efficiency:** The difference in efficiency between concepts is assessed using the average *flight time* and average *flight distance*. Also the *number of aircraft* in the simulation will be considered.

D. Traffic Scenario

1. Testing Region

Origins and destinations are defined at ground level, in a grid pattern of 17 x 17 airports. The spacing between airports is 30 nm, based on the distance between airports (including small ones) in Europe. With 289 (17 x 17) airports, the resulting simulation area covers 480 by 480 nautical miles. Aircraft are spawned at 0 ft and have to perform a climb to their cruise altitude. To ensure that aircraft have a cruise-phase in their flight, the minimum distance between origin and destination is selected to be 240 nm. The maximum flight distance is set to 450 nm. Using these settings, initial simulations showed a uniform distribution of flight lengths, which is used for the vertical distribution of aircraft.

In the vertical plane, the experiment area is positioned between 5,000 ft[§] and 12,700 ft. This allows for 8 Layers, separated by 1,100 ft. In combination with a vertical separation requirement of 1,000 ft, this ensures that cruising aircraft in different layers will not detect a conflict with each other.

When aircraft descend to the airport, they are deleted from the simulation when reaching an altitude of 4,000 ft.

2. Simulation Time

The simulation consisted of three phases. The first one was the build-up phase; during this period of time aircraft were generated and after

[§]To allow aircraft to be spawned at 0 ft, and include a limited climbing/descending time, the lower altitude of the experiment area is set at 5,000 ft.

approximately 60 minutes the average aircraft density reached a stabilized state.

After 60 minutes, the measurement phase could start and the logging of data began. It was chosen to set the measurement time to 60 minutes.

Until 180 minutes, new flights were created. This ensures that aircraft, spawned during the simulation phase, finished their flight with the average density of aircraft in the airspace. The simulation ended when all aircraft reached their destination, after approximately 240 minutes.

For the simulations without conflict resolution, ASAS was turned on after 45 minutes. Since conflict resolution was not performed during these simulations, this does not affect the results of the simulation. When conflict resolution was enabled, it was chosen to do this from the beginning. To speed up the simulation, ASAS was only performed every four seconds during the first 30 minutes, every two seconds between 30 and 45 minutes simulation time, and after that every second.

E. Simulation Procedure and Data Logging

As mentioned in Section V.D.2, the simulation consisted of three phases, each with a different purpose. In this section, the type of data that was logged, during which simulation phase it was logged and the logging procedure will be shortly elaborated on. Two types of logging are used: periodic and event-based.

Periodic Logging

Periodic logging kept track of the traffic situation with a fixed interval of 30 seconds. For every aircraft in the experiment area, the position, speed and heading is logged. Besides that, the conflict situation is logged with the same interval, which includes the t_{cpa} locations. This is used for the number of instantaneous conflicts. The periodic logging was active during the measurement phase, from 60 minutes to 120 minutes.

Event-based Logging

An overview of all conflicts and intrusions that occurred during the simulation time, from 60 minutes to 120 minutes, is used to assess the performance of the airspace concepts. The conflict logging includes information on different relevant times regarding the conflict; the t_{cpa} , the time at which the aircraft get in conflict ($t_{in,conf}$) and the time they get out of the conflict ($t_{out,conf}$). Also the state of the aircraft and information on the conflict location is logged. Conflicts that are detected using the CP module are included as well. For the intrusions, the location of the most severe intrusion is logged.

To assess the efficiency performance of the different airspace concepts, flight time and flight distance of the flights are kept track of. These are logged as soon as an aircraft is deleted from the simulation because it reached its destination.

F. Hypotheses

In this section, the hypotheses regarding the extent of the benefits of the Layers concept compared to the Free Flight concept are presented. First, the hypotheses regarding the conflict probability model are presented. Second, the effect of airspace design on capacity will be discussed.

Conflict Probability Model

1. Based on the theoretical model for a layered airspace, the first hypothesis is that due to the *sorting effect* for cruising aircraft in a layered airspace, the number of conflicts between cruising aircraft will decrease significantly with a reduction in heading range per layer.
2. The conflict probability relates to the climb angle by the volume searched for conflicts. With a decrease in climb angle, and thereby a decrease in vertical speed, the instantaneous volume searched for conflicts decreases as can be observed in Figure 7. However, as a direct result of reducing the climb angle, the climb/descent phase of the flight will increase in length, and the ratio between cruising and climbing/descending

aircraft changes: at any given moment in time, due to a reduction in climb angle, relatively more aircraft will be climbing/descending. Since the volume searched for conflicts by climbing/descending aircraft increases for a lower climb angle, it is hypothesized that the instantaneous number of conflicts increases. Since the model accounts for the climb angle, the k -values are not expected to show significant variation.

3. For the derivation of the theoretical model, one assumes a constant true airspeed for all aircraft. By introducing a variation in true airspeed between aircraft, two-dimensional simulations do not show a significant variation in number of conflicts. Therefore, it is expected that the introduction of speed variations will not significantly affect the results for a three-dimensional airspace.

Effect of Airspace Design on Capacity

4. A reduction in heading range per layer, results in a lower conflict probability between aircraft when no resolution maneuvers are applied. Furthermore, due to this effect, it is also expected that the number of new conflicts due to resolution maneuvers decreases. Between the different Layers concepts, the stability performance is hypothesized to improve with reducing the heading range per layer and will be the metric limiting the capacity.
5. Where one expects the stability to increase for a decrease in heading range per layer, the efficiency is expected to decrease for a decrease in heading range per layer and become more important in assessing the capacity. Aircraft are less able to select an optimal cruise altitude for their flight distance, and therefore have a reduced efficiency.
6. For the low traffic densities, it is hypothesized that Free Flight will have advantages regarding the efficiency of the system compared to a layered airspace. Using the Free Flight concept, aircraft will be able to select a cruise altitude suitable for the distance between the origin and the destination.
7. For high traffic densities, the efficiency is not expected to limit the capacity. Due to the separation of aircraft using height rules, the seventh hypothesis is that the Layers concept will have advantages regarding the safety and stability performance compared to the Free Flight concept.
8. The primary priority rules for the Layers concept are chosen, such that the cruising aircraft is solving the conflicts with climbing and descending aircraft. Due to the effect of a reduced relative velocity between cruising aircraft in a layered airspace, it is expected that cruising aircraft have less new conflicts due to conflict resolving than climbing/descending aircraft would have. When the secondary priority settings are used, it is hypothesized that this will result in more new conflicts due to conflict resolving, and therefore reduces the capacity of the airspace.
9. When considering the priority settings for the Free Flight concept, it is hypothesized that the primary settings will result in a slightly higher capacity limit than the secondary settings. The difference is the priority for conflicts that involve one cruising and one climbing descending aircraft; with the primary settings, the cruising aircraft solves the conflict, and with the secondary settings, both aircraft solve the conflict. When performing a resolution maneuver, aircraft have to search for conflicts in an additional volume. This additional volume is smaller for a cruising aircraft than for a climbing/descending aircraft, and therefore the expected number of conflicts is slightly lower for primary settings.

VI. Results

In this section, the results of the simulations are presented. This is done separately for the conflict probability model, in Section VI.A, and the effect of airspace design on capacity, in Section VI.B. In both

parts, the effect of the relevant independent variables on the dependent variables are discussed.

The theoretical models assume a homogeneous density distribution in the airspace. Therefore, first, the density distribution during the simulations is evaluated. An example for the Free Flight scenario with an instantaneous traffic count of 1331 aircraft is provided in Figure 10. An instantaneous traffic count of 1331 aircraft corresponds to a desired average density of $58 \text{ aircraft}/10,000 \text{ nm}^2$. This example is a good reflection of the findings for other concepts and traffic scenarios.

It can be observed that the traffic is not evenly distributed over the complete experiment area. Since the theoretical model uses the assumption of evenly distributed traffic, this affects the prediction capability of the model. This results in an increase of the k -values to compensate for the uneven distribution of traffic. In order to reduce the effect of the variation of density in the airspace, it is chosen to post-process the results and filter on the position of aircraft; only data generated by aircraft flying with a lateral and longitudinal position between -2 and 2 decimal degrees is used for the analysis of the results. This corresponds to a size of the experiment area of 240 nm by 240 nm .

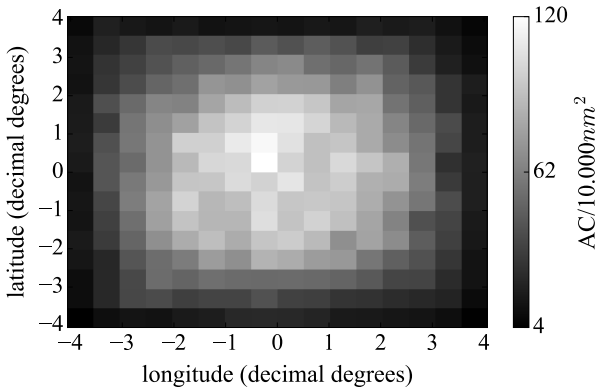


Figure 10. The average density distribution for the Free Flight concept, with 1331 instantaneous aircraft.

A. Validation of Conflict Probability Model

In Section III.B the theoretical relationship between the expected number of conflicts and number of aircraft has been discussed, and in this section the results of the simulations to validate the model are presented. To validate the conflict probability model, the number of instantaneous conflicts and the number of instantaneous aircraft of the simulations without conflict resolution have to be considered.

The simulation results are fitted to the conflict probability model in a least-square error sense to determine the value for k , the parameter used to match the simulation results and the model. An overview of the model parameters can be found in Table 6. The closer k is to a value of 1.0, the more accurate the model is in predicting the number of instantaneous conflicts. For a value greater than 1.0, the model is underestimating the number of conflicts. And for a value less than 1.0, the model is overestimating the number of conflicts. In Figure 11 an example of the model fitting is presented for the Free Flight concept, and in Figure 12 for the Layers 45 concept. This represents the method that is used to obtain the results in the following sections.

Table 6. Model parameters for the standard settings

Model Parameter	Value	Unit
d_{sep_h}	5.0	nm
d_{sep_v}	1000.0	ft
v	554.0	kts
t	300.0	s
A	$57.6e^3$	nm^2
V	$57.6 \cdot 10^3 \times 7,700$	$\text{nm}^2 \times \text{ft}$
γ	2.84	0
$ \gamma _{avg}$	0.39	0

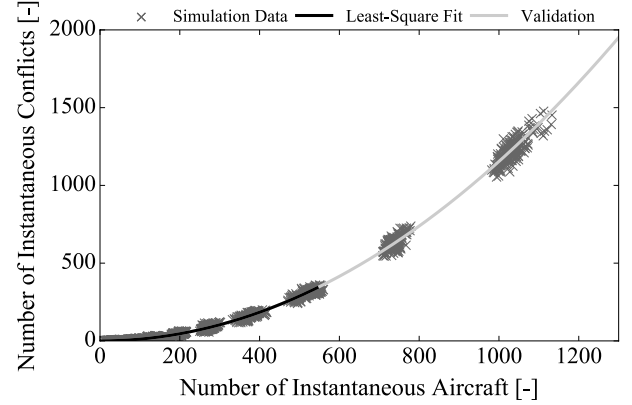


Figure 11. Free Flight: simulation results, least-square fit using Equation 21 (black line) and validation for higher densities (gray line).

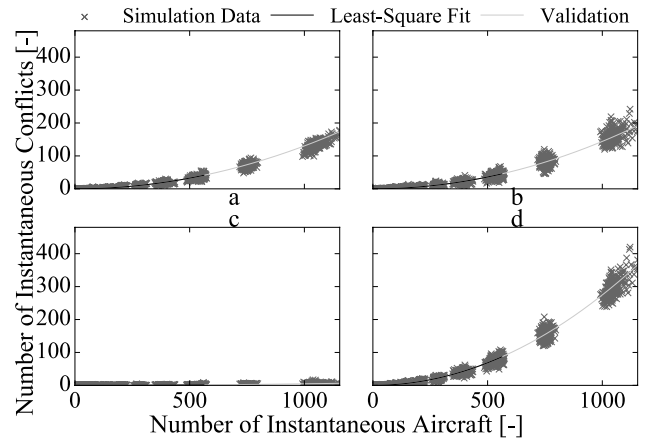


Figure 12. Layers 45: simulation results, least-square fit using Equation 23 (black line) and validation for higher densities (gray line). Subfigures a,b,c and d represents the cruising versus cruising, cruising versus C/D, C/D versus C/D and the total number of conflicts, respectively.

From Figure 11 and Figure 12, one can observe that the model can be fitted to the results at low number of instantaneous aircraft, indicated with the black line. This can be used to predict the number of conflicts at a high number of instantaneous aircraft, see the line indicated in gray. Despite a fixed inaccuracy of the model, the binomial random variable approach is a good predictor for the expected number of instantaneous conflicts. Comparable results are obtained for the other Layers concepts, which can be found in Appendix B of the report.

Next the results for the effect of a layered airspace on the conflict probability will be presented. After that, the effect of changes in vertical speed and the effect of variations in airspeed will be discussed.

1. Effect of a Layered Airspace on the Conflict Probability

Using the method described above, the simulation results have been fitted to the model by determining the k -values that fit the data in a least-square error sense. The k -values resulting from fitting the model to the simulation results are presented in Table 7, where k_1 , k_2 and k_3 are the constants used to match the theoretical model with the simulation results for the different conflict types of the Layers concept. Note that for the Free Flight concept and the Layers concepts a different model applies, as discussed in Section III.B. Using the model, the expected number of conflicts as a function of the instantaneous number of aircraft is visualized in Figure 13 for all concepts.

Table 7. Results of fitting the model to the simulation results.

	Free Flight	Layers 360	Layers 180	Layers 90	Layers 45
$k[-]$	1.03	-	-	-	-
$k_1[-]$	-	1.30	1.44	1.66	2.18
$k_2[-]$	-	1.77	1.73	1.45	1.23
$k_3[-]$	-	1.23	1.24	0.96	0.73

In order to fit the theoretical model with the simulation results, k -values significantly deviate from 1.0. This indicates that the model, without fitting it to simulation results, is not accurate in predicting the expected number of conflicts. For the cruising versus cruising conflicts and mixed (cruising versus climbing/descending) conflicts, the model shows an underestimation. For the climbing/descending versus climbing/descending conflicts, the model is overestimating the number of conflicts for the Layers 360 and Layers 180 concepts, and underestimating the number of conflicts for the Layers 90 and Layers 45 concepts. Also, for the prediction of conflicts between cruising aircraft, the model loses accuracy for a decrease in heading range per layer.

In Figure 13 significant differences can be observed in the number of conflicts between the different concepts. When splitting the total number of conflicts in the three classes as discussed in Section III.B, it becomes clear how the different concepts relate to each other; The cruising versus climbing/descending conflicts and climbing/descending versus climbing/descending conflicts show only a minor difference between the concepts. These results can be found in Appendix B. However, the cruising versus cruising conflicts reflect the significant difference between the concepts, as presented in Figure 14.

The expected number of conflicts for the Free Flight concept is greater than for the Layers 360 concept. The only difference is the a priori separation of cruising aircraft using altitude rules, which significantly influences the conflict probability.

When looking at the different layered airspace concepts, one can observe a decrease in the number of conflicts for a decrease in heading range per layer. This indicates that, even when climbing/descending

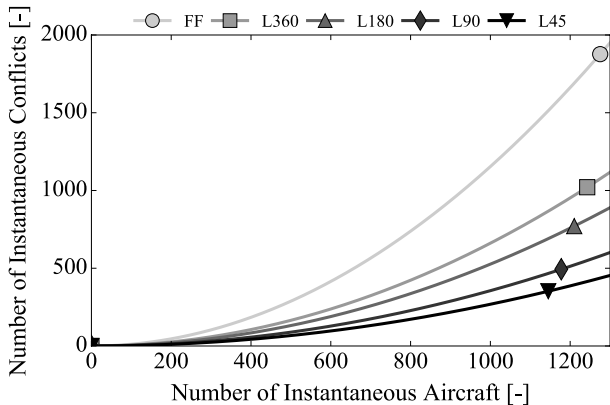


Figure 13. A comparison of the total number of conflicts for all concepts. The model are presented, that have been fitted to the simulation results with the k -values as described in Table 7.

aircraft are introduced, reducing the relative velocity between cruising aircraft using the layered airspace concepts, positively affects the conflict probability.

The deviation of the k -values that can be observed in Table 7, can partly be explained by the conflict detection method. The detection of conflicts in the conflict probability model is based on the t_{cpa} . When taking a closer look at the conflict detection module in BlueSky, t_{cpa} is actually not the direct criterium for a conflict; when t_{inconf} is less than the look-ahead time for the aircraft, a conflict is detected. Two aircraft can therefore be in conflict before the t_{cpa} is less than the look-ahead time. The difference is visualized in Figure 15. To assess the prediction capabilities of the model, filtering of the conflicts is applied in the post-processing; only conflicts with a t_{cpa} less than the look-ahead time are considered, since these can be predicted by the model. When performing a new model fit this results in k -values as presented in Table 8.

Table 8. Results of fitting the model to the simulation results: Conflicts are filtered based on t_{cpa} .

	Free Flight	Layers 360	Layers 180	Layers 90	Layers 45
$k[-]$	0.92	-	-	-	-
$k_1[-]$	-	1.15	1.21	1.23	1.35
$k_2[-]$	-	1.65	1.61	1.34	1.12
$k_3[-]$	-	1.05	1.09	0.82	0.64

Comparing the results before and after the filtering procedure, it can be observed that the underestimation reduced significantly. However, the model still lacks accuracy for a prediction of the number of conflicts. Therefore the following assumption is tested; the theoretical relationship between the heading band, α , and the conflict probability is a triangular probability density function for heading difference between two uniformly distributed headings [11], as explained in Section II.B. A triangular probability density function, for headings between 0 and α , indicates that the average conflict angle equals $\frac{1}{3}\alpha$. When computing the average conflict angle from the conflicts that occurred during the simulation, it is found that the results do not satisfy this assumption. This is tested before and after filtering the results on the experiment area. In Table 9 the measured average conflict angles are presented for the Layers concepts. When correcting α for these conflict angles, a new model fit is performed and the results of this fit are presented in Table 10.

From Table 10 it can be concluded that the model is able to predict the expected number of conflicts more accurately when all assumptions are met. This means that the criterium for a conflict is that t_{cpa} is less than the look-ahead time, and the headings are uniformly distributed within the heading range.

Concluding, when comparing Layers 360 and Free Flight, a priori separation of cruising aircraft in the vertical direction reduces the con-

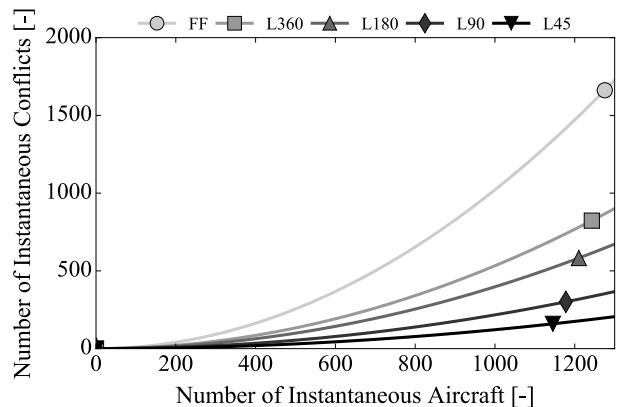


Figure 14. Overview of the conflicts between cruising aircraft, using the resulting least-square fit for all concepts.

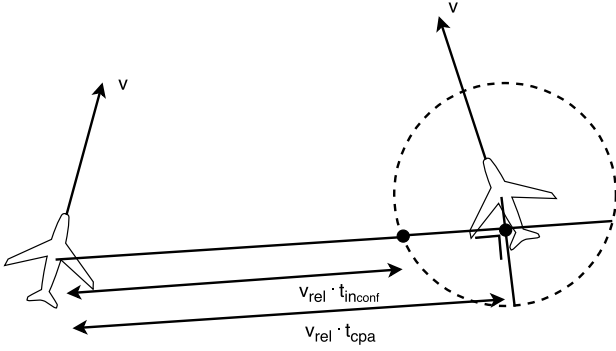


Figure 15. Visualization of difference between t_{inconf} , the first moment of intrusion, and the t_{cpa} , moment of most severe intrusion.

Table 9. Measured average conflict angle during the simulations.

	Average Conflict Angle [deg]
Layers 360	112
Layers 180	82
Layers 90	41
Layers 45	22

Table 10. Results of fitting the model to the simulation results: Conflicts are filtered based on t_{cpa} and α is corrected according to the measured average conflict angle.

	Layers 360	Layers 180	Layers 90	Layers 45
k_1 [-] (not corrected)	1.15	1.21	1.23	1.35
k_1 [-] (corrected)	1.15 ¹	0.99	0.93	0.93

¹ This angle is not corrected in the computation for the k-values, since the relative velocity effect is not present for the Layers 360 concept.

flict probability. And as expected, a reduced heading range per layer results in a reduced expected number of conflicts. It is found that the model performs better when a homogenous traffic distribution is used, and only conflicts with a t_{cpa} less than the look-ahead are considered.

2. Effect of Variation in Climb Angle

The effect of the climb angle is analyzed for the Free Flight and the Layers 45 concepts. The same traffic scenarios are used as for the simulations discussed in Section VI.A.1, but the flight path angle, γ , during climbing/descending phases of the flights is varied; simulations are performed with a γ of 2.8° and 1.4° .

Since the traffic scenarios do not change and the vertical speed of the aircraft does, the ratio of cruising/climbing/descending aircraft is affected. The model does take this into account.

First the results for the Free Flight concept are presented. The total number of instantaneous conflicts is compared with the standard simulations in Figure 16 and a new model fit is performed. The corresponding k-values can be found in Table 11.

Table 11. Free Flight: Effect of variation in climb angle on the conflict probability model.

	$\gamma = 2.8^\circ$	$\gamma = 1.4^\circ$
k [-]	0.92	1.07

A decrease in the vertical speed results in an increasing climb/descent time. The Free Flight concept has no direct benefit for aircraft flying at cruise altitude; the conflict probability is not affected by a priori separation rules. Therefore the effect of reducing the climb angles only affects the results minimally, as can be seen in Figure 16. Since the ratio between cruising/climbing/descending aircraft is affected by the change in vertical speed, the total number of conflicts increases. This can be explained by the larger volume searched for conflicts by aircraft, see Equation 21.

Next, the results for the change in vertical speed for the Layers 45 concept are presented. The results regarding total number of instantaneous conflicts are visualized in Figure 17 and the k-values to fit the model with the results are presented in Table 12.

For the Layers 45 concept, a reduction in the climb angle significantly affects the total number of conflicts. In contrast to the results for Free Flight, now it is possible to look at the model for each conflict type. From Table 12, a shift from overestimation to underestimation in the climbing/descending - climbing/descending conflicts can be found. When considering the number of conflicts, the largest change in number of conflicts is observed for the conflicts that involve a climb-

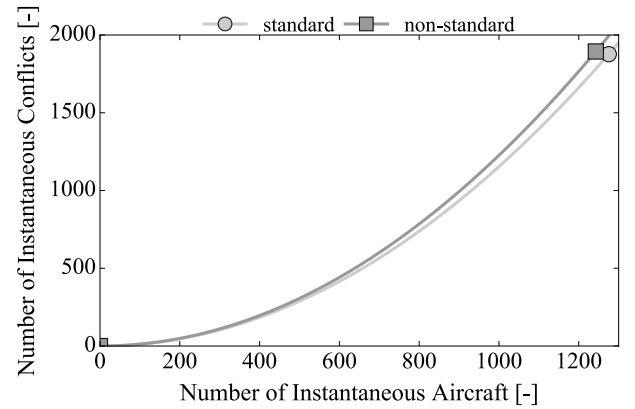


Figure 16. Free Flight: Effect of variation in climb angle on conflict probability. Here *standard* represents the simulations with a γ of 2.8° , and *non-standard* represents a γ of 1.4° .

Table 12. Layers 45: Effect of variation in climb angle on the conflict probability model.

	$\gamma = 2.8$ [deg]	$\gamma = 1.4$ [deg]
k_1 [-]	0.93	1.01
k_2 [-]	1.12	1.23
k_3 [-]	0.64	1.48

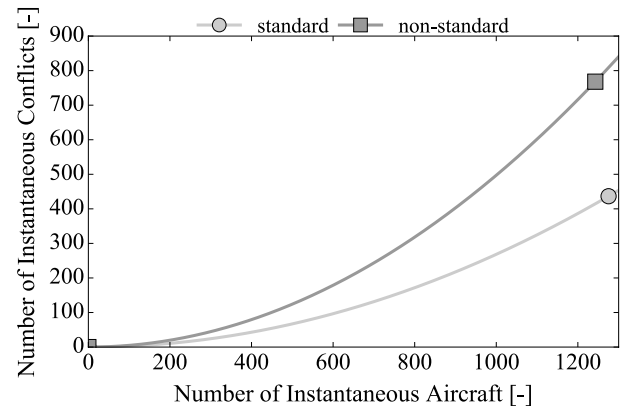


Figure 17. Layers 45: Effect of variation in climb angle on conflict probability. Here *standard* represents the simulations with a γ of 2.8° , and *non-standard* represents a γ of 1.4° .

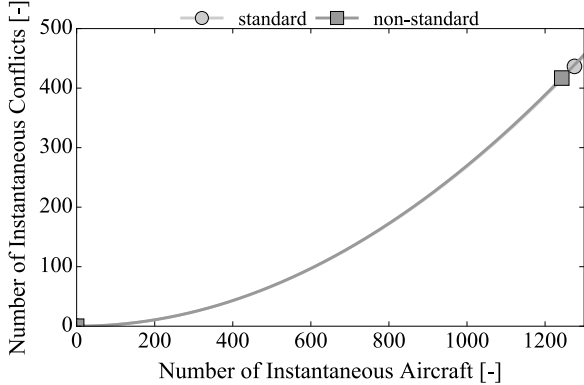


Figure 18. Layers 45: Effect of variation in true airspeed on conflict probability. Here *standard* represents the simulations with a constant true airspeed of 554 *kts*, and *non-standard* represents a uniformly distributed airspeed between 480 *kts* and 600 *kts*.

Table 13. Layers 45: Effect of variation in true airspeed.

	Constant Airspeed	Uniformly Distributed Airspeed
k_1 [-]	0.93	0.99
k_2 [-]	1.12	1.24
k_3 [-]	0.64	0.94

ing/descending aircraft. The biggest advantage of a layered airspace concept is that the conflict probability for cruising aircraft is reduced. By reducing the vertical speed, it takes longer for aircraft to reach their layer and profit from this reduced conflict probability. This explains the significant increase in the total number of conflicts.

3. Effect of Variation in Airspeed

The last sensitivity analysis that is performed regarding the conflict probability model is the effect of a uniformly distributed airspeed, instead of using a speed of 554 *knots* for all aircraft. For the uniformly distributed airspeed, the speeds are distributed between 480 *knots* and 600 *knots*. A comparison of the results of the simulations with a constant airspeed and the simulations with a variation in airspeed is presented in Figure 18. The k -values that result from fitting the simulation results and the model are presented in Table 13.

As can be observed, a variation in the speed distribution does not significantly influence the total number of conflicts. A small shift between conflict types is visible, but the total number of conflicts show very similar results. It can be concluded that, using a limited uniform speed distribution does not affect the conflict probability significantly.

B. Effect of Airspace Design on Capacity

In this section, the results regarding the effect of airspace design on capacity are presented. The different airspace concepts are discussed using the safety, stability and efficiency performance metrics as presented in Section IV. First, the results for the simulations using the standard settings are discussed. Secondly, the effect of the priority rules is assessed using a second set of simulations.

1. Effect of a Layered Airspace on the Capacity

Safety

The total number of conflicts and the total number of intrusions were found to be significantly lower when altitude rules were applied in the airspace, see Figure 19 and 20. Using a priori separation in the vertical direction has a larger positive influence on the conflict count than a uniform distribution in vertical direction of all traffic, which is used for Free Flight. It can also be observed that increasing the level of structure, by limiting the relative velocity per layer, has a positive effect on the conflict count.

Noticeable is the grouping of the Layers 360 and Layers 180 concepts and the Layers 90 and Layers 45 concepts. The grouping of the Layers 90 and Layers 45 concepts in Figure 19 and 20 can be explained by considering the effect of resolving conflicts on the results: the average conflict angle during simulations with conflict resolution shows a significant difference with simulations without conflict resolution. This is presented in Table 14. An increase in average conflict angle can be represented by an increasing heading range per layer. As predicted by the model described in Section II.B, an increase in heading range will result in an increase in number of conflicts.

The increase in average conflict angle can be observed for the Layers 90 and Layers 45 concepts. This can be explained by taking a closer look at the resolution maneuvers that aircraft perform to solve a conflict. In Table 15, the average heading change that would be required to solve a conflict at the first moment of detection is presented for the five airspace concepts. It can be observed that the average required heading change increases with a decrease in heading range per layer; conflicts with a lower conflict angle require a larger heading change to solve the conflict. An increased heading change to solve conflicts, results in new, secondary conflicts with a larger conflict angle.

In Figure 21 the results for the intrusion prevention rate are shown. This represents the ability of an airspace concept to solve conflicts, such that intrusions are avoided. It can be noted that the concepts show similar results; without conflict resolution an IPR of approximately 30% is realized. This means that if these conflicts would not be solved, they would not result in intrusions, and are false conflicts. This can partly be explained by the intended trajectory changes of aircraft. For example, a conflict between two cruising aircraft is solved since one of the aircraft starts descending towards the destination. Another reason

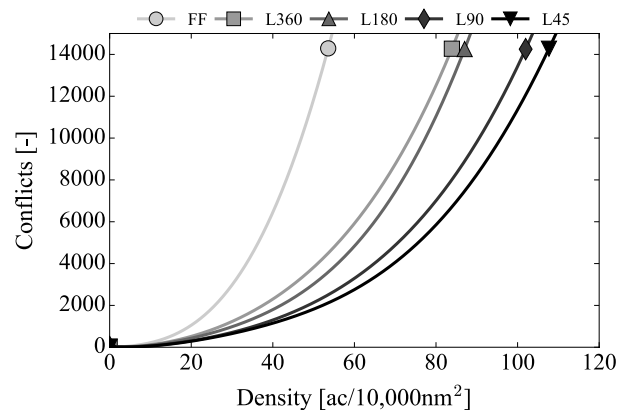


Figure 19. Overview of the total number of conflicts during the simulation time, with the conflict resolution module active.

Table 14. Measured average conflict angle during the simulations, with and without conflict resolution.

	Average Conflict Angle [deg]	
	without CR	with CR
Free Flight	112	115
Layers 360	112	116
Layers 180	82	84
Layers 90	41	57
Layers 45	22	48

Table 15. Average change in heading that would be required to solve the conflict at first moment of detection, for simulation with conflict resolution.

	Average Heading Change [deg]
Free Flight	1.8
Layers 360	2.4
Layers 180	3.1
Layers 90	4.3
Layers 45	5.0

for false conflicts is the variation in true airspeed for climbing and descending aircraft; the true airspeed changes during the climb/descent, and therefore can result in false conflict predictions. The IPR in case of conflict resolution varies between 95% and 98% for all concepts, meaning that almost all of the predicted intrusions are avoided. One can not observe a clear distinction between the IPR metric and the different limitations in heading band for the concepts.

Finally the safety can be assessed by looking at the intrusion severity. In Figure 22 the average severity of an intrusion can be found. It can be observed that the average intrusion severity greatly

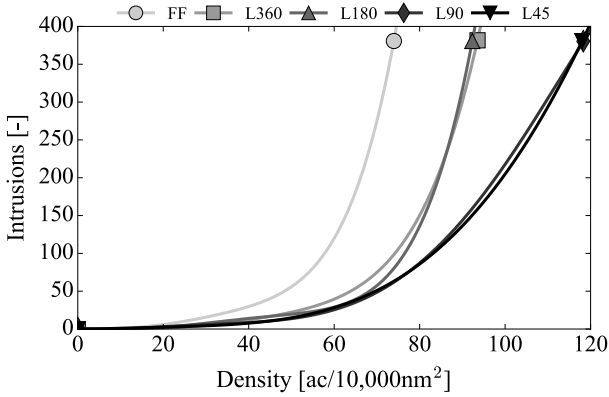


Figure 20. Overview of the total number of intrusions during the simulation time, with the conflict resolution module active.

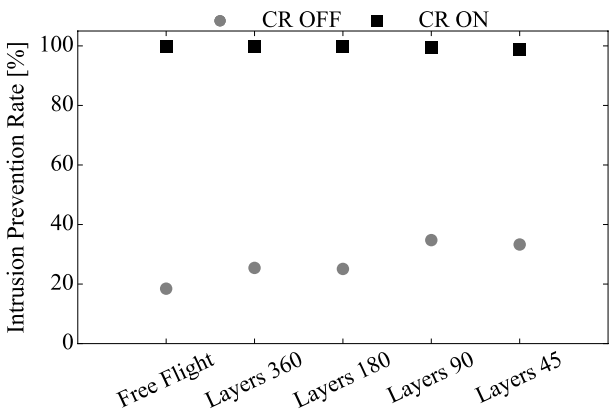


Figure 21. The average intrusion prevention rate for each concept.

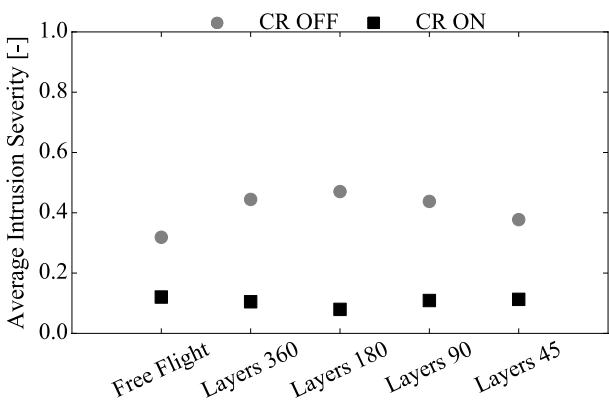


Figure 22. The average intrusion severity for each concept.

reduces when using conflict resolution maneuvers, as expected. When no conflict resolution is applied, the Free Flight concept has a lower average than the other concepts; the vertical traffic distribution in the Free Flight concept is not restricted by the layers altitudes. This results in a higher number of intrusions with a low severity. For the layered concepts, a slight decrease in average severity can be observed for a decrease in heading range per layer.

Stability

Using the domino effect parameter it is possible to assess the stability of the airspace concepts. The DEP is an indication for the stability by considering the increment (or decrement) in number of conflicts due to resolving conflicts. The theoretical model for the DEP is described in Section IV.B, and the model is fitted to the simulation results by selecting a ρ_{max} such that the model matches with the results, see Figure 23. The simulation results and the fitted model for all concepts can be found in Appendix B of the report. The results for all concepts are visualized in Figure 24 and an overview of the ρ_{max} per concept is presented in Table 16.

Table 16. The ρ_{max} values for all concepts.

	ρ_{max} [ac/10,000nm ²]
Free Flight	81
Layers 360	168
Layers 180	162
Layers 90	200
Layers 45	215

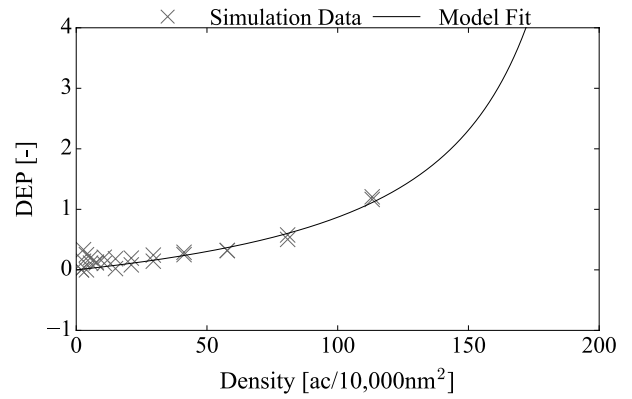


Figure 23. Simulation results and fitted model for the Layers 45 concept.

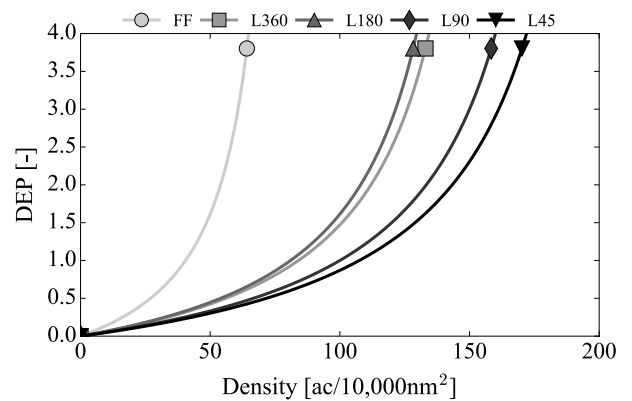


Figure 24. Comparison of the domino effect parameter.

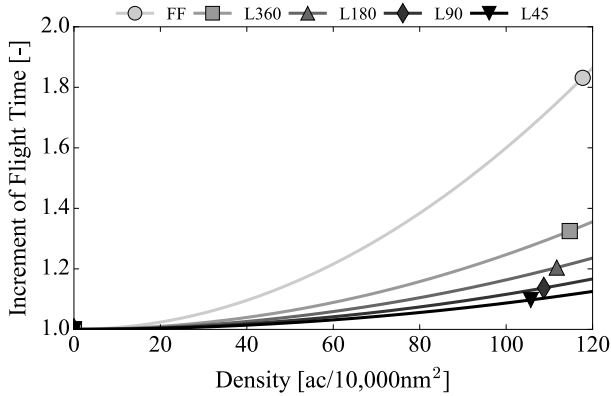


Figure 25. Increment in flight time of the scenarios with CR compared to without CR.

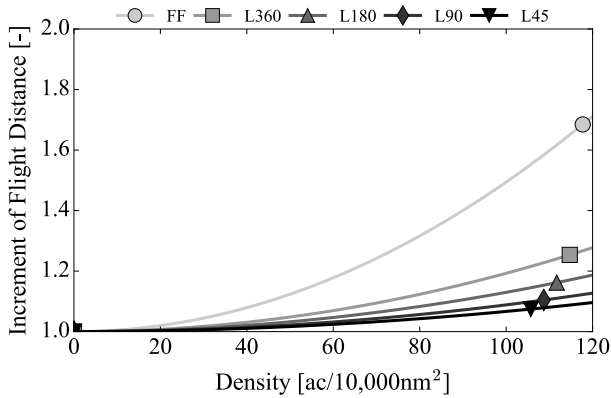


Figure 26. Increment in flight distance of the scenarios with CR compared to without CR.

It can be observed that the layered airspace concept have a significantly higher ρ_{max} than the Free Flight concept. Comparable to the safety assessment, a priori separation of cruising aircraft positively influences the performance on stability. Regarding the layered airspace concepts, the Layers 360 and Layers 180 show comparable results, as do the Layers 90 and Layers 45. This can be explained by looking at the average conflict angle during the simulations, see Table 14. The average conflict angle for the Layers 45 concepts increases significantly for the simulations with CR compared to without CR. Due to the violation of the height rules, an increase in number of conflicts can be observed. The average conflict angle of the Layer 45 concept increases more than for the Layers 90 concept, explaining why these concepts show a comparable DEP performance.

Efficiency

The third and final performance metric that is used to compare the capacity of the different concepts is efficiency. As explained in Section IV.C, a good method to assess the efficiency is to look at the average flight time and flight distance. The increase in time and distance due to conflict resolution is presented in Figure 25 and 26 respectively. Note that these results show the increment in time and distance for simulations with conflict resolution compared to simulations without conflict resolution for the same concept. A direct comparison between concepts is therefore not possible.

Both, flight time and flight distance show comparable results. The layered airspace concepts show a lower increment of time and distance due to conflict resolution than the Free Flight concept. This is expected, since the Free Flight concepts shows a significantly higher number of conflicts in Figure 19. When considering the layered airspace concepts, again a decrease in heading range per layers results in a reduced incre-

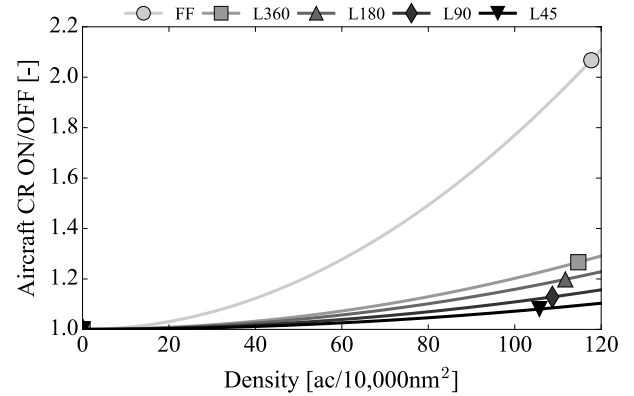


Figure 27. Number of aircraft in the simulation, presented as the ratio between the number of aircraft in the simulations with CR and without CR.

ment of flight time and distance.

Besides the flight time and flight distance, one can also look at the number of aircraft in the simulation. For the simulation without CR, a relatively constant number of aircraft is observed. The simulations with CR show an increase in traffic count for an increase in desired density. In Figure 27 the ratio of average number of aircraft in the simulation with CR over without CR is presented. The lower this ratio is, the better an airspace concept is able to process the flights.

The Free Flight concept shows the highest increase in traffic count. With a decrease in heading range per layer, a decrease in ratio can be observed. This means that with a decreasing heading range per layer, the airspace concept is performing better in processing the desired number of flights.

2. Effect of Priority Rules on the Results

A second set of simulations were performed to compare the effect of the priority rules on the results, using primary and secondary settings. The main difference is the priority between cruising and climbing/descending aircraft; the primary settings for the layered airspace, as well as the Free Flight airspace, prescribe that the cruising aircraft solves the conflict. For the Free Flight concept, the secondary settings prescribe that both aircraft solve the conflict, and for the Layers concepts, the climbing/descending aircraft solves the conflict. A complete overview of the priority settings can be found in Table 4 and 5. First, the results for Free Flight are presented. Secondly, the effect of new priority rules on the performance for the Layers 45 concept is discussed.

The performance of the Free Flight is assessed using the same performance parameters as in Section VI.B.1. For the Free Flight concept, the most noticeable difference in performance due to the new priority rules is observed in the domino effect parameter. This is presented in Figure 28. The other performance metrics show comparable results for both priority settings.

From Figure 28 it can be observed that the new priority rules have a reduced performance on stability. The difference is the priority between cruising versus climbing/descending aircraft. When the cruising aircraft solely solves the conflict, this results in a lower increment of new conflicts due to conflict resolving than when both aircraft solve the conflict together. This can be explained by looking at the volume searched for new conflicts; this is greater for a climbing/descending aircraft than for a cruising aircraft.

Finally, the results for the comparison of the Layers 45 simulations with different priority rules is discussed. The most noticeable differences can be observed in the domino effect parameter and the number of intrusions. In Figure 29 the performance on the domino effect parameter is presented and in Figure 30 the total number of intrusions is presented.

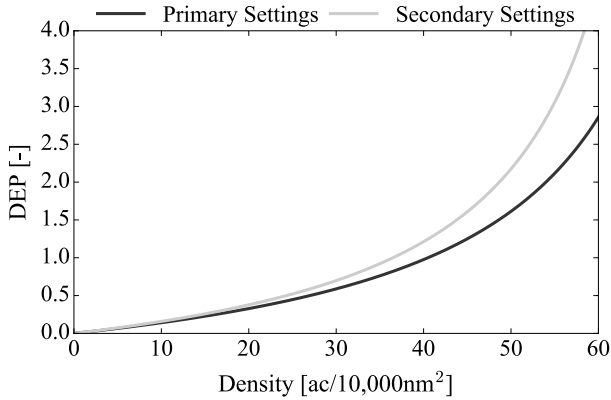


Figure 28. Free Flight: Effect of priority settings on the DEP. The values for ρ_{max} for the standard settings and the non-standard settings are 81 and 73 respectively.

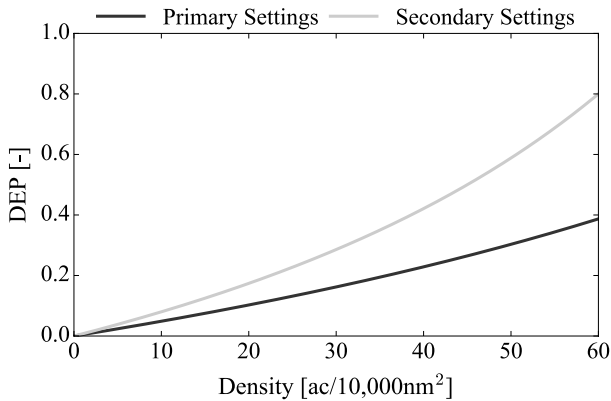


Figure 29. Layers 45: Effect of priority settings on the DEP. The values for ρ_{max} for the standard settings and the non-standard settings are 215 and 135 respectively.

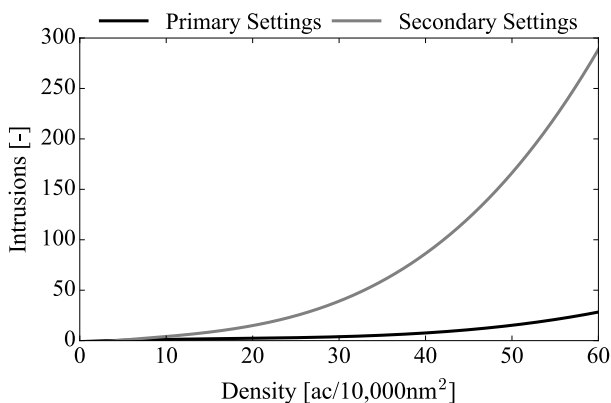


Figure 30. Layers 45: Effect of priority settings on the number of intrusions.

The secondary priority settings, where the climbing/descending aircraft solves the conflicts with cruising aircraft, show a significant decrease in ρ_{max} . It can be concluded that the secondary priority settings results in significantly more conflicts due to conflict resolving than the primary settings. This can be explained by the relative velocity component that is used in the conflict probability model and the area/volume searched for conflicts. The conflict probability for cruising aircraft in a

layered airspace is positively influenced by the design of the airspace. When a climbing/descending aircraft solves the conflict, one does not utilize the positive effect of a reduced conflict probability.

Besides a reduced performance on stability, a significant increase in the number of intrusions can be observed in Figure 30. This can be explained as follows; when a cruising aircraft solves the problem, new conflict with other cruising aircraft have a relatively low relative velocity due to the layered airspace design. However, when the climbing/descending aircraft solves the problem, new, short-term conflicts might occur with a large relative velocity. In fact, the combination of time and relative velocity results in significantly more intrusions. It can be concluded that the primary priority settings greatly improve the robustness of the system and the performance on safety, stability and efficiency.

VII. Discussion

The goal of this research is to describe and validate the theoretical relation between airspace parameters and the probability that aircraft encounter a conflict. Also, a quantitative comparison of the Free Flight and the Layers concepts is performed in terms of capacity, by assessing the impact of the heading range per flight level on safety, stability and efficiency metrics. Using large-scale, fast-time simulations five airspace concepts are compared; Free Flight and layered airspace concepts with heading ranges per layer of 360, 180, 90 and 45 degrees.

First, the validation of the conflict model is discussed in Section VII.A, and second, the effect of a layered airspace on capacity is discussed in Section VII.B. The discussion is based on the hypotheses that are presented in Section V.F. Finally, in Section VII.C, recommendations for future research are proposed.

A. Validation of Conflict Probability Model

The first hypothesis is that the number of conflicts between cruising aircraft will decrease significantly with a decrease in heading range per layer, as predicted by the theoretical model. This can be explained by looking at the different types of conflicts; only minor differences are observed between conflicts that involve climbing/descending aircraft. Since the traffic is distributed evenly in vertical direction over the airspace, an equal number of aircraft is climbing/descending through the airspace. Therefore the number of conflicts that involve a climbing/descending aircraft does not significantly vary with a variation in the layered airspace. However, when looking at conflicts between cruising aircraft, the reduction in conflicts due to a reduced relative velocity is clearly visible. In order to be able to use the model to accurately predict the expected number of conflicts, filtering of the conflicts was required. It was found that the theoretical model does not predict all the instantaneous conflicts that are observed in the simulation results. Types of conflicts that are not predicted by the model are conflicts with a t_{cpca} larger than the look-ahead time, but a t_{inconf} within the look-ahead time. The t_{inconf} is a direct criterion for conflicts in BlueSky. Although the model is not predicting all conflicts, a reduction in the number of conflicts between cruising aircraft is observed for a reduction in the heading range per layer. Therefore the first hypothesis is accepted.

Since the conflict probability relates to the climb angle by the volume searched for conflicts, it is hypothesized that the number of conflicts increases with a decrease in climb angle. For the Free Flight airspace, a slight increase in the number of conflicts is observed; when flying at a lower γ , more time is needed to climb to the desired cruise altitude. This increase in time increases the total airspace volume searched for conflicts. The Layers 45 concept shows a significant increase in number of conflicts; the benefits of a layered airspace, the *spreading effect* and *reduced relative velocity effect*, are only utilized by cruising aircraft. Since the flight path angle decreases, the climb/descent phase takes longer, and therefore reduces the cruising time. Since the k -values, used to match the model and the simulation results, do not vary significantly for a change in climb angle, the second hypothesis is accepted.

The last hypothesis regarding the validation of the conflict probability model is that the introduction of speed variations will not significantly affect the results for a three-dimensional airspace. This is

tested by introducing a uniformly distributed speed, instead of a constant speed for all aircraft. Changing the velocity settings from an equal speed for all aircraft of 500 kts, to a uniform distribution between 450 and 550 kts, did not significantly affect the results, and therefore, the third hypothesis is accepted.

Comparing the Free Flight and the Layers 360 concepts, the only difference is a discretization of the cruise altitude to the predefined layers. In the results, a clear trend is visible that a discrete separation of aircraft in the vertical direction positively influences the conflict probability. In a layered airspace, cruising aircraft in different layers do not get into conflict with each other; the predefined separation reduces the total number of conflict pairs, as well as the volume searched. For conflicts between cruising aircraft, the vertical aspect is removed from the conflict probability. This is not the case for Free Flight, where cruising aircraft can get into a conflict with all other cruising aircraft.

The model does not predict the number of conflicts with full accuracy, but with an over- or underestimation. As yet can be observed in the density distribution of the simulations, it is not fully heterogeneous. This can partly be solved by selecting a smaller area, but cannot be avoided completely. A second effect that could cause the over- or underestimation is the average conflict angle that is observed in the simulation results; the derivation of the theoretical model for the conflict probability assumes that the average conflict angle is $\frac{1}{3}\alpha$, based on the triangular probability density function for two uniformly distributed headings [11]. However, in the results of the simulations, it is observed that the average conflict angle is larger. Since this is observed before and after filtering the results on a smaller experiment area, this could be a side effect of the simulation design; the size of the square shape of the experiment area, in combination with the requirements on the flight distance might have biased the heterogeneous distribution of the headings between the origins and destinations. This could be solved by designing a larger experiment area, but this would also stress the limits of the simulation software. Also, the layers with a relatively high altitude have less cruising time compared to the lower layers, due to the different climbing times. This results in a different number of instantaneously cruising aircraft between layers, where the model is using the average. This also contributes to a uneven distribution of traffic.

B. Effect of Airspace Design on Capacity

The fourth hypothesis describes the expected effect of a layered airspace on the capacity; the stability performance is hypothesized to improve with reducing the heading range per layer and to be the metric limiting the capacity. However, considering the results for all performance metrics, the safety shows the steepest trend in loss of performance and limits the capacity. This indicates that the fourth hypothesis is false, however, for a complete conclusion the efficiency metric should be reconsidered, see Section VII.C. The three performance metrics with respect to the fourth hypothesis will be discussed next.

For the total number of conflicts, a decreasing trend for a decrease in heading range can be observed. However, the total number of intrusions does not show the same trend. It can clearly be observed that the Layers 45 and Layers 90 show comparable results, despite the different heading range, as well as the Layers 360 and Layers 180 concepts.

When assessing the stability, again the grouping of the Layers 90 and Layers 45 concepts, and the Layers 360 and Layers 180 concepts is visible. The grouping of the result can be explained by looking at the average conflict angle; the average conflict angles for the Layers 90 and Layers 45 concepts are comparable, as well as for the Layers 360 and Layers 180 concepts. When performing conflict resolution at layered concepts with a small heading range (like the 45 degrees), one easily violates the layer rules during the CR maneuver. This results in more conflicts due to the higher relative velocity, resulting in more maneuvers.

Also, by analyzing the resolution maneuver, it is observed that the average required heading change to solve a conflict, increases with a decrease in heading range per layer; in order to solve conflicts using heading changes between aircraft with a small relative velocity, requires resolution maneuvers with a relatively large heading change. This could be improved by implementing an adjusted CR strategy, as will be discussed in Section VII.C.

The last performance metric is the efficiency. The results for the flight distance and time show a clear improved performance trend for

a decrease in heading range. Combining all performance metrics, the efficiency does not seem to limit the capacity at traffic densities that are simulated.

At low densities, an increase in heading range per layer was hypothesized to positively influence the efficiency of the system, since aircraft will be able to select an optimal cruise altitude for their flight distance. Over the complete range of densities, implementing a layered airspace structure and a reduced heading range per layer positively influence the performance in flight time and distance. Work done can not be considered, and therefore the effect of selecting a more preferred cruise altitude for fuel efficiency is not visible in the results. While the results regarding flight time and distance do not support the fifth hypothesis, it is not possible to reject it due to the failed measurement of the work done.

For the sixth hypothesis, it is expected that the Free Flight concept shows a better efficiency at low traffic densities than a layered airspace concept. Again, the flight time and flight distance are the measurements used for efficiency during this research, instead of the work done. The average flight time and distance show an decreased efficiency for Free Flight compared to a layered airspace, but it is not possible to reject the sixth hypothesis due to the failed measurement of the work done.

For high traffic densities, the seventh hypothesis is that the Layers concept will have advantages regarding the safety and stability performance compared to the Free Flight concept. All the metrics indicate the same trend; a priori separation of traffic using height rules positively influences the performance compared to the Free Flight concept. The explanation starts with the number of conflicts. Comparing the Layers concepts and Free Flight, a significant reduction is observed for the Layers concepts. When less conflicts occur, less conflict resolution maneuvers are required. This directly affects the stability and efficiency; less conflict resolution means a smaller volume searched for new conflicts and a smaller flight distance and time. The seventh hypothesis can therefore be accepted.

The eighth hypothesis discusses the effect of the priority rules on the capacity for the Layers concept. The influence of the priority settings is clearly visible when comparing the simulations with different settings: for the Layers concepts, a great decrease of performance is visible when the climbing/descending aircraft solves the conflicts with cruising aircraft, instead of the cruising aircraft. The primary settings, where the cruising aircraft solves the conflicts, utilizes the benefits of a reduced conflict probability and thereby improves the robustness of the system. The eighth hypothesis is accepted.

The last hypothesis, regarding the Free Flight concept, is that the primary priority rules result in a higher capacity than the secondary rules. The difference in results is best visible when looking at the Domino Effect Parameter; a clear decrease in ρ_{max} is visible for the secondary settings, compared to the primary settings. Therefore, including the rule that cruising aircraft solve the conflicts with climbing/descending aircraft has a positive influence on the capacity, and the last hypothesis is accepted.

For both the Free Flight and the Layers concepts, an increase in capacity is visible when cruising aircraft solve conflicts with climbing/descending aircraft. In a real life operational situation, this might feel counter-intuitive for the pilots; when an aircraft is cruising towards its destination, it has to deviate from its course to solve conflicts and create space for climbing/descending aircraft. Where this might seem unfair for the cruising aircraft, the total system achieves an increased capacity. To conclude, cruising aircraft have to perform resolution maneuvers to create space for climbing/descending aircraft, but will get the favor returned when they have to climb/descent.

C. Recommendations for Future Research

Theoretical Model

The theoretical model for conflict probability is based on t_{cpa} locations. Types of conflicts that are not modeled are conflicts with a t_{cpa} greater than the look-ahead time, but t_{inconf} less than the look-ahead time. For practical applications, using the t_{inconf} for conflict detection makes most sense; the first moment of conflict should already be avoided (t_{inconf}), instead of the most severe intrusion (t_{cpa}). Also, conflicts with a negative t_{cpa} , which are still intrusions, are counted as conflict in BlueSky, but not accounted for in the model. This could, for example, be solved by adding an

extra term to the conflict probability model, or considering a larger area searched for conflicts. Future research could extend the conflict probability model in order to predict these type of conflicts as well.

Effect of Height Errors on Conflict Probability and Airspace Capacity

As suggested in the research by Ford [9], the ability of aircraft to fly at a specific altitude, and the height-keeping errors that arise from a number of sources, could affect the number of conflicts in the vertical plane. While the simulations for this research assume that aircraft can fly precisely at the selected altitude, this does not have to be the case in the real world. In the design of the Layers concepts, the layers are separated by the vertical separation criterium plus an extra margin of 100 ft. However, since no height-keeping errors are simulated, it is unknown what the effect of such errors is on the conflict probability and airspace capacity. When the height-keeping errors frequently introduce conflicts between aircraft in different layers, this could significantly affect the conflict probability and airspace capacity. Future research could include these errors, and analyze the effect using different height-keeping performance models and different altitude margins between layers.

Implementation of Conflict Resolution

When performing conflict resolution at layers concepts with a small heading range (like the 45 degrees), one easily violates the layer rules during the CR maneuver. Besides, the results show that the average heading change to solve conflicts increases for these concepts. Both effects result in more conflicts due to the higher relative velocity, resulting in more maneuvers and a snow-ball effect. A recommendation is to analyse the effect of the implementation of the MVP Conflict Resolution method in combination with obeying the layer rules. Options for a different implementation could be; limit the heading change of cruising aircraft during a resolution maneuver, or initiate an altitude change to a layer that corresponds to the heading of the resolution maneuver, or prioritize speed changes for the resolution maneuver.

In general, increasing the look-ahead time, and thereby detecting conflicts in an earlier stage, results in less severe heading changes during the CR maneuver. However, the experiment area is designed, such that the climb/descent phase is shorter than the look-ahead time. Therefore, it is expected that increasing the look-ahead time for the same simulation will not affect the average conflict angle for cruising versus climbing/descending conflicts.

Effect of Simulation Experiment Design

In the simulations used for this research, layers with a high altitude have less cruising time than layers with a low altitude. This is due to the different climbing and descending times, which are not taken into account in the scenario generation. This results in a different number of instantaneously cruising aircraft between layers, where the conflict probability model is using the average. Therefore effect on fitting the simulation results with the model might not be significant. However, for the capacity analysis the influence might be significant, since the lower part of the airspace might get saturated before the upper part of the airspace does. For future research, this can be taken into account when designing the simulations.

Conflict Prevention

The conflict prevention module that is implemented in BlueSky has a limited functionality; only for aircraft that are cruising and intend to start climbing/descending use the conflict prevention module. This could be extended and used for all aircraft that want to change their state, including conflict resolving in the horizontal plane. The conflict prevention module could influence the effect of conflict resolving, and thereby affect all performance metrics. Also, using intent in the conflict detection could significantly reduce the number of false conflicts; when aircraft are planning on changing their state, for example leveling of from climb to cruise or starting a descent to their destination, before the conflict would occur, this could be ignored in the conflict detection.

Measuring Work Done

One of the limitations of this research is the failed measurement of the *work done* by aircraft. The results could be biased towards the less fuel efficient airspace concepts, since the flight time and distance are considered as alternative. A recommendation for future research is to correct the measurement of the work done by aircraft, in order to get a better understanding of the influence of a layered airspace on the efficiency.

VIII. Conclusion

This work investigated the effect of a layered airspace on conflict probability and capacity. First, the conflict probability model is extended for application in a three-dimensional airspace and fast-time simulations are used to validate the theoretical relations. The following conclusions can be drawn regarding the conflict probability model:

- The results regarding the validation of the conflict probability model show that the model can be used to predict the instantaneous number of conflicts. Especially when fitting the model to the simulation results at low densities, it can be used to accurately predict the number of conflicts, for the same type of scenarios, at high density.
- A reduction in conflicts between cruising aircraft, as a result of a reduction in heading range per layer, is clearly visible in the simulation results. The *sorting effect* results in a significant reduction in the number of conflicts between cruising aircraft. Only minor differences are observed between the different airspace concept for conflicts that involve climbing/descending aircraft.
- Two additional analyses have been performed; first, the conflict probability model can be used to predict the effect of a change in climb/descent angle of aircraft. Second, introducing uniformly distributed speeds, instead of a constant true airspeed for all aircraft, does not significantly influence the results regarding the conflict probability model.

Moreover, fast-time simulations have been performed to assess the impact of the heading range per layer on the safety, stability and efficiency metrics. The analysis of the effect of a layered airspace on capacity results in the following conclusions:

- The safety metric, assessed using the total number of conflicts and intrusions, shows the steepest trend in loss of performance. The results show a clear improvement in performance for a decreasing heading range in terms of safety.
- When comparing the Free Flight and Layers 360 airspace concepts, using the three metrics safety, stability and efficiency, the Layers 360 concept shows a clear increase in capacity. The only difference with the Free Flight concept is a discretization of the cruise altitudes using the predefined layers. It can be concluded that a priori separation of traffic using height rules positively influences the performance compared to the Free Flight concept.
- By comparing simulations with different sets of priority rules, it can be concluded that cruising versus climbing/descending conflicts can best be solved by the cruising aircraft. When cruising aircraft solve the conflict, the complete ATM system shows an improved performance on safety, stability and efficiency. This holds for the layered airspace, as well as for the Free Flight concept.

References

- [1] SESAR Consortium, "SESAR Concept of Operations," Tech. rep., SESAR Consortium, July 2007.
- [2] NextGen Joint Planning and Development Office, "Concept of Operations for the Next Generation Air Transportation System," Tech. rep., Federal Aviation Administration, June 2007.
- [3] Hoekstra, J. M., Ruigrok, R. C. J., and Van Gent, R., "Free flight in a crowded airspace?" *Progress in Astronautics and Aeronautics*, Vol. 193, 2000, pp. 9.

- [4] Bilimoria, K. D. and Lee, H. Q., "Properties of Air Traffic Conflicts for Free and Structured Routing," *AIAA Guidance, Navigation, and Control Conference and Exhibit*, Aug. 2001.
- [5] Krozel, J., Peters, M., Bilimoria, K. D., Lee, C., and Mitchell, J. S., "System performance characteristics of centralized and decentralized air traffic separation strategies," *Fourth USA/Europe air traffic management research and development seminar*, 2001.
- [6] Hoekstra, J. M., van Gent, R. N., and Ruigrok, R. C., "Designing for safety: the 'free flight' air traffic management concept," *Reliability Engineering & System Safety*, Vol. 75, No. 2, 2002, pp. 18.
- [7] Sunil, E., Hoekstra, J., Ellerbroek, J., Bussink, F., Nieuwenhuisen, D., Vidosavljevic, A., and Kern, S., "Metropolis: Relating Airspace Structure and Capacity for Extreme Traffic Densities," *ATM seminar 2015, 11th USA/EUROPE Air Traffic Management R&D Seminar*, 2015.
- [8] RTCA Inc., "Final report of the RTCA task force 3: Free Flight Implementation," Tech. rep., Radio Technical Commission for Aeronautics, Washington DC, Oct. 1995.
- [9] Ford, R. L., "On the use of height rules in off-route airspace," *Journal of Navigation*, Vol. 36, No. 02, 1983, pp. 269–287.
- [10] Jardin, M. R., "Analytical relationships between conflict counts and air-traffic density," *Journal of Guidance, Control, and Dynamics*, Vol. 28, No. 6, 2005, pp. 1150–1156.
- [11] Hoekstra, J. M., Maas, J., Tra, M., and Sunil, E., "How do layered airspace design parameters affect airspace capacity and safety?" *7th International Conference on Research in Air Transportation*, Philadelphia, 2016.
- [12] Leiden, K., Peters, S., and Quesada, S., "Flight level-based dynamic airspace configuration," *Proceedings of the 9th AIAA Aviation Technology, Integration and Operations (ATIO) Forum. American Institute of Aeronautics and Astronautics*, 2009.
- [13] Irvine, R. and Shaw, C., "Layers of parallel tracks: a speculative approach to the prevention of crossing conflicts between cruising aircraft," Sept. 2004.
- [14] Irvine, R. and Hering, H., "Towards Systematic Air Traffic Management in a Regular Lattice," *7th AIAA ATIO Conf, 2nd CEIAT Int'l Conf on Innov and Integr in Aero Sciences, 17th LTA Systems Tech Conf; followed by 2nd TEOS Forum*, 2007, p. 7780.
- [15] Paielli, R. A., "A Linear Altitude Rule for Safer and More Efficient En-route Air Traffic," *Air Traffic Control Quarterly*, Vol. Vol. 8, 2000.
- [16] Bilimoria, K. D., Sheth, K. S., Lee, H. Q., and Grabbe, S. R., "Performance evaluation of airborne separation assurance for free flight," *Air Traffic Control Quarterly*, Vol. 11, No. 2, 2000, pp. 85–102.
- [17] "ProfHoekstra/bluesky," <https://github.com/ProfHoekstra/bluesky>, Accessed: 2015-11-29.
- [18] Bussink, F., Hoekstra, J. M., and Heesbeen, B., "Traffic Manager: A Flexible Desktop Simulation Tool Enabling Future ATM Research," *24th Digital Avionics Systems Conference*, Washington DC, Oct. 2005.
- [19] Nolan, M. S., *Fundamentals of Air Traffic Control*, Wadsworth Publishing Company, Belmont, California, second edition ed., 1994.
- [20] Maas, J., "A Quantitative Comparison of Conflict Resolution Strategies for Free Flight," MSc Thesis, Faculty of Aerospace Engineering, Delft University of Technology, June 2015.
- [21] Eurocontrol, "High-Density 2015 European Traffic Distributions for Simulation," March 2000.

Part II

Preliminary Thesis Report

Chapter 1

Introduction

Since the early days of aviation, all over the world, a highly centralized Air Traffic Management (ATM) system has been used to control aircraft. The foundations for this system originate in the United States; due to the rapid growth of air traffic in the 1920's, the United States Department of Commerce started to regulate the use of airways in 1926 [11].

The first Airway Traffic Controls Units (ATCU) were developed by the major airlines operating in the U.S. airspace in 1935 to control en-route traffic using radio communications. A few years later the U.S. federal government acquired these units and implemented standardized Air Traffic Control (ATC) procedures, forming the basis for the current ATM system [11]. Since then, the basic components of en-route ATC have not changed, and consist of air routes that are defined by ground-based navigational aids in the horizontal plane and flight levels in the vertical plane, as well as Air Traffic Controllers (ATCo) who are responsible for the separation between aircraft [12].

The tasks of ground controllers include the services of providing safe and efficient flight, sometimes extended with the task of reducing noise and emissions [13, 14]. In order to structure the areas for which controllers are responsible, the airspace is divided into a number of Flight Information Regions (FIR), each with its own ATC. A FIR can be subdivided into sections, each with its own ATCo, used to limit the number of aircraft under the supervision of the controllers. In Figure 1-1 an example airspace structure of en-route airspace in Europe is presented, in which the highly organized system is clearly visible.

1-1 Air Traffic Demand vs. Capacity

One of the most important issues for the current ATM system is the limited capacity due to the limits on the controllers' workload, and their ability to deal with the complex situations that occur under their supervision [15]. Airspace structure and other procedural elements are important factors in reducing the complexity for the controller. Standardizing the flow patterns, as for the current ATM system, helps controllers by reducing overall complexity as well as reducing the perceived workload [16]. As presented by the long term forecast of

Eurocontrol, the European organization for the safety of air navigation, in Figure 1-2, it is expected that the European air traffic demand will increase between 10% and 170% over the next 35 years [2].

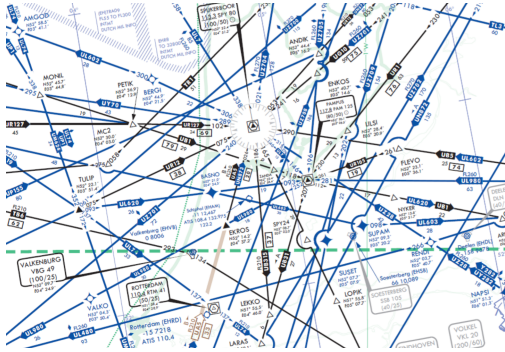


Figure 1-1: Example of the highly structured airways in the current ATM system [1]

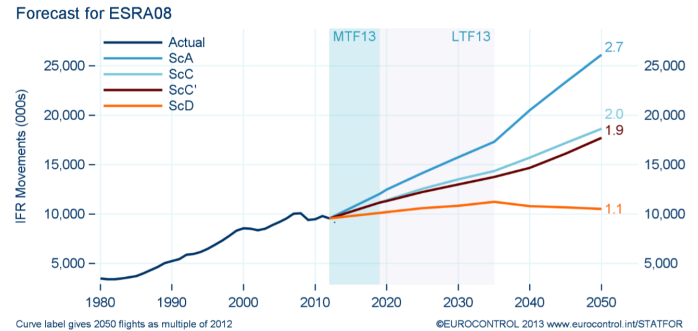


Figure 1-2: Long Term ATM Forecast by Eurocontrol [2]

In general there are two options to deal with the increasing demand; by improving the current ATM system or by introducing a fundamentally new system. The first option, to improve the current, centralized ATM system, is focussed on reducing the controllers' workload in order to increase the airspace capacity. Two important research projects with the goal of dealing with the increasing demand in the current ATM system are the Single European Sky ATM Research (SESAR) project and NextGen, organized by the European Union and the United States, respectively. As stated by the European Commission [17], other constraints that limit the capacity are caused by:

- On average, flights within the European airspace are 49 km longer than they would be when flying a direct (great-circle) route.
- En-route delays, that already have been reduced to 0.5 minute per flight
- Fragmentation of airspace, with 16 different control centers within Europe

Some improvement of the centralized system can be gained by developing automation tools to assist controllers or restructuring the airspace sectors [18]. Regardless, the centralized ATM system is approaching its saturation level [19, 20].

Since the ATCo workload is found to be the main bottleneck for increasing capacity, the second option to improve capacity is by implementing a distributed ATM system; the traffic separation responsibility is moved from the ATCo to the individual aircraft. This will be elaborated on in section 1-2.

1-2 Distributed Air Traffic Management

Introducing a fundamentally new airspace structure and moving the separation task to the cockpit, also referred to as a distributed system, has become an important topic of research for

substantially increasing the airspace capacity [6, 21, 4, 22]. A distributed system may require innovative safety management techniques due to the new dimension in conflict handling. But when the equipment in the cockpit is equally reliable as the equipment on the ground, a distributed system could potentially increase safety and efficiency, and thereby increase airspace capacity by several orders of magnitude compared to the current ATM system [6].

Most research performed on new airspace concepts is of a qualitative nature, especially when an attempt is made to compare different concepts. The Metropolis project [3] is one of the first research projects to distinguish qualitative differences between multiple airspace concepts. The results of the research show that a distribution of traffic over the complete airspace is the key in dealing with extremely high traffic densities and minimizing the occurrence of conflicts, see Figure 1-3. The two concepts that show the most promising results are the Full Mix and Layers concept.

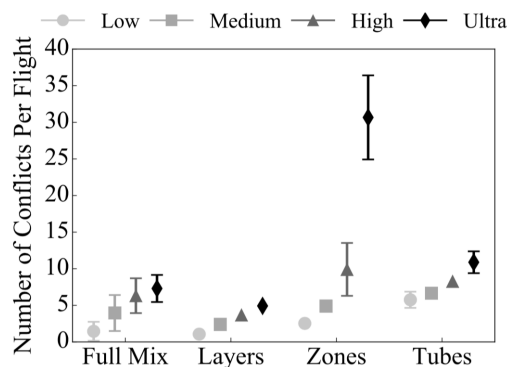


Figure 1-3: Number of conflicts (with conflict resolution) for different airspace concepts and traffic demand levels [3]

In the Full Mix airspace concept, aircraft can determine their own flight path with four degrees of freedom; there are no constraints on longitudinal, lateral or vertical position and speed. Due to the lack of constraints, this concept is often also referred to as Free Flight. The original concept for Free Flight is described in the report of the RTCA Free Flight Task Force [23].

The Layers concept applies predefined vertical airspace segmentation to influence conflict probability, while keeping the airspace structure relatively flexible. Segmentation of the airspace in altitude bands is used to limit the freedom in vertical flight path of aircraft, while the other degrees of freedom remain available. The resulting airspace consists of layers, as visualized in Figure 1-4, with a specific heading range for each layer. Due to the limited heading range, the relative velocity between aircraft will be reduced and this is expected to positively influence the safety and stability of the airspace [24], while the effect on efficiency is kept to a minimum, as can be seen in Figure 1-5 and Figure 1-6.

While the Metropolis results indicate that implementing a layered structure can improve capacity compared to Full Mix, the extent of the capacity benefit is unknown [3]. Furthermore, the influence of the heading range per altitude and the corresponding performance for Layers also needs to be determined. Therefore, in this thesis, the performance of the Layers and Full Mix concepts will be questioned on a quantitative level, using a systematic variation in the heading range per flight level.

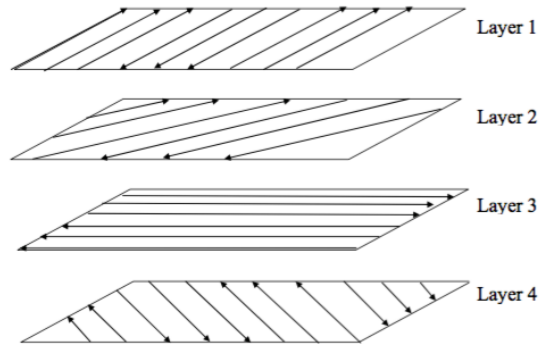


Figure 1-4: A layered airspace concept: using altitude rules as a priori separation method

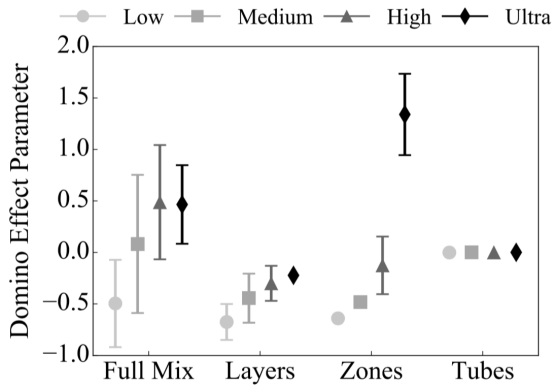


Figure 1-5: Domino Effect Parameter (DEP) for different airspace concepts and traffic demand levels; The DEP is inversely related to the stability of a system [4, 3]

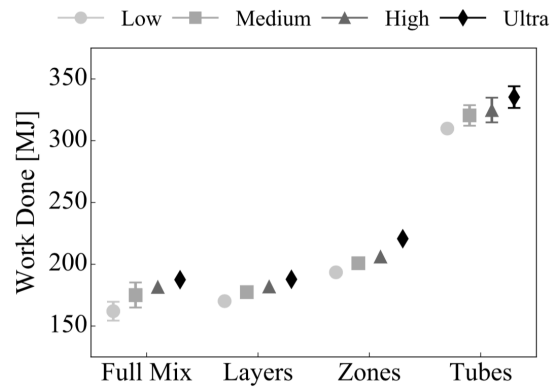


Figure 1-6: Effect of traffic demand on system efficiency for different airspace concepts; The efficiency is measured through the average work done to complete a flight [3]

1-3 Thesis Objective and Research Questions

The main objective of this research is to quantitatively compare the Full Mix and the Layers concepts in terms of capacity, by assessing the impact of the heading range per altitude on safety, stability and efficiency metrics using large-scale simulation experiments.

The following research question, with a set of sub-questions, has been defined to complete the research objective:

What is the effect of the Layers concept, considering different heading ranges per flight level, on capacity compared with the Full Mix concept?

1. How are different limitations in heading range per flight level affecting the safety and stability for the Layers concept?
2. Using large-scale simulation experiments, what is the limiting metric for the Layers concept, with different heading ranges per flight level: safety, stability or efficiency?

3. What is the relation between the heading range per flight level and capacity, considering the Full Mix and the Layers concepts?
4. What are the advantages of the Layers concept, compared to the Full Mix concept on a quantitative level?

The research scope of this thesis will be limited using the following assumptions:

- Only en-route airspace will be considered
- Random, heterogeneous traffic patterns will be used for the simulations
- Simulated aircraft will be of the same type using the same performance limits
- Atmospheric influences, for example wind, are not considered during the simulations

1-4 Research Approach

To answer the research questions presented in section 1-3, the thesis is split in two phases, the preliminary thesis and the main thesis. In Figure 1-7 a roadmap is presented in which five steps can be distinguished.

The first step includes the literature review. This literature review will focus on the different airspace structure concepts that will be investigated and the theoretical method to relate airspace structure to capacity. An overview of the different steps to relate the airspace concept parameters to capacity is presented in Figure 1-8. The airspace capacity is evaluated using three metrics: by assessing the safety and stability through conflict probability and by assessing the efficiency using the work done by aircraft to complete their flight.

The following questions will be answered during the literature review:

1. How can airspace capacity be described as a function of conflict probability, using safety and stability metrics?
 - (a) What is the definition of conflict probability?
 - (b) How does Conflict Detection & Resolution (CD&R) influence the conflict probability?
 - (c) How can the conflict probability be derived from experiments for different airspace concepts?
 - Are random variable models suitable for modeling the conflict probability?
 - What random variable models can be used to obtain the conflict probability from experiments?
 - How can random variable models be used to describe the relation between the number of instantaneous conflicts and airspace density?
2. How can airspace capacity be assessed using the efficiency metric?

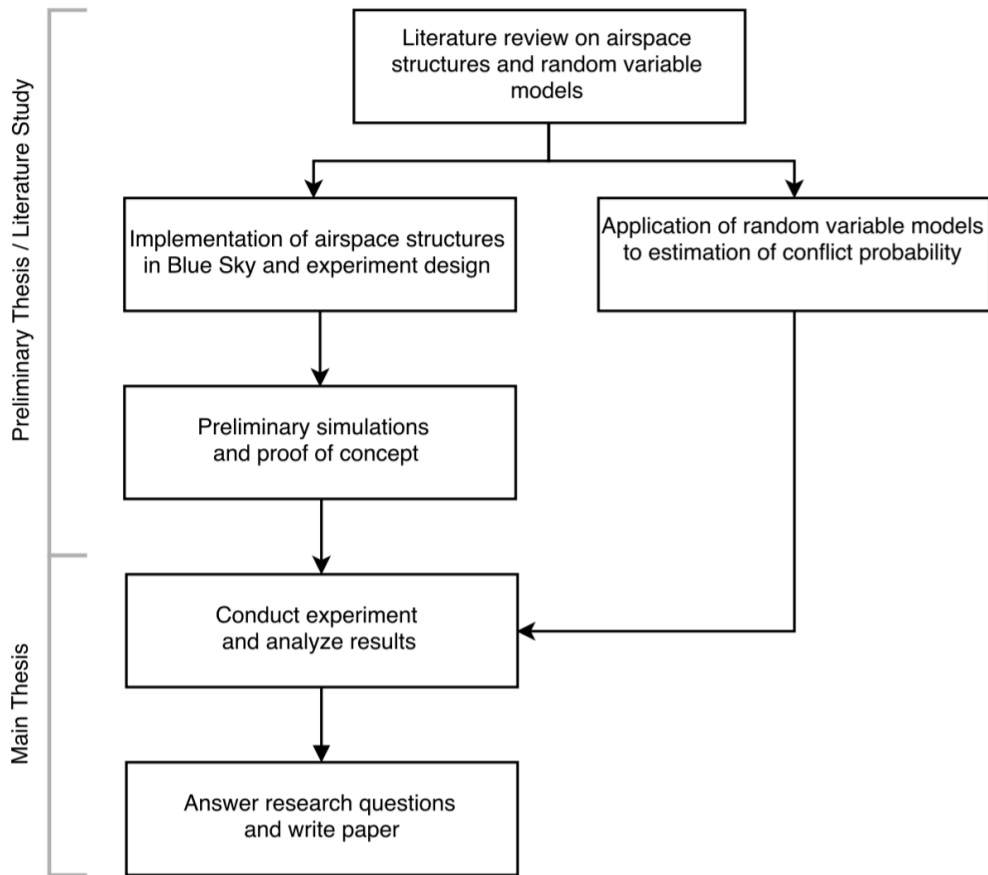


Figure 1-7: Road map of the research approach used during the Preliminary Thesis and Main Thesis

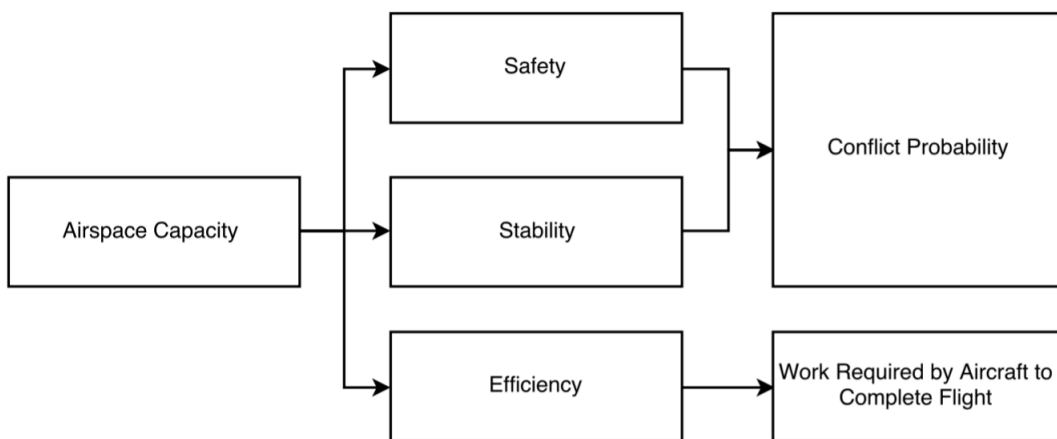


Figure 1-8: Relating concept parameters to capacity

In the second step of the road map, airspace structure will be implemented in BlueSky, the ATM tool that will be used for the simulations. Parallel to this implementation, the application of random variable models to estimate the conflict probability will be investigated in more depth. The last step during the preliminary thesis is a proof of concept; the simulation set-up will be defined and the first simulations will be performed.

The second phase of this research, the main thesis phase, consists of two steps. The simulations will be performed for the layered airspace structure concept. Using different Layer designs, the effect of structure will be analyzed and compared with the theory developed during the Preliminary Thesis phase. This includes the application of the random variable models to estimate the conflict probability and modeling of airspace capacity limits using the conflict probability and the Domino Effect Parameter. The system efficiency is obtained by measuring the difference in total work required for flights in simulations with different Layers concepts and with and without resolution maneuvers. Finally, a conference or journal paper will be written to present the final results of the thesis.

1-5 Outline of the Report

This report presents the results of the preliminary thesis phase. In chapter 2 the Literature Review is presented including a review on fundamental airspace concepts, conflict probability and the translation to airspace capacity. Second, in chapter 3 the two-dimensional theory regarding conflict probability is extended to a three-dimensional situation. In chapter 4 the experiment design will be presented. This includes a description of the simulation software, the traffic scenarios, independent and dependent variables and lastly a hypothesis regarding the conflict probability and airspace utilizations. A conclusion is presented in chapter 5.

Chapter 2

Literature Review

In this chapter, the literature review is presented. The concept of airspace structure, including a overview of the current airspace, Full Mix, Layers and Zones, is presented in section 2-1. A theoretical model to describe the conflict probability, in terms of airspace parameters, such as separation minima and heading range per altitude, is presented in section 2-2. This includes a model for a two-dimensional airspace and a method to estimate the conflict probability using random variable models from empirical data. Finally, in section 2-3, the translation is made between the safety, stability and efficiency metrics to capacity of an airspace.

The derivations in this chapter are presented such that they are clear without any prior knowledge. All the steps used for the derivations are mentioned in the text, though, not always presented in the equations.

2-1 Airspace Structure

"The difficulty of safely separating a large number of aircraft can be reduced through careful design of airspace structure" [3]. In this context, structure can be seen as an a priori means of separation and organization of air traffic. For a human controller, who is responsible for the separation between aircraft, structure can be used as a basis for simplifying abstractions and to limit the potential future states of air traffic situations [15]. In short, for a centralized ATM system, this means that ground controllers can use structure to facilitate the task of ensuring safe separation between aircraft.

During the last decades, increased navigation capabilities have enabled the possibility for direct routing operations. Direct routing would result in, for example, greater fuel efficiency, reduced flight time and increased airspace capacity [25]. However, in order to use the advantages of direct routing, the freedom that aircraft have in determining their flight path needs to increase, and an alternative method of separation responsibility is required; the separation task is moved from the ATCo to the individual aircraft, resulting in a system with a distributed responsibility. When the separation responsibility is moved to each individual aircraft, safe separation becomes entirely dependent on the Airborne Separation Assurance

Systems (ASAS). Dependent on the airspace structure, limitations to the solution space of ASAS can be imposed.

In the following sections airspace concepts with different levels of structure, varying from restrictions on 4 degrees of freedom to no restrictions, will be discussed. First, in subsection 2-1-1 the current airspace structure is presented. Three other conceptual designs will be described in subsection 2-1-2 to subsection 2-1-4, named Full Mix, Layers and Tubes.

2-1-1 Current Airspace Structure

The current airspace structure is characterized by the highly centralized ATM system to control aircraft in en route airspace. The basic components of en-route ATC have not changed since the beginning of its development of the system in the 1930's, and consists of air routes that are defined by ground-based navigational aids in the horizontal plane, and flight levels in the vertical plane [11, 12].

The separation task is centralized as ground controllers are responsible for providing safe and efficient flight [14]. In order to structure the areas for which controllers are responsible, the airspace is divided into a number of Flight Information Regions (FIR), each with its own ATC. A FIR can be subdivided into sections, each with its own ATCo, used to limit the number of aircraft under the supervision of the controllers. In Figure 2-1 an example of the airspace structure in Europe are presented, in which the highly organized system, with different FIR's, is clearly visible.

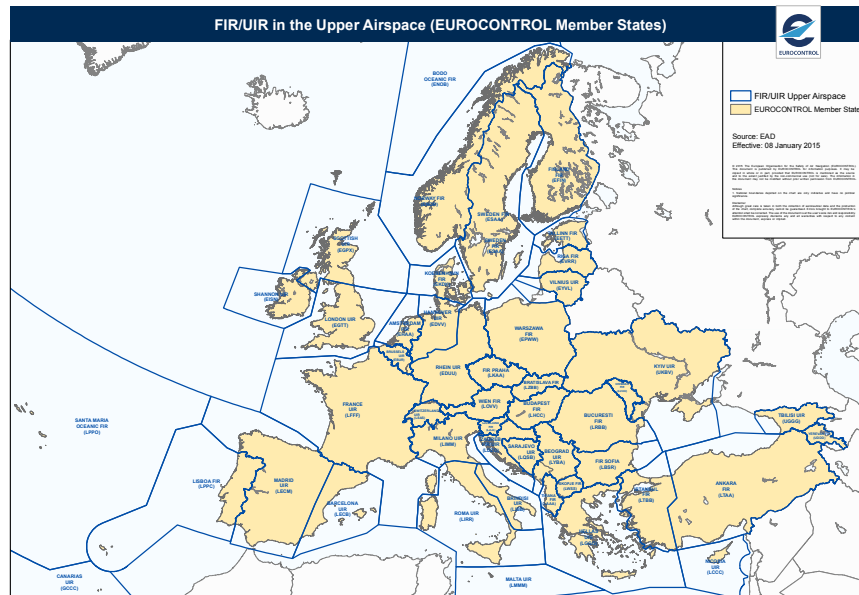


Figure 2-1: Example of the highly structured ATM system, indicating the division of the airspace in different FIR's [5]

2-1-2 Full Mix / Free Flight

The Full Mix concept, using the direct routing philosophy, is often the topic of extensive research projects regarding capacity, safety and efficiency of ATM systems [6, 21, 4, 22]. In this concept, all structure is removed from the design of the airspace and aircraft can determine their own flight paths, see Figure 2-2; there are no restrictions in longitudinal or lateral position, altitude and speed (4 Degrees of Freedom). The original concept for Full Mix / Free Flight is described in the report of the RTCA Free Flight Task Force [23]. The design philosophy for the Full Mix concept is that a decentralized system increases the flexibility for the airlines, while improving the level of safety [23].

In such a system the separation responsibility is decentralized and moved to the cockpit of each individual aircraft. A distributed system may require innovative safety management techniques due to the new dimension in conflict handling. But when the equipment in the cockpit is equally reliable as the equipment on the ground, a distributed system could potentially increase safety and efficiency, and thereby airspace capacity by several orders of magnitude compared to the current ATM system [6]. In the Full Mix concept, ASAS systems are allowed to perform resolution maneuvers using all four degrees of freedom.

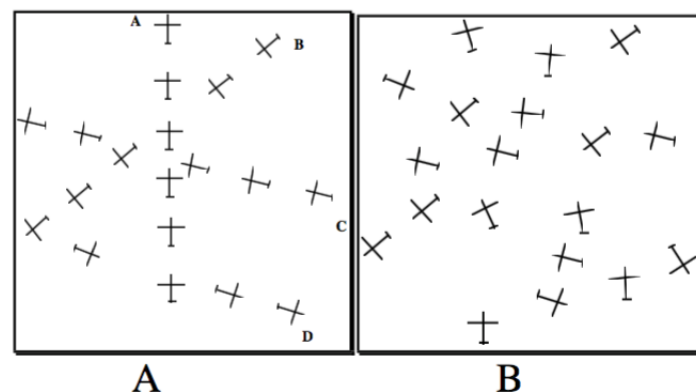


Figure 2-2: Schematic representation of the unstructured Full Mix concept (B) compared with the current centralized ATM system (A) [6]

2-1-3 Layers

The Layers concept uses height rules to describe the relation between the altitude for an aircraft and the direction of its track. "Qualitative considerations suggest that these height rules enhance intrinsic safety" [24] as they can be interpreted as predefined vertical separation to influence the conflict probability. For the implementation of the Layers concept, segmentation of the airspace in altitude bands is used and within each layer the allowed heading range is limited, leaving 3 Degrees of Freedom: longitudinal and vertical position and speed. This limitation in heading per flight level results in a lower relative velocity between aircraft and therefore is expected to result in enhanced safety. A downside to this concept is the potential decrease in efficiency. Since the altitude of the flight path will directly follow from the flight track, aircraft might not be cruising at the optimum flight level. This limitation is expected

to increase the fuel used compared with the Full Mix concept. In Figure 2-3 a schematic overview of the Layers concept is presented.

Set of Layers	315° to 360°	Fl 120
	270° to 315°	Fl 110
	225° to 270°	Fl 100
	180° to 225°	Fl 90
	135° to 180°	Fl 80
	90° to 135°	Fl 70
	45° to 90°	Fl 60
	0° to 45°	Fl 50

Figure 2-3: Schematic overview of the Layers concept, with 45° heading range per flight level

The implementation of height rules to define the airspace can be used in many different ways [24, 26, 27, 28, 29]. The variation in Layer concepts is mainly the result of a different heading range per altitude band. A specific implementation of the Layers concept can already be found for cruising aircraft in parts of the current airspace where Visual Flight Rules (VFR) apply [30]. This specific implementation uses hemispheric altitude rules to separate aircraft that fly in Eastern and Western direction. This rule requires aircraft with a heading between 0° and 179° to fly at an odd flight level, an integral multiple of 1000 ft, and aircraft with a heading between 180 and 359 at an even flight level. A Layer concept that utilizes the height rules to maximum is the 'linear altitude rule': the cruising altitudes for an aircraft is a linear function of the heading. "This rule spreads the traffic vertically and provides a default vertical separation that is proportional to the path crossing angle" [29].

Since the Layers concept is also a decentralized ATM system, ASAS is used for separation between aircraft. The height rules are a pre-defined part of the system, and therefore the resolution space of the ASAS is limited. For climbing and descending aircraft the same resolution maneuvers as in the Full Mix concept are allowed. The resolution space of cruising aircraft is limited to combined heading and speed maneuvers.

2-1-4 Tubes

Trajectory-Based Operations (TBO) can be used to limit the freedom of aircraft by pre-planning the flight path, making sure the aircraft does not encounter conflicts during the flight. When the flight trajectory is defined before take-off and time constraints are included at certain waypoints during the flight, this becomes a 0 Degree of Freedom airspace concept. An example of airspace that uses TBO, extended with the constraint that only predefined trajectories can be used, is the Tubes concept; fixed routes in the airspace are defined using nodes, as visualized in Figure 2-4, and time constraints. The advantages of using such a structured concept cannot be found in flying the optimal trajectory, but instead the system improves the predictability of service and travel time [31].

By placing different tube layers on top of each other with a decreasing grid size, aircraft can optimize their trajectory based on flight distance; the small grid size for low altitudes create

flexibility in planning short flight, while long flights can profit from the longer tubes sizes at high altitudes [3].

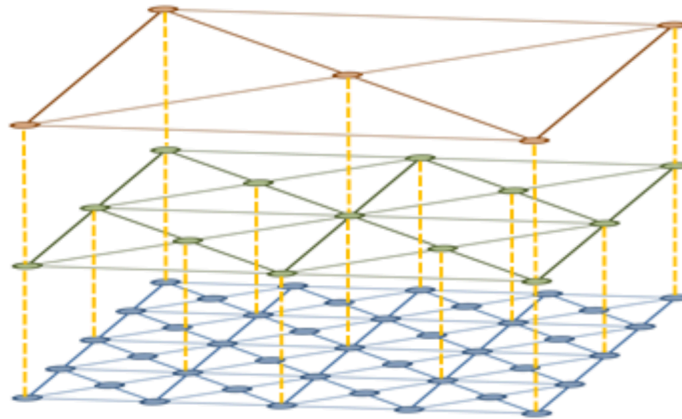


Figure 2-4: Example of airspace structure in the Tubes concept [3]

2-1-5 Concepts that will be evaluated in the Thesis assignment

Based on the promising Metropolis [3] results and the relatively straightforward way of varying the level of structure, the layered airspace structure will be evaluated in this research. The Full Mix concept will also be evaluated and will be used as a benchmark for comparing the performance through safety, stability and efficiency metrics. It is chosen to size the airspace such that the layers with a heading range per altitude band, α , of 45 degree can be implemented, resulting in 8 required flight levels. A schematic overview is presented in Figure 2-3. Using a maximum of 8 flight levels results in the possibility to use the following selections for α : 360°, 180°, 90°, 45°.

2-2 Conflict Probability and Random Variable models

The expected number of conflicts is a key parameter for assessing the airspace capacity using the safety and stability metrics. Since it is expected that the number of conflicts is affected by airspace parameters, such as separation minima and heading range per flight level, a theoretical model will be presented to describe this relation.

The probability that two aircraft are in conflict can be defined as p . This probability is independent of traffic density and who is responsible for the separation between aircraft [6]; the ATCo in a centralized ATM system or the pilot in a decentralized environment. Secondly, it is assumed that, without any prior knowledge of aircraft paths, it is equally likely that one aircraft will be in conflict with any other aircraft [7]. This assumption only holds when there are no conflict resolution maneuvers. Therefore, the theoretical model derived in this section can only be used to estimate the number of conflicts when no conflict resolution is used, E_{nr} .

Another assumption that will be made is that performance parameters are equal for all aircraft. When considering air traffic, not all aircraft will have the same performance, and

therefore the conflict probability could be different for each aircraft. Though, for this thesis, the objective is to investigate the dependency on the airspace concept, and to avoid that the variation in performance affects the results, this is eliminated from the experiment.

The assumptions listed above, imply that the probability that two aircraft will have a conflict can be described by a random variable model. The suitability, and application of random variable models to obtain the conflict probability from empirical data is described in subsection 2-2-1. In subsection 2-2-2 to subsection 2-2-4, a theoretical model for the conflict probability is presented and verified.

2-2-1 Application of Random Variable Models to Predict Airspace Capacity

The number of conflicts in an environment of distributed air traffic have proven to be predictable using random variable models [7]. In this subsection, first the methodology for estimating the conflict probability using random variable models will be presented. Secondly, the available random variable models and their applicability will be discussed.

How can the conflict probability be estimated using random variable models?

The main assumption used by Jardin [7] is that without any prior knowledge of aircraft paths it is equally likely that one aircraft will be in conflict with any other aircraft. Using this assumption, the instantaneous number of conflict for any aircraft can be modeled as a binomial random variable. The conflict probability p is chosen by fitting the data in a least square error sense. In Figure 2-5 the results of his experiments and the conflict probability estimation are presented.

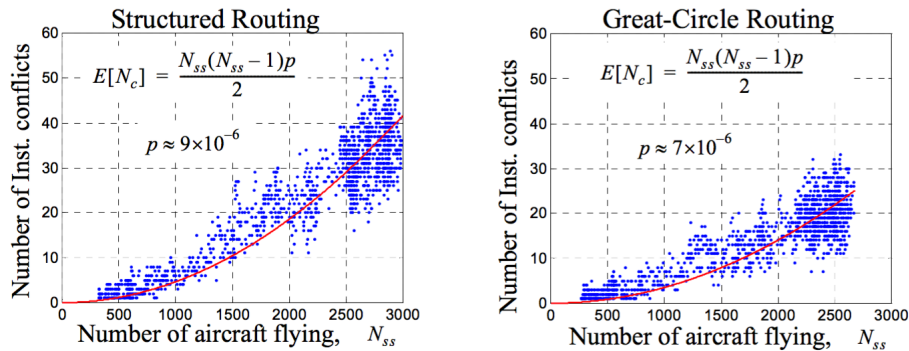


Figure 2-5: Conflict counts for structured and great-circle routes [7]

What random variable models are applicable to the problem?

Random variable models can be divided in two categories: continuous and discrete random variable models. Clearly the estimation of conflict probability between two aircraft is a discrete random variable problem: either an aircraft is in conflict or it isn't, without anything in between. Therefore in the remainder of this report, only discrete random variable models are considered.

In Table 2-1 a overview of discrete random variable models and a short description of these models is presented.

Table 2-1: Overview of discrete random variable models [9, 10]

Discrete random variable distributions	Description
Bernoulli	Probability distribution of a random variable with only two possible outcomes: failure or success.
Binomial	Probability distribution for n repeated Bernoulli trials assumed that for each trial the probability of success remains constant.
Poisson	The Poisson probability distribution is a convenient approximation of the Binomial distribution for large n and small p .
Hypergeometric	Distribution for k successes in n trials if K successes occur in N trials.
Negative Binomial	Probability distribution for the number of independent trials that is required to obtain r successes.
Geometric	Probability distribution for the number of independent trials that is required to obtain one success.
Discrete Uniform	Probability distribution in which all possible outcomes of the trial are equally likely

When considering these conditions of the various models and their application to estimating the conflict probability between two aircraft, the following random variable models are considered potentially suitable: Binomial and Poisson distributions. The following assumptions considering the conflict probability will be applied:

- n identical trials: the conflict probability between all sets of two aircraft is identical.
- trials are independent: the conflict probability of one set of aircraft does not affect the conflict probability of any other set of aircraft.
- probability of success remains constant: the conflict probability is equal for each set of aircraft.

The Binomial distribution

$$p_{\underline{x}}(k) = \binom{n}{k} p^k (1-p)^{n-k} \quad (2-1)$$

$$E[X] = np \quad (2-2)$$

With the random variable \underline{x} the number of successes in n trials and p the probability of success in a single trial. Then $p_{\underline{x}}(k)$ is the probability that k successes occur in n trials.

The Poisson distribution

$$p_{\underline{x}}(k) = e^{-\lambda} \frac{\lambda^k}{k!} \quad (2-3)$$

$$E[X] = \lambda \quad (2-4)$$

With the random variable \underline{x} the number of successes in n trials and λ equal to $n \cdot p$, the number of trials times the probability of success in a single trial.

The binomial distribution is expected to be best suitable, considering the match between the mathematical description of the problem and the general application of the binomial random variable model.

2-2-2 Centralized vs. Decentralized Conflict Probability

The expected number of conflicts for a ground controller, responsible for the separation of N aircraft, can be described by the product of the number of combinations of any two aircraft, $\binom{N}{2}$, times the conflict probability for two aircraft, p [6]. This relation is presented in Equation 2-5.

$$E_{ground} = \binom{N}{2} \cdot p \quad (2-5)$$

The expected number of conflicts for a single aircraft, responsible for its own separation, can be expressed using Equation 2-6 [6]. It is the product of the number of other aircraft, $N - 1$, times the conflict probability p .

$$E_{air} = (N - 1) \cdot p \quad (2-6)$$

Equation 2-6 can be rewritten to the total number of expected (instantaneous) conflicts, E , by taking the sum over all aircraft, as presented in Equation 2-7. A factor $\frac{1}{2}$ is included since conflicts are counted twice due to the summation over all aircraft

$$E_{total} = \frac{N(N - 1)}{2} \cdot p \quad (2-7)$$

With N the steady-state number of aircraft flying and p the probability that any one aircraft will have a conflict with any other aircraft at a given instant of time. In Figure 2-6 an example is presented for the relation between the number of aircraft and the expected number of conflicts for an ATCo (E_{ground}), using Equation 2-5, and a pilot (E_{air}), using Equation 2-6.

From this figure, a clear difference in estimated number of conflicts that need to be solved by an ATCo or by a pilot can be seen. For an ATCo, the expected number of conflicts increases quadratically with the number of aircraft. This becomes a linear relationship when the number of estimated conflicts for a pilot is considered [6].

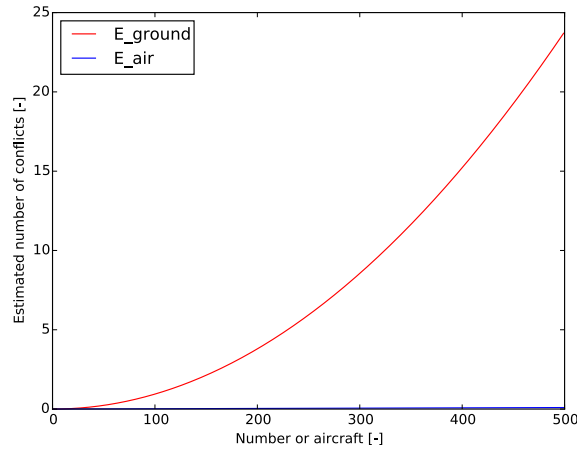


Figure 2-6: Relation between number of aircraft and expected number of conflicts for an ATCo (ground) and pilot (air). A conflict probability of $1.9e-4$ is used to generate this example.

2-2-3 2D-model for Theoretical Conflict Probability

Equation 2-7 can be extended by defining the conflict probability as a function of airspace parameters. First, the area searched for conflicts by an aircraft is considered [7]. This is visualized in Figure 2-7 and can be approximated as a function of horizontal separation distance, D_{sep} , the velocity, V , and the time interval used, t , as presented in Equation 2-8. This approximation is valid for: $V \cdot t \gg D_{sep}$.

A conflict does not necessarily occur when the areas of two aircraft, using D_{sep} , overlap, but it does when the areas using $\frac{D_{sep}}{2}$ overlap.

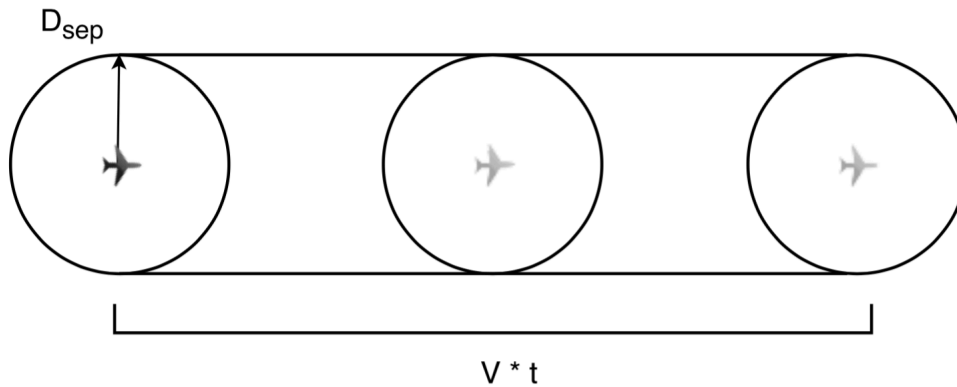


Figure 2-7: The area searched for conflicts; using a linear extrapolation of the flight path based on the speed, V , and the look-ahead time, t

$$\Delta A = 2 \cdot \frac{D_{sep}}{2} \cdot V \cdot t \quad (2-8)$$

The probability that two aircraft occupy the same area, element ΔA , can be defined as Δp ,

see Equation 2-9. Where A is the total area of the airspace considered.

$$\Delta p = \left(\frac{\Delta A}{A} \right)^2 \quad (2-9)$$

Then, when taking the sum over all elements, this results in the probability p as a function of ΔA and A . The parameter p_0 is used to account for other parameters that influence the conflict probability and match the theoretical model to results from simulations:

$$p = p_0 \frac{\Delta A}{A} \quad (2-10)$$

Combining Equation 2-8 and Equation 2-10 results in the relation described by Equation 2-11 to relate conflict probability to separation distance, speed and interval time [7].

$$p = p_0 \left[\frac{D_{sep} \cdot V \cdot t}{A} \right] \quad (2-11)$$

Secondly, the conflict probability can be related to the average relative velocity between aircraft with the same cruise altitude [8]. It is assumed that the conflict probability relates proportionally to $\frac{V'}{V}$, with V' the relative velocity between two aircraft and V the speed of the aircraft, see Equation 3-12. Again, the parameter p_0 is used to account for other parameters that influence the conflict probability and match the theoretical model to results from simulations. The relative velocity, V' , is visualized in Figure 2-8 can be defined by Equation 2-13.

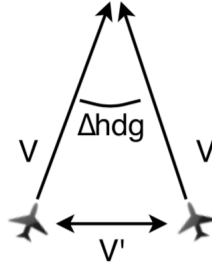


Figure 2-8: Relation between heading difference and relative velocity

$$p = p_0 \frac{\Delta V'}{V} \quad (2-12)$$

$$V' = 2 \cdot V \cdot \sin\left(\frac{1}{2} \Delta hdg\right) \quad (2-13)$$

Using the assumption that there is no prior knowledge of aircraft paths, the heading of both aircraft can be modeled as two uniform distributed random variable models. The absolute heading between two aircraft can be represented by the probability distribution in Figure 2-9 and Equation 2-14. This probability density function is a function of heading range per flight

level, α . Since the average relative velocity is based on the $\sin(\frac{1}{2}\Delta hdg)$, one cannot simply use the average heading difference. Instead, the average of the $\sin(\frac{1}{2}\Delta hdg)$ needs to be used to obtain the average relative velocity, using Equation 2-15 [8].

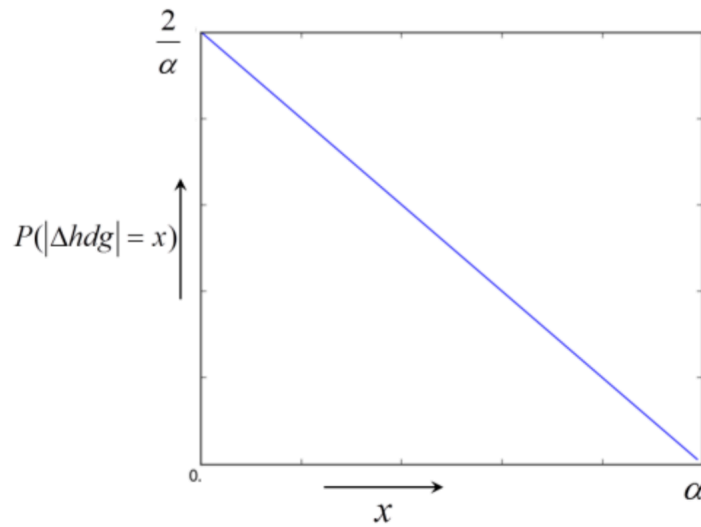


Figure 2-9: Probability distribution for the absolute heading difference between two uniform distributed random variables [8]

$$P(|\Delta hdg| = x) = \frac{2}{\alpha^2} \cdot (\alpha - x) \quad (2-14)$$

$$V' = 2 \cdot V \cdot \int_0^\alpha \frac{2}{\alpha^2} \cdot (\alpha - x) \sin\left(\frac{x}{2}\right) dx \quad (2-15)$$

When performing the integration over the probability density function, this results in a conflict probability as presented in Equation 2-17 [8].

$$V' = 2 \cdot V \cdot \left[\frac{1}{\alpha} - \frac{2}{\alpha^2} \sin\left(\frac{\alpha}{2}\right) \right] \quad (2-16)$$

Substituting Equation 2-16 in Equation 3-12, and including a factor p_0 , used to match the theoretical model with empirical data, results in Equation 2-17, describing the relation between the conflict probability and the heading range per flight level.

$$p = p_0 \left[\frac{1}{\alpha} - \frac{2}{\alpha^2} \sin\left(\frac{\alpha}{2}\right) \right] \quad (2-17)$$

Equation 2-7 can now be extended using Equation 2-11 and Equation 2-17 resulting in the following definition for the expected number of conflicts:

$$E_{nr} = \frac{N(N-1)}{2} p_0 \left(\frac{D_{sep} \cdot V \cdot t}{A} \right) \left(\frac{1}{\alpha} - \frac{2}{\alpha^2} \sin\left(\frac{\alpha}{2}\right) \right) \quad (2-18)$$

Equation 2-18 can be used to predict the effect of changing the airspace parameters on the expected number of conflicts. In Figure 2-21 the predicted effect of decreasing the separation distance with a factor two is presented and Figure 2-22 the effect of changing the heading range of a flight level.

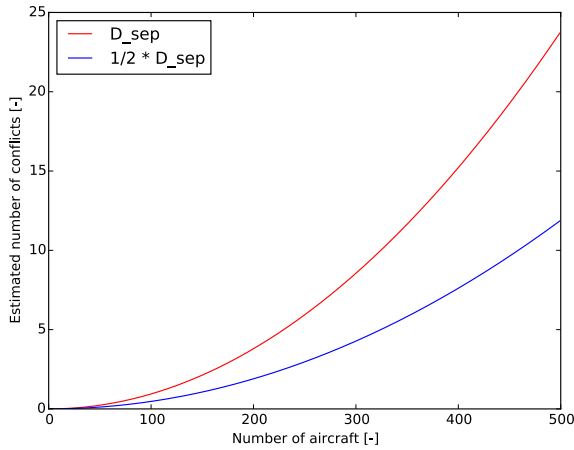


Figure 2-10: Effect of separation distance on expected number of conflicts. A conflict probability of $1.9e-4$ and $9.5e-5$ are used for D_{sep} and $\frac{D_{sep}}{2}$, respectively.

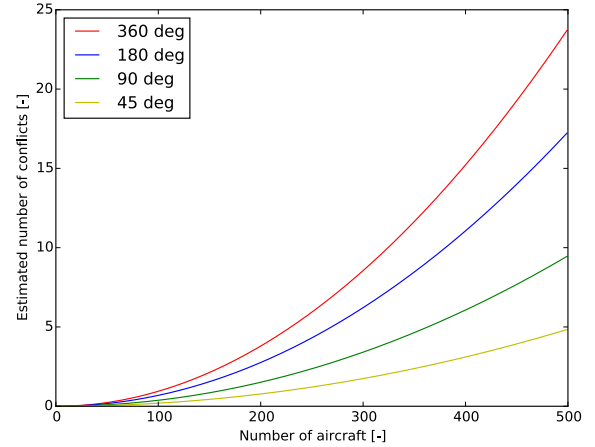


Figure 2-11: Effect of heading limitations on expected number of conflicts. A conflict probability of $1.9e-4$ is used for the 360° heading band, and scaled accordingly for the other heading bands.

In Figure 2-21, the linear relation between the separation distance and the estimated number of conflicts is clearly visible; reducing the horizontal separation by a factor 2, results in a reduction of estimated number of conflicts by a factor 2, for the same number of aircraft. The relation between the heading range and the estimated number of conflicts is less clear, since it scales using the relation in Equation 2-17. It can be observed, from Figure 2-22, that reducing the allowed heading band per flight level, reduces the estimated number of conflicts.

2-2-4 Verification of the 2D-model

In this section, the 2D-model will be verified using large-scale simulations. In this simulation, aircraft position data, including speed and heading, are randomly generated. By linearly extrapolating their flight path, the conflicts within their look-ahead time are counted. Equation 2-18 is used for the theoretical model and fitted to the experimental using an average fit for p_0 .

The results for the vertical separation distance, the look-ahead, the speed and heading range effects are presented next.

Separation Distance

In Table 2-2 the simulation parameters are presented. The results are presented in Figure 2-12 and Figure 2-13. From these results, it can be observed that the theoretical linear

relation (blue) between conflicts and horizontal separation distance is a good approximation for number of conflicts counted in the experiments (red).

Table 2-2: Setting for simulations regarding the horizontal separation requirements

Average traffic density [1/10.000nm ²]	5
Look-ahead time, t [sec]	300
Area size [nm ²]	100.0000
Heading range, α [deg]	360
Speed, V [m/s]	400

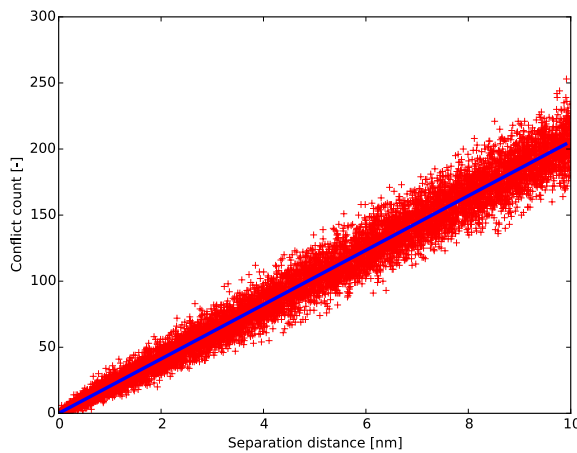


Figure 2-12: Simulations with a randomly selected separation distance: theoretical (blue) and results of simulations (red)

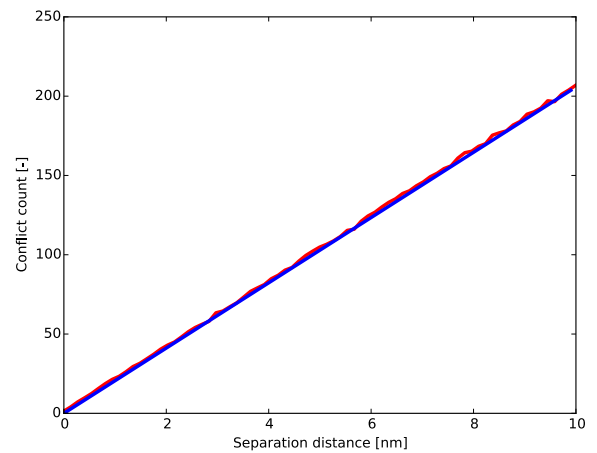


Figure 2-13: Simulations with a randomly selected separation distance: theoretical (blue) and average of simulations (red)

Look-Ahead Time

In Table 2-3 the simulation parameters are presented. The results are presented in Figure 2-14 and Figure 2-15. The theoretical model suggests a linear relation between number of conflicts and look-ahead time (blue), verified by the experimental results (red).

Table 2-3: Setting for simulations regarding the look-ahead time

Average traffic density [1/10.000nm ²]	5
Separation distance [nm]	5
Area size [nm ²]	100.0000
Heading range, α [deg]	360
Speed, V [m/s]	400

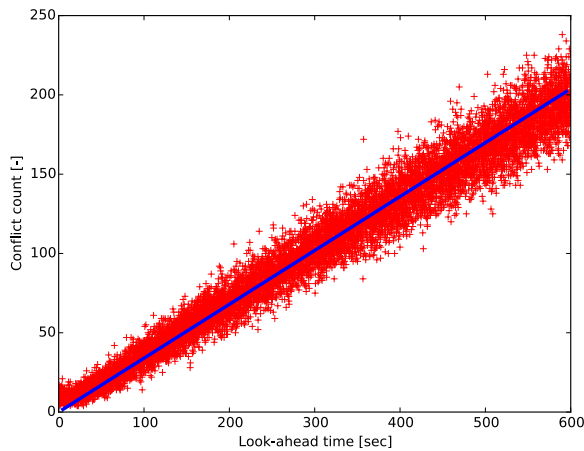


Figure 2-14: Simulations for the look-ahead time : theoretical (blue) and results of simulations (red)

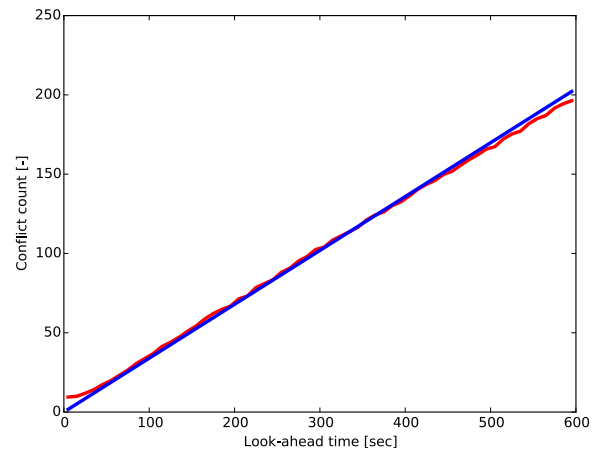


Figure 2-15: Simulations for the look-ahead time: theoretical (blue) and average of simulations (red)

Speed

In Table 2-4 the simulation parameters are presented. The speeds are equal for all aircraft within the same simulation, but are randomly selected between 250 kts and 600 kts per experiment. The results are presented in Figure 2-16 and Figure 2-17. Comparable to the separation distance and look-ahead time, the theoretical model predicts a linear relation between conflicts and speed of the aircraft. It can be observed that the theoretical model (blue) is a good approximation for number of conflicts counted in the experiments (red).

Table 2-4: Setting for simulations regarding the speed

Average traffic density [1/10.000nm ²]	5
Separation distance [nm]	5
Area size [nm ²]	100.0000
Heading range, α [deg]	360
Look-ahead time, t [sec]	300

Heading Range

In Table 2-5 the simulation parameters are presented. The results are presented in Figure 2-18 and Figure 2-19. Per simulation, a random restriction on the heading range is applied. Compared with the results from the simulations (red), the theoretical model (blue) is a good approximation for the relation between the number of conflicts and the heading range.

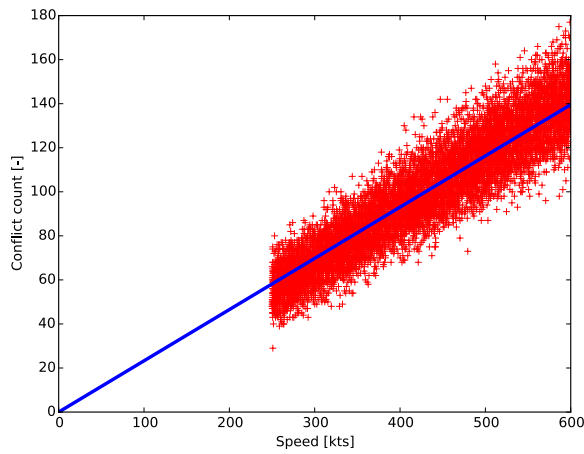


Figure 2-16: Simulations with a randomly selected speed: theoretical (blue) and results of simulations (red)

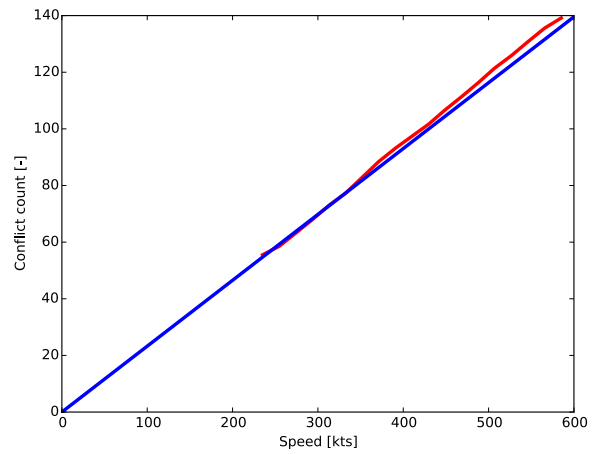


Figure 2-17: Simulations with a randomly selected speed: theoretical (blue) and average of simulations (red)

Table 2-5: Setting for simulations regarding the heading range

Average traffic density [1/10.000nm ²]	5
Separation distance [nm]	5
Area size [nm ²]	100.0000
Speed, V [m/s]	400
Look-ahead time, t [sec]	300

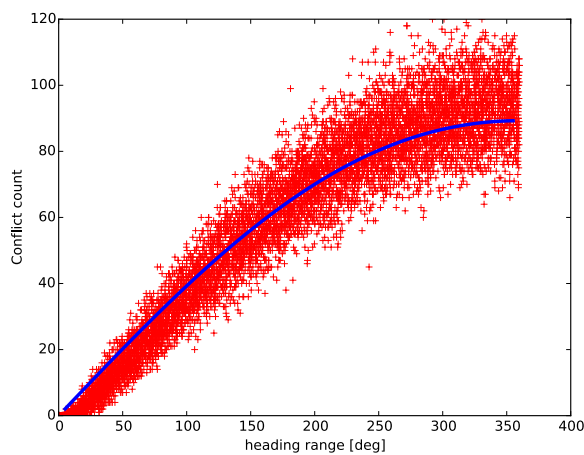


Figure 2-18: Simulations for the heading range: theoretical (blue) and results of simulations (red)

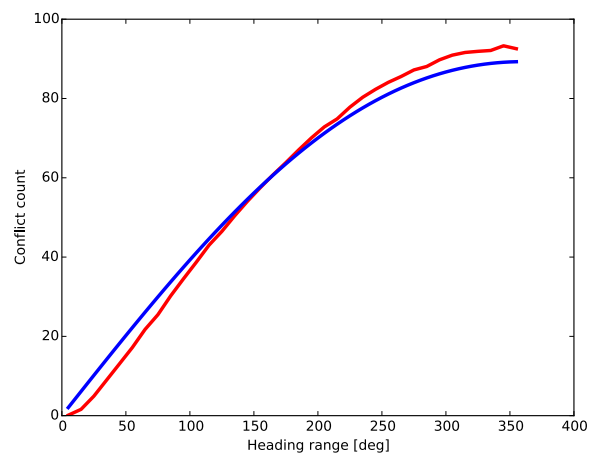


Figure 2-19: Simulations for the heading range: theoretical (blue) and average of simulations (red)

2-3 Airspace Capacity

The capacity of an airspace can be assessed by multiple performance metrics; safety, stability and efficiency. In the subsection 2-3-1, it is explained how the safety metric can be measured and how it limits the capacity. The stability of a system can be expressed using the Domino Effect Parameter (DEP), explained in subsection 2-3-2. Finally, the efficiency metric is discussed in subsection 2-3-3.

2-3-1 Safety

When considering the capacity of airspace, safety is of utmost importance. It can be related to the ability of an airspace concept to prevent a Loss of Separation (LoS). Safety can be analyzed by considering the number of conflicts, a predicted LoS, and the number of intrusions, the actual LoS. If the application of a new height rule results in a reduced conflict and intrusion count, then it can be said that this new rule is intrinsically safer than the old rule [24].

Considering the safety of an airspace concept, the capacity can be assessed as follows: "A high number of conflicts and a steep rate of growth of conflicts would suggest that the airspace is nearing saturation" [7].

2-3-2 Stability

The stability of an airspace concept can be inversely related to the Domino Effect Parameter. This parameter describes the process of an increment in conflicts due to conflict resolving by the ASAS system; "Resolving conflicts may create new conflicts with neighboring aircraft, which in turn may create additional conflicts during subsequent conflict resolutions" [4]. Bilimoria [32] describes that "one possible measure of the DEP is the incremental number of aircraft that get drawn into conflicts by other aircraft that are trying to resolve their own conflicts". The DEP can be defined by Equation 2-19 [32] and is visualized using Figure 2-20. E_{nr} is the total number of conflicts in a simulation without conflict resolution and E_{wr} is the total number of conflicts with conflict resolutions.

$$DEP = \left(\frac{S_2}{S_1} - 1 \right) = \left(\frac{E_{wr}}{E_{nr}} - 1 \right) \quad (2-19)$$

Next, a theoretical model is presented to relate the DEP to the capacity of the airspace structure. This methodology is a combination of the methods described by Hoekstra [6] and Jardin [7]. This model is derived for a 2D airspace, comparable with one flight level in the Layers concept.

In defining the total number of conflicts with resolution the most important assumption is that the conflict rate, the average number of conflicts per unit distance, is constant whether or not conflict resolution is applied [7].

The expected number of conflicts without resolution, E_{nr} , can be expressed as a function of the conflict rate, r_c , and the average distance travelled by an aircraft, D , as presented in Equation 2-20.

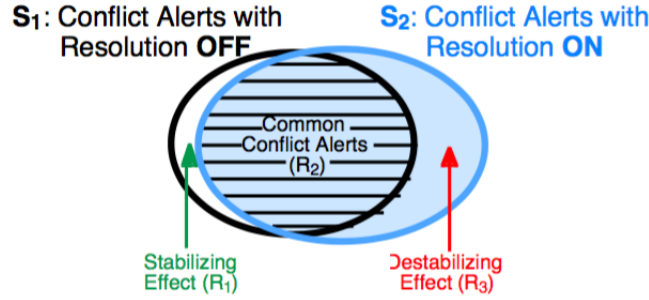


Figure 2-20: Visualization of the Domino Effect Parameter [7]

$$E_{nr} = D \cdot r_c \quad (2-20)$$

Summing over all aircraft and using the expected number of conflicts without conflict resolution, Equation 2-20 can be rewritten for the average conflict rate:

$$r_c = \frac{E_{nr}}{N \cdot D} \quad (2-21)$$

When conflict resolution is applied, the distance travelled is modeled to increase as a function of the number of conflicts. The average distance travelled by an aircraft is extended by the number of conflicts without resolution, E_{nr} , times a factor k resulting in Equation 2-22. The factor k "is a constant model parameter, which includes both the average amount of extra path distance flown as a result of conflict resolution and the effective extra path distance searched for conflicts per conflict resolution" [7].

$$E_{wr} = (D + k \cdot E_{nr})r_c \quad (2-22)$$

When Equation 2-22 is applied to all aircraft and summed, this results in the following equation for the expected number of conflicts with conflict resolution:

$$E_{wr} = \frac{N \cdot D \cdot r_c}{1 - k \cdot r_c} \quad (2-23)$$

By substituting Equation 2-21 into Equation 2-23, E_{wr} can be defined as a function of E_{nr} :

$$E_{wr} = \frac{E_{nr}}{\left(1 - k \cdot \frac{E_{nr}}{N_{ac} \cdot D}\right)} \quad (2-24)$$

It is assumed that the airspace density is constant over a given area and time, therefore the number of aircraft N is:

$$N = \rho_{ac} \cdot A \cdot t \cdot \frac{V}{D} \quad (2-25)$$

Substituting Equation 2-18, Equation 2-24 and Equation 2-25 in Equation 2-19 results in the following relation for the Domino Effect Parameter:

$$DEP = \left(\frac{1}{\left(1 - \frac{1}{\rho_{max}} \left(\rho_{ac} - \frac{1}{A}\right)\right)} - 1 \right) \quad (2-26)$$

With ρ_{max} defined as Equation 2-27. It can be observed that the theoretical maximum airspace capacity is a function of multiple airspace parameters. ρ_{max} can be determined by fitting Equation 2-26 to empirical data.

$$\rho_{max} = \frac{2}{k \cdot p_0 \cdot D_{sep}} \cdot \left(\frac{\alpha}{1} - \frac{\alpha^2}{2} \frac{1}{\sin\left(\frac{\alpha}{2}\right)} \right) \quad (2-27)$$

Equation 2-26 can be simplified using the fact that ρ_{ac} is much greater than $(1/A)$ and rewritten, resulting in Equation 2-28. This is the same relation between aircraft density and DEP as obtained by Jardin [7]. In Figure 2-21 and Figure 2-22, the expected effect of changing the horizontal separation and the heading range per flight level are presented.

$$DEP = \left(\frac{\rho_{ac}}{\rho_{max} - \rho_{ac}} \right) \quad (2-28)$$

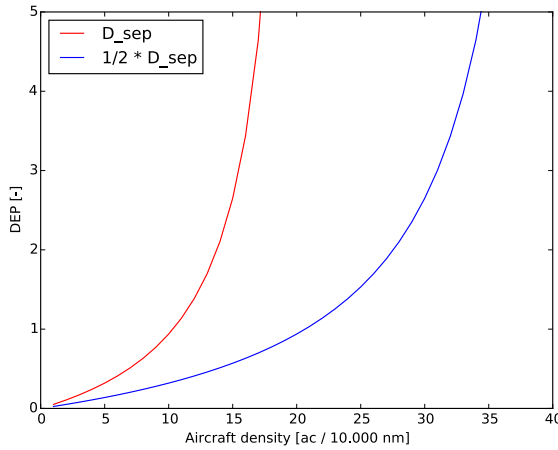


Figure 2-21: Effect of separation distance on expected number of conflicts. A conflict probability of $1.9e-4$, and k of 3 are used for the standard horizontal separation of 5 nm, and scaled accordingly for $\frac{D_{sep}}{2}$

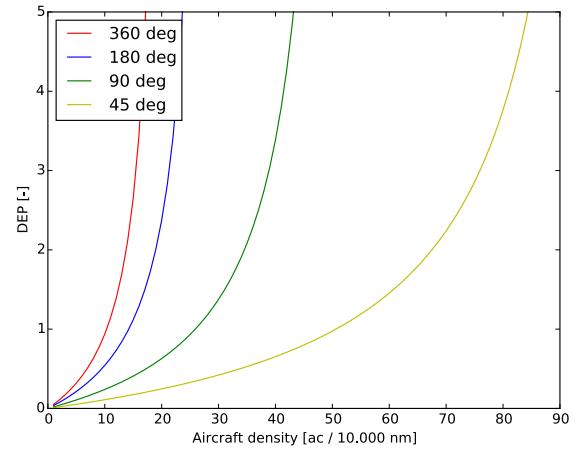


Figure 2-22: Effect of heading limitations on expected number of conflicts. A conflict probability of $1.9e-4$, and k of 3 are used for the 360° heading band, and scaled accordingly for the other heading bands

From Figure 2-21, one can observe the linear relationship between the DEP and the reduction in horizontal separation distance. This indicates that the theoretical maximum capacity will also increase linearly. For the effect of the heading band on the DEP, the relationship is less clear. One can observe an increase of the aircraft density for a decreasing heading band per flight level.

To assess the capacity due to stability limitations, the theoretical model described in this section can be matched with empirical data. This will yield a value for ρ_{max} , the theoretical maximum capacity.

2-3-3 Efficiency

The third performance metric that will be considered is the efficiency of the aircraft. The efficiency will be analyzed using the average work done by aircraft to complete their flight. This metric shows the result of conflict resolutions as well as concept dependent in-efficiency on the flight compared to the preferred trajectory. As mentioned by Krozel et al [4] the additional work done relates to the Direct Operating Cost for an airliner, an important consideration for every airline. Per flight, the work done, W , can be obtained using Equation 2-29.

$$W = \int_{path} \mathbf{T} \cdot d\mathbf{s} \quad (2-29)$$

With \mathbf{T} the thrust of an aircraft and \mathbf{s} the displacement vector.

Comparable with assessing the safety of an airspace concept, a steep rate of growth of the work required to complete a flight would suggest that the airspace is nearing saturation.

Conflict Modelling in 3D

When a three-dimensional airspace is considered, climbing and descending aircraft might affect the total number of conflicts within that airspace. In literature, the conflict probability is only described for 2D scenarios, as discussed in chapter 2. This chapter will extend the models described in literature such that they can be applied to 3D scenarios. For the derivations, it is assumed that there are no resolution maneuvers.

First, in section 3-1 the conflict probability relation with the area searched by aircraft is extended to the three-dimensional situation. To account for climbing/descending aircraft, the total number of conflicts can be split in three classes [33]: level versus level, climbing/descending versus climbing/descending (C/D v. C/D) and mixed (level versus C/D). The estimated number of conflicts for three classes is described in section 3-2 to section 3-4. Finally, in section 3-5 an overview for the estimation of conflicts for the Full Mix and Layers concept is presented, for the 2D and 3D situations.

3-1 3D-model for Theoretical Conflict Probability

The 2D-model as presented in subsection 2-2-2 can be modified to predict the number of conflicts in a 3D airspace by including the 3D airspace parameters. The area searched for conflicts by an aircraft becomes a volume defined by the horizontal and vertical separation criteria, the velocity, vertical velocity and the time interval used. A side-view of the situation is presented in Figure 3-1.

Since $V \cdot t \gg D_{sep}$, the volume can be simplified, and the simplified side-view is presented in Figure 3-2. The distance x_1 depends on the flight path angle, γ (see Equation 3-1), and the separation minima, D_{sep} and h_{sep} , and is defined using Equation 3-2.

$$\gamma = \tan^{-1} \left(\frac{v_s}{V_H} \right) \quad (3-1)$$

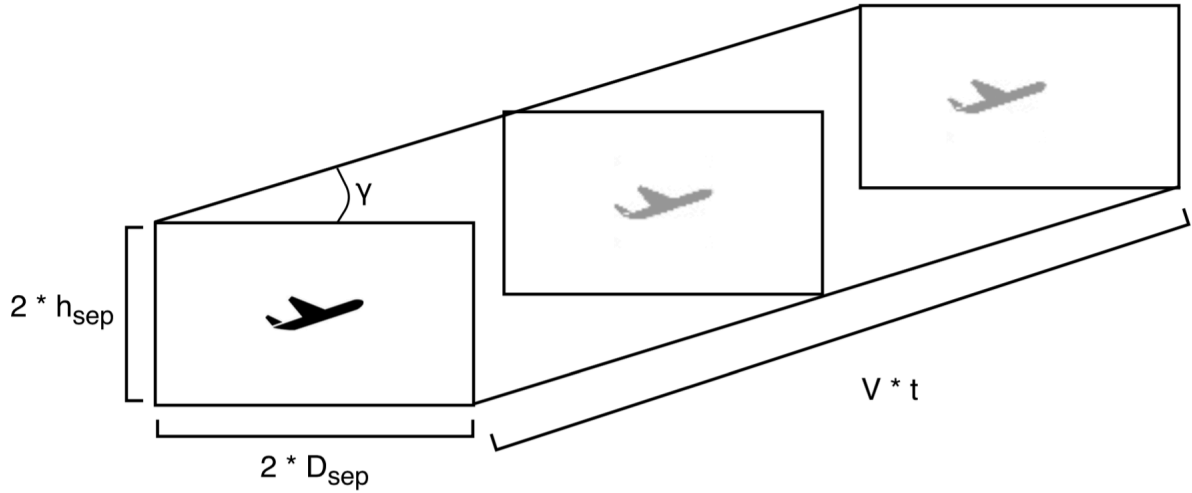


Figure 3-1: The side-view on the volume searched for conflicts; using a linear extrapolation of the flight path based on the speed, vertical speed, separation criteria and the look-ahead time

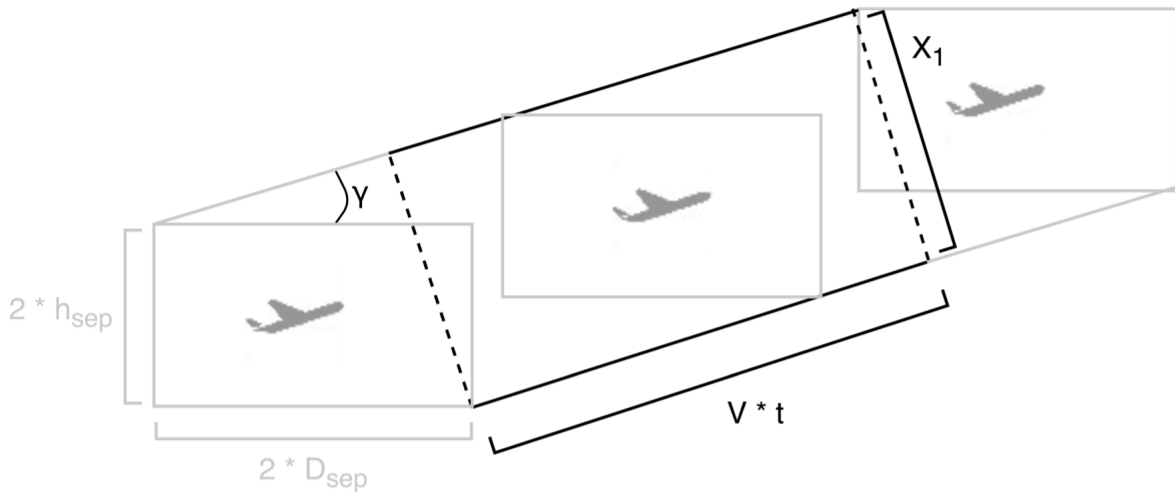


Figure 3-2: Graphical representation of the side-view of the simplified volume searched by a climbing aircraft

$$x_1 = 2 \cdot D_{sep} \cdot \sin(\gamma) + 2 \cdot h_{sep} \cdot \cos(\gamma) \quad (3-2)$$

The resulting volume searched by a climbing or descending aircraft is defined by Equation 3-3. A conflict does not necessarily occur when the volumes of two aircraft, using D_{sep} and h_{sep} , overlap, but it does when the areas using $\frac{D_{sep}}{2}$ and $\frac{h_{sep}}{2}$ overlap.

$$\Delta V_{CD} = [2 \cdot \frac{D_{sep}}{2} \cdot \sin(\gamma) + 2 \cdot \frac{h_{sep}}{2} \cdot \cos(\gamma)] \cdot (2 \cdot D_{sep}) \cdot V \cdot t \quad (3-3)$$

Since the vertical speed, v_s , is small compared with the velocity vector, V , the flight path

angle, γ , will also be small. For small angles of the flight path, the assumptions in Equation 3-4 and Equation 3-5 can be used to simplify the model.

$$D_{sep} \cdot \sin(\gamma) = D_{sep} \cdot \gamma \quad (3-4)$$

$$h_{sep} \cdot \cos(\gamma) = h_{sep} \quad (3-5)$$

Using these approximations, the area searched by aircraft for conflicts can be simplified to Equation 3-6. For vertical speeds up to 8,000 ft/min, the difference in area searched between the exact solution and the approximation is presented in Figure 3-3. It can be concluded that for climbing speeds of the average medium to large sized aircraft, of around 2,000 ft/min, the simplifications are a good approximation.

$$\Delta V_{CD_{approx}} = [D_{sep} \cdot \gamma + h_{sep}] \cdot D_{sep} \cdot V \cdot t \quad (3-6)$$

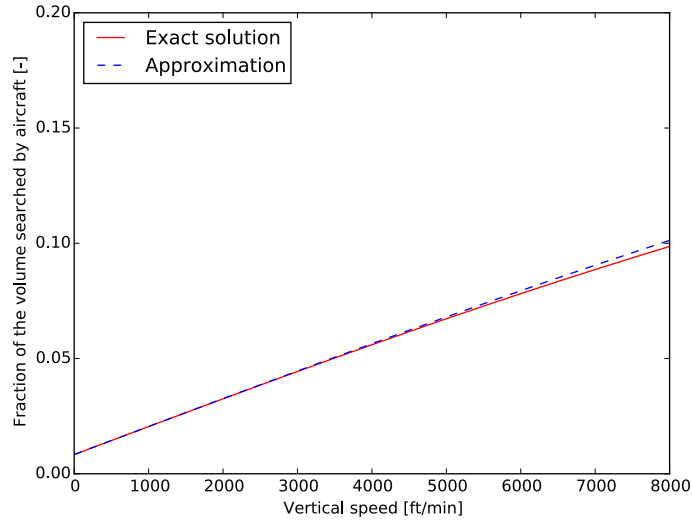


Figure 3-3: The difference between the exact solution and the approximation of the volume searched by aircraft, for a vertical speed up to 8,000 ft/min

For a cruising aircraft, the volume searched can be defined by extending Equation 2-8 with the vertical separation requirement, h_{sep} , presented in Equation 3-7. When the vertical speed, hence the flight path angle γ , is zero, Equation 3-3 becomes Equation 3-7, as expected.

$$\Delta V_{level} = D_{sep} \cdot h_{sep} \cdot V \cdot t \quad (3-7)$$

Next, the findings of this section will be used to extend the model for the estimated number of conflicts to the three situations as discussed in the introduction.

3-2 Level vs. Level Aircraft

The probability that two level aircraft occupy the same area, element ΔV_{level} , can be defined as Δp_{level} , see Equation 3-8.

$$\Delta p_{level} = \left(\frac{\Delta V_{level}}{V_0} \right)^2 \quad (3-8)$$

Then, when taking the sum over all elements this results in the probability p as a function of ΔV_{level} and V_0 :

$$p = p_0 \frac{\Delta V_{level}}{V_0} \quad (3-9)$$

$$p = p_0 \left(\frac{h_{sep} \cdot D_{sep} \cdot V \cdot t}{V_0} \right) \quad (3-10)$$

3-3 Climbing/Descending vs. Climbing/Descending Aircraft

The probability that two climbing/descending aircraft occupy the same area, element ΔV_{CD} , can be defined as Δp_{CD} , see Equation 3-11.

$$\Delta p_{CD} = \left(\frac{\Delta V_{CD}}{V_0} \right)^2 \quad (3-11)$$

Then, when taking the sum over all elements this results in the probability p as a function of ΔV_{CD} and V_0 :

$$p = p_0 \frac{\Delta V_{CD}}{V_0} \quad (3-12)$$

$$p = p_0 \left(\frac{[D_{sep} \cdot \gamma + h_{sep}] \cdot D_{sep} \cdot V \cdot t}{V_0} \right) \quad (3-13)$$

3-4 Climbing/Descending vs. Level Aircraft

When a combination of climbing/descending aircraft is considered, the probability that two aircraft occupy the same area can be defined as $\Delta p_{CD/level}$, see Equation 3-14.

$$\Delta p_{CD/level} = \frac{\Delta V_{CD}}{V_0} \cdot \frac{\Delta V_{level}}{V_0} \quad (3-14)$$

Equation 3-14 can be simplified by defining the area searched by aircraft to be related to the absolute average vertical velocity, and therefore the absolute average flight path angle, γ .

$$\Delta p_{CD/level} = \left(\frac{\Delta V_{avg}}{V_0} \right)^2 \quad (3-15)$$

This relation can be used to express the conflict probability, p , as a function of the average flight path angle, see Equation 3-16. And finally, also the expected number of conflicts can be expressed as a function of the average flight path angle, Equation 3-17.

$$p = p_0 \frac{\Delta V_{avg}}{V_0} \quad (3-16)$$

$$p = p_0 \left(\frac{[D_{sep} \cdot \gamma_{avg} + h_{sep}] \cdot D_{sep} \cdot V \cdot t}{V_0} \right) \quad (3-17)$$

3-5 Overview of Conflict Estimation for Layers and Full Mix

In this section, an overview is presented for the estimation of the total number of conflicts for the Full Mix and Layers concept. This will be done for the two-dimensional situation, as discussed in chapter 2, and for the three-dimensional situation discussed in this chapter.

Full Mix: 2D

For a two-dimensional airspace, using the Full Mix concept, the total number of conflicts can be estimated using Equation 3-18.

$$E_{total} = \frac{N(N-1)}{2} p_0 \left(\frac{D_{sep} \cdot V \cdot t}{A} \right) \quad (3-18)$$

Full Mix: 3D

For the Full Mix concept, there is no effect of the limitation in heading range on the conflict probability and therefore no differentiation of the conflict probability between cruising and climbing/descending aircraft. The hypothesis is that this model, Equation 3-19, can be used to estimate the total number of conflicts in the airspace.

$$E_{total} = \frac{N(N-1)}{2} p_0 \left(\frac{[D_{sep} \cdot \gamma_{avg} + h_{sep}] \cdot D_{sep} \cdot V \cdot t}{V_0} \right) \quad (3-19)$$

Layers: 2D

When an airspace is designed using the Layers concept, the heading range per flight level affects the conflict probability, as explained in chapter 2. For a two-dimensional situation, this estimation of the total number of conflicts is defined by Equation 3-20.

$$E_{total} = \frac{N(N-1)}{2} p_0 \left(\frac{D_{sep} \cdot V \cdot t}{A} \right) \left(\frac{1}{\alpha} - \frac{2}{\alpha^2} \sin \left(\frac{\alpha}{2} \right) \right) \quad (3-20)$$

Layers: 3D

The estimation of the total number of conflicts for a three-dimensional airspace, using the Layers concept, requires a distinction between the three classes discussed in the beginning of this chapter. The parameter L is introduced because the number of flight levels becomes important in estimating the number of conflicts. It is assumed that the number of cruising aircraft is uniformly distributed over the L number of flight levels. The estimated number of conflicts is a summation of the three different classes of conflicts as presented in Equation 3-21.

$$\begin{aligned}
 E_{total} = & \frac{N_{level} \left(\frac{N_{level}}{L} - 1 \right)}{2} p_{01} \left(\frac{D_{sep} \cdot V \cdot t}{A} \right) \left(\frac{1}{\alpha} - \frac{2}{\alpha^2} \sin \left(\frac{\alpha}{2} \right) \right) + \\
 & \frac{N_{CD} (N_{CD} - 1)}{2} p_{02} \left(\frac{[D_{sep} \cdot \gamma + h_{sep}] \cdot D_{sep} \cdot V \cdot t}{V_0} \right) + \\
 & N_{CD} \cdot N_{level} \cdot p_{03} \left(\frac{[D_{sep} \cdot \gamma_{avg} + h_{sep}] \cdot D_{sep} \cdot V \cdot t}{V_0} \right) \quad (3-21)
 \end{aligned}$$

Experiment Design

The effect and expected benefits of the Layers concept will be tested and compared with the Full Mix concept using data obtained from an Air Traffic Management experiment. Fictive traffic will be simulated to measure the performance on safety, stability and efficiency for the Full mix concept and the Layers concept, with multiple variations in heading range per flight level. The experiment serves two goals:

1. To determine the influence of the heading range per flight level on the performance for the Layers concept
2. To quantitatively compare the Full Mix and the Layers concepts in terms of capacity

This chapter describes the experiment to be conducted during the main thesis. First, in section 4-1 the simulation environment, BlueSky, will be discussed. This includes a short explanation regarding the software, and the implementation of the Layers concept. The traffic scenario, including the test region, experiment time and traffic demand, is discussed in section 4-2. The independent and dependent variables are discussed in section 4-3 and section 4-4, respectively. Finally, the hypothesis is presented in section 4-5.

4-1 Simulation environment: BlueSky

BlueSky is an open-source tool for performing research on Air Traffic Management and Air Traffic Flows. It can be used to simulate, analyze and visualize air traffic on a global scale [34]. It is developed in the programming language Python in combination with a user-friendly interface. BlueSky is capable of simulating hundreds of aircraft at the same time and traffic scenario's can easily be created and introduced using the command stack of BlueSky, including a time stamp. The implementation of the Layers concept, the airspace concept that will be evaluated during this research, is discussed in subsection 4-1-1. The ASAS method used for detecting and resolving conflicts is discussed in subsection 4-1-2.

4-1-1 Implementation of Layers Concept

The implementation of the Layers concept includes two aspects. The first aspect is the altitude selection of the aircraft based on the height rules that apply for the specific Layer concept. When resolution maneuvers are applied to avoid intrusions an aircraft may need to deviate from its route. The second aspect involves the trajectory recovery by selecting the appropriate waypoint for navigation after being involved in a resolution maneuver.

Altitude Selection

The first aspect of the layers implementation, the altitude selection, will be solved by defining waypoints along the routes of aircraft. This way the horizontal traffic pattern does not vary per Layer concept, but the altitude rules of the different Layers can easily be included. When there are multiple layers with the same heading band a selection of layer will be made using the flight distance between origin and destination. Depending on the number of allowed flight levels per heading range, the available traffic will be distributed equally over these flight levels; for example, when two flight levels are available, approximately 50% of the flights, with the shortest distance, will be assigned to the lowest available flight level. The remaining 50%, with the longest flight distance, will be assigned to the highest available flight level.

Trajectory Recovery

Selecting the appropriate waypoint for navigation can become important when resolution maneuvers are required relatively close to an active waypoint, this is visualized in Figure 4-2. In an extreme case, it could happen that an aircraft passes a waypoint in its route during a resolution maneuver, but needs to reach the exact coordinates of the waypoint to activate the next one. This could result in a heading of the aircraft outside the heading range in case of the Layers concept. To that aircraft fly far outside the heading envelope of a Layer, it will be implemented that the next waypoint needs to be selected when the difference between the required heading to the active waypoint and the heading of the initially defined route is more than half the heading range of the flight level, $\frac{\alpha}{2}$. This difference in heading is defined as δ and is visualized in Figure 4-1. Using this logic, the next waypoint can be selected and the flight path is more realistic, see Figure 4-2 and Figure 4-3. An overview for the implementation of this trajectory recovery method is presented in Figure 4-4.

$$\delta \leq \frac{\alpha}{2} \quad (4-1)$$

As can be seen in Figure 4-4, the selection of the waypoint that meets the requirement for δ can be an iterative process. A maximum of 5 iterations for selecting the next waypoint will be included after each resolution maneuver; the time that the aircraft deviates from the initial flight path will be minimized, resulting in a minimal violation of the Layers concept. When the active waypoint is the destination, no other waypoints can be selected anymore and the restrictions on the heading are no longer active. After all, the aircraft needs to reach its destination.

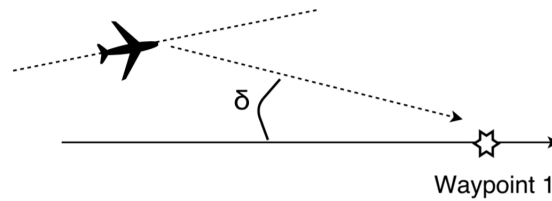


Figure 4-1: Graphical representation of δ , the deviation between the heading of the initially defined route and the required heading to fly to the active waypoint

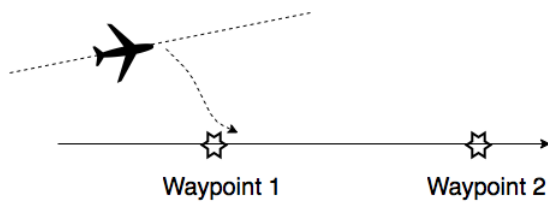


Figure 4-2: Flight path using the regular waypoint selection

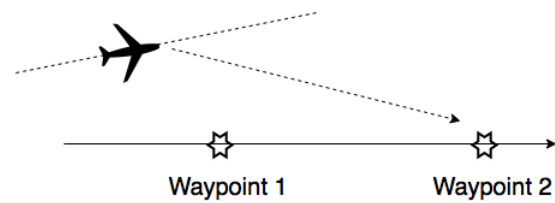


Figure 4-3: Flight path with adjusted waypoint selection

4-1-2 Airborne Separation Assurance System

The Airborne Separation Assurance System used in the simulations consists of Conflict Detection and Conflict Resolution modules. Predicted conflicts are solved using the Modified Voltage Potential method, implemented in BlueSky as described in [35].

The look-ahead time for conflict detection is set to 300 seconds. When conflicts are resolved within this look-ahead time, the heading changes are relatively small, in the order of a few degrees, minimizing the effect on the altitude rules.

A vertical separation of 1,000 ft and horizontal separation of 5 nm are applied as separation minima [11].

The types of resolution maneuvers that are allowed depend on the airspace concept. Using the Full Mix concept, speed, horizontal and vertical maneuvers are allowed, where cruising aircraft in the Layers concept are limited to speed and horizontal resolution maneuvers.

4-2 Traffic Scenario

In this section the design of the traffic scenario will be discussed. First, in subsection 4-2-1 the lay-out of the test region will be discussed. The required duration of the simulations will be discussed in subsection 4-2-2 and finally the traffic demand is presented in subsection 4-2-3.

4-2-1 Test Region

Two options for the shape of the test region have been investigated: A circular test region, figure 4-5, and a square test region, figure 4-6. Besides the area shape, there are also two options for the traffic generation: all aircraft with origins on the ground and climb to the

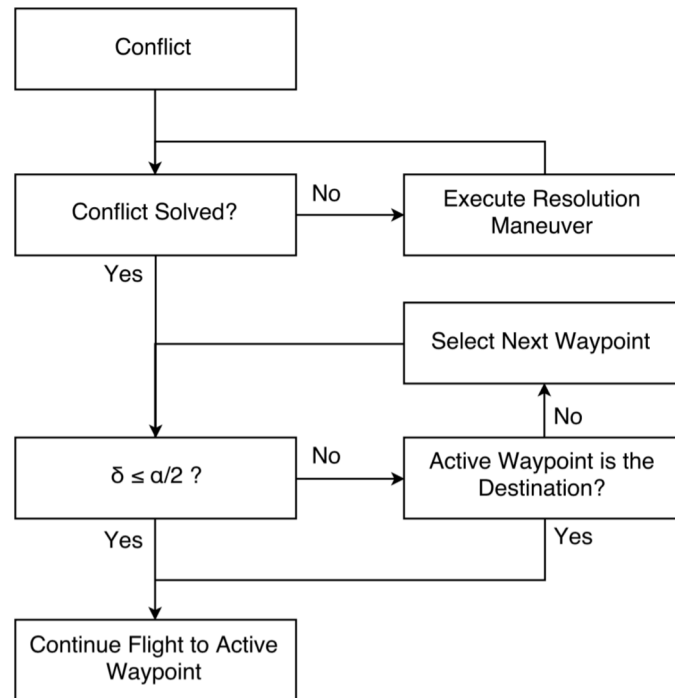


Figure 4-4: Flow Chart for trajectory recovery logic, used in case of a conflict between two aircraft

desired altitude, Figure 4-6, or aircraft are generated at cruise altitude, Figure 4-5. Two combinations in which all four options are represented; Design 1, section 4-2-1, combines the circular shape with traffic generation at cruise altitude and Design 2, section 4-2-1, combines the square test region with traffic generation at ground level.

Design 1

The circular test region concept is based on research by Jardin [7] and Krozel et al [4] and is used for 2D simulations comparing the system performance of structured routing and Free Flight. A graphical representation of this concept can be found in Figure 4-5. The inner, yellow cylinder defines the experiment area with the destinations for the aircraft on the outline of the cylinder. When the aircraft reach their destination they will be deleted from the simulation. The origins of the aircraft are positioned on the outer, blue cylinder. By separating the origins and destinations it will be avoided that aircraft are generated and encounter an intrusion before they can execute a resolution maneuver.

The pro's and cons of this concept, taking into account that traffic conditions should be as equal as possible for all airspace concepts, are presented next.

Pro's:

- Simulation of en route traffic only; no climbing and descending phase due to origins and destinations on the ground.

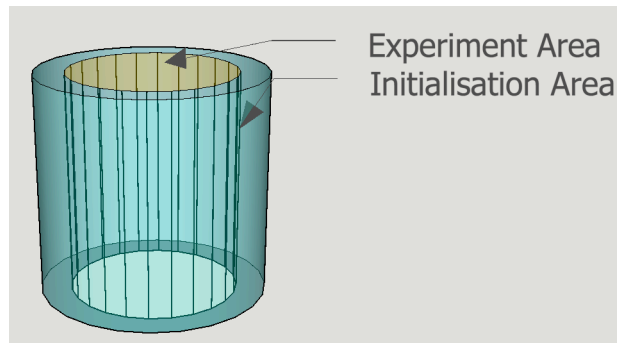


Figure 4-5: Example of circular test region with origins and destinations at cruise altitude

Cons:

- Altitude selection cannot be based on flight distance: The flight levels with lower altitudes will only be used at the border area, while the higher flight levels will have a high concentration of aircraft in the middle area.
- The height of the origins and destination, randomly selected on the cylinders, may create strange traffic patterns that are highly influenced by the traffic generation method instead of the airspace structure.

Design 2

The development of a square test area is based on research by E. Sunil et al [3]. It was used for comparing four airspace concepts and their system performance under the influence of UAV's and PAV's. In Figure 4-6 a graphical interpretation of this concept is presented. The top, yellow square in the figure represents the experiment area. The origins and destinations are positioned on the ground of the initialisation area. The pro's and cons of this concept are presented next.

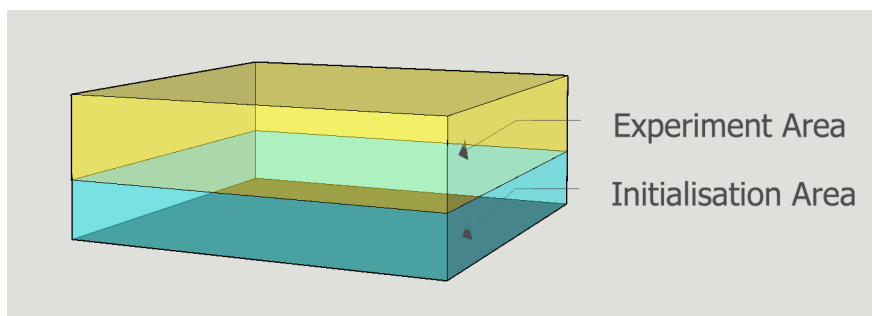


Figure 4-6: Example of square test region with origins and destinations of the ground

Pro's:

- Origins and destinations equally distributed on the ground of the test region. Therefore more uniform distribution of short and long flights over the entire test region.

- For all concepts a climbing and descending part is included in the flight, minimizing the influence of the different concepts, not caused by the height rules, on the traffic pattern.

Cons:

- Climbing and descending phases of the flight are included in the simulation. Therefore less comparable with en route traffic only.
- Climbing and descending may create false conflict warnings due to prediction method.
- Traffic density on boundaries of the experiment area may be significantly lower than the inner parts of the experiment area, especially in the 'corners' of the experiment area.

Conclusion Regarding Test Region

Considering the pro's and cons discussed in the previous sections, it is decided to design a test area with the following characteristics:

- Aircraft are generated with origins and destinations at ground level
- The initialization area will be sized such that aircraft generated on the edge have sufficient time to climb and enter the experiment area in cruise. This allows generation of aircraft that enter the experiment area in cruise, the phase of flight interesting for en route capacity.
- A square test region increases the number of possible origin-destination pairs for long distance flights, and avoids a concentrating of this traffic in the center region

This concept is best applicable for different airspace structure designs with minimum impact on the results of the simulation.

Test Region Sizing

The sizing of the test region is based on the airspace structure concepts that will be implemented (altitude sizing) and the flight distance (longitudinal and lateral sizing). The minimum distance that an aircraft should fly is obtained using the following assumptions:

- A minimum cruise time of 30 minutes; main focus for this research is the en-route traffic. By requiring a minimum cruise time, it is avoided that aircraft are climbing and directly descending
- A climb from the origin to the highest altitude included in test region
- A descent from the highest altitude in the test region to the destination

For the implementation of the Layers concept it is chosen to use 8 flight levels. This will be elaborated upon in section 4-3. For the initialization area the following dimensions have been set:

- First 1,000 ft without conflict resolution; to avoid that aircraft have to start a conflict resolution maneuver straight after initialization
- Then 4,000 ft with conflict resolution active; this way, conflicts that would occur when entering the experiment area can be resolved in time, not affecting the conflict count

The resulting altitudes are presented in Figure 4-7 including an overview of the flight phases for the minimum distance.

The climb rate and descent rate used in the simulations is 2000 ft/min, based on the performance of a Boeing 747. An average cruise speed of 530 kts is used in the calculation of the cruise distance. This results in a minimum distance between an origin-destination pair of approximately 310 nm.

For the area it is important to take the DEP into account. When the test region is too small and flights too short, the DEP can, and most probably will, be biased. To avoid this, the area has to be sized large enough and this will be evaluated during the simulations.

The size of the experiment area is 500 nm x 500 nm. In figure 4-8 the area is plotted on a map of Europe for reference. The longest flight would be 707 nm, with an average cruise speed and no resolution maneuvers will take approximately 1 hour and 30 minutes.

The origins and destinations points are located on a grid, with a distance of 10 nm between two airports equal to twice the horizontal separation distance, resulting in 1156 airports in total. Using this distance between airports it will be avoided that aircraft are generated directly encountering an intrusion.

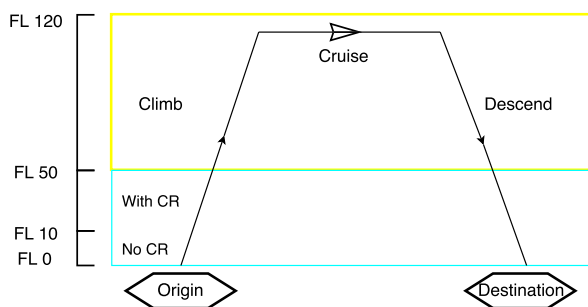


Figure 4-7: Simplified visualization of different phases of flight



Figure 4-8: Size of the test region compared with the size of France

4-2-2 Experiment Time

The experiment time consists of three phases. The first one is the build-up phase; during this period of time aircraft will be generated and after approximately 60 minutes average aircraft density reaches the required aircraft density. After the required density is obtained, the measurement phase can start. It is chosen to set the measurement time to 60 minutes.

Finally, to not influence any of the experiment metrics, all aircraft should finish their flight. This also takes approximately 60 minutes, resulting in a total simulation time of 180 minutes.

4-2-3 Traffic Demand

The traffic demand scenarios can be defined in terms of aircraft density and instantaneous number of aircraft flying. Based on research by Jardin [7] and Krozel [4] and a high-density traffic distribution for simulation purposes as defined by Eurocontrol [36] the densities have been defined, varying from 2 to 50 aircraft per 10.000 nm^2 .

Using the test region that is defined in section 4-2, this results in the number of instantaneous aircraft varying between 500 (2 aircraft per 10.000 sq. nm. x 25 for the total area x 8 flight levels) and approximately 10.000 (50 x 25 x 8).

4-3 Independent Variables

The two independent variables of the experiment are the airspace concept and the traffic demand. The selection of the values for these variables will be explained in this section, and an overview is presented in Table 4-1.

Airspace Concept

The Layers concept is based on the heading range per flight level. In order to have an equal number of flight levels per heading range, the number of flight levels needs to double with respect to the 'previous' concept. This means, to go from 360° to 180° heading range, the number of flight levels goes from one to two. To go from 45° to 22.5° heading range, the number of flight levels goes from eight to sixteen. This, in combination with limiting the total number of aircraft that need to be simulated, results in the choice for a maximum of eight flight levels, with the smallest heading range of 45° per flight level.

Traffic Demand

The method for selecting the traffic demands is based on the chosen variation in airspace concepts: for the Layers concept, the heading range per flight level starts at 360°, and is reduced with a multiplication of 0,5 to obtain the next heading range per flight level. This, in combination with the theoretical model explained in subsection 2-3-2, suggests that capacity limits also scale with a multiplication. In order to have sufficient data points, and due to the unpredictability of the effect of climbing/descending aircraft, it is chosen to use a multiplication factor of 1.25 for the traffic demand. Starting with a aircraft density of 2 aircraft per 10.000 nm^2 , this results in the traffic demands as stated in Table 4-1, with a highest traffic density of 45,5 aircraft per 10.000 nm^2 .

Table 4-1: The independent variables of the experiment

Independent Variable	Definition
Airspace concept	Full Mix Layers, with a heading range per altitude band of 360°, 180°, 90°, 45°
Traffic demand	2,0/2,5/3,1/3,9/4,9/6,1/7,6/9,5/11,9/14,9/18,6/23,3/29,1/36,4/45,5 aircraft per 10.000 nm^2

Total Number of Experiment Conditions

For each of the 195 experiment conditions (5 x 15), two repetitions are performed. Additionally, the scenario's are performed with and without conflict resolution, resulting in a total of 300 simulation runs (5 concepts x 15 demand scenarios x 2 repetitions x 2 conflict resolution settings).

4-4 Dependent Variables

Three different categories of dependent variables will be used to quantitatively compare the level of structure: safety, stability and efficiency. An explanation of the metrics can be found in section 2-3 and a short overview is presented in Table 4-2.

Table 4-2: The dependent variables of the experiment

Performance Metric	Dependent Variable
Safety	Conflicts Intrusions
Stability	Domino Effect Parameter
Efficiency	Work done

4-5 Hypotheses

In this section, the hypotheses regarding the extend of the benefits of the Layers concept compared to the Full Mix concept is presented. First, a few statements are presented regarding the variation in heading range per altitude for the Layers Concept. Second, the expected difference between the Full Mix and the Layers concept will be discussed.

Expected results for a systematic variation in the heading range per flight level

- Based on the two-dimensional simulations (section 2-2-4), the first hypothesis is that the number of conflicts between cruising aircraft will reduce with a reduced heading range per flight level

- Considering a three-dimensional airspace, it is expected that the average climbing and descending time increases with a reducing heading range per flight level: therefore the second hypothesis is that the number of conflicts involving at least one climbing/descending aircraft will increase with a reduction in heading range per flight level
- Third, the stability performance is expected to improve with reducing the heading range per flight level and will be the metric limiting the capacity. On the other hand, the efficiency is expected to decrease and become more important in assessing the capacity.

The benefits of a layered airspace structure compared with the Full Mix concept

- For the lower range of traffic densities, it is expected that the Full Mix will have advantages regarding the efficiency of the system. Using the Full Mix concept, aircraft will be able to select a cruise altitude suitable for the distance between the origin and the destination.
- For high traffic densities, the efficiency is not expected to limit the capacity. Due to the separation of aircraft using height rules, the hypothesis is that the Layers concept will have advantages regarding the safety and stability performance compared to the Full Mix concept.

Conclusion/Summary

In this Preliminary thesis report, the results of the literature study and the experiment design are presented. The main objective of this thesis is to quantitatively compare the Full Mix and the Layers concepts in terms of capacity, by assessing the impact the heading range per altitude on safety, stability and efficiency metrics.

The current ATM system consists of air routes that are defined by ground-based navigational aids in the horizontal plane and flight levels in the vertical plane, as well as air traffic controllers who are responsible for the separation between aircraft. One of the most important issues for the current ATM system is the limited capacity due to the limits on the controllers' workload, and their ability to deal with the complex situations that occur under their supervision.

The combination of limits on the controllers workload, and an increase in traffic demand that could be as high as 170% over the next 35 years, results in that the current ATM system is approaching its saturation level. In order to deal with an air traffic demand that is several orders higher than the current situation, research into fundamentally new airspace concepts is required. Previous research indicated that the Full Mix and the Layers concepts are the most promising when it comes to dealing with high density traffic, while satisfying safety, stability and efficiency requirements. While the Metropolis [3] results indicate that implementing a layered structure can improve capacity compared to Full Mix, the extent of the capacity benefit is unknown. Furthermore, the influence of the heading range per altitude and the corresponding performance for Layers also needs to be determined. Therefore, in this thesis, the performance of the Full Mix and the Layers concepts will be questioned on a quantitative level.

First, the conflict probability is expressed as a function of airspace parameters, such as look-ahead time and heading range per flight level, based on literature. Since performance of the airspace will be assessed for a three-dimensional situation, and the literature only provides the two-dimensional situation, this has been extended to the three-dimensional situation for Full Mix and Layers. The conflict probability will be determined for both airspace concepts; random variable models will be used to estimate the conflict probability using empirical data obtained from simulations where the conflict resolution is not active.

The performance of the Full Mix and Layers concept will be evaluated using safety, stability and efficiency metrics. In order to analyze the performance differences between Full Mix and Layers on a quantitative level, a systematic variation in heading range per flight level for the Layers concept will be assessed: 360°, 180°, 90°, 45° heading range per flight level. A theoretical model is presented to predict the capacity, and simulations will be performed to generate empirical results. The theoretical model is used to estimate the capacity as a function of the Domino Effect Parameter, a metric that can be inversely related to stability. This model includes the influence of airspace parameters, such as heading range per altitude, look-ahead distance and separation minima. A high number of conflicts, a steep rate of growth of conflicts or the DEP, or a steep decrease in efficiency would suggest that the airspace is nearing its saturation.

In the next phase of the thesis, experiments will be performed to validate the theoretical model. The experiments will be conducted using the BlueSky ATM simulation software. The dependent variables of the experiment are the airspace concept (5 variations) and traffic demand (39 levels). In total, 195 scenarios will be simulated, using two repetitions and with two conditions for the ASAS system; with and without resolution maneuvers. The independent variables can be categorized using safety, stability and efficiency. Safety will be evaluated using the number of conflicts and intrusions. The stability is inversely related to the Domino Effect Parameter, which is a parameter that describes the process of an increment in conflicts due to conflict resolving by the ASAS system. Finally, the efficiency is analyzed by comparing the average work required by aircraft to complete their flights.

Part III

Appendices

Appendix A

Validation of Conflict Probability Model using Two-dimensional Simulations

Based on literature [?, 8], the following model is used to predict the instantaneous number of conflicts:

$$E = \frac{N(N-1)}{2} \cdot k \cdot \frac{2 \cdot d_{seph} \cdot v \cdot t}{A} \cdot \frac{2\pi}{\alpha} \left(1 - \frac{2}{\alpha} \sin \frac{\alpha}{2}\right) \quad (\text{A-1})$$

The variables used in Equation A-1 are explained in Table A-1. The model is validated using large-scale simulations for four different heading ranges; 360 degrees, 180 degrees, 90 degrees and 45 degrees. A number of aircraft, between 0 and 500, are randomly initialized in the experiment area, A , and conflict detection is applied. In Table A-2 the other model parameters are summarized.

Using 1,000 random initializations, the results are obtained as presented in Figure A-1,A-2,A-3 and A-4. The k -value obtained by fitting the model in least-square error sense to the simulation results. Intrusions at the initialization are not counted as conflicts.

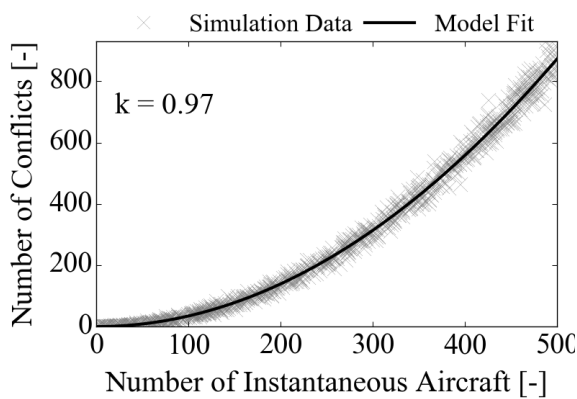
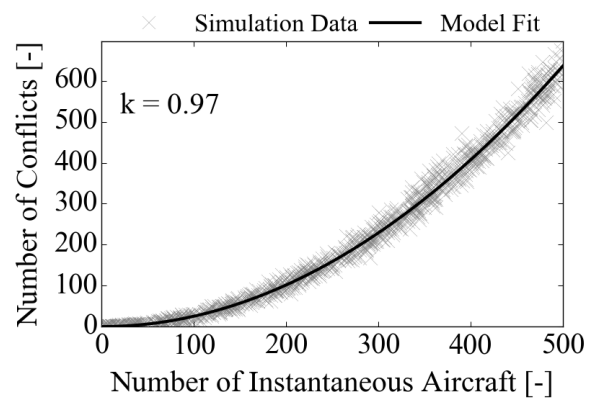
It can be observed that, for the 360 and 180 degrees heading range the model is very accurate in predicting the number of conflicts. The accuracy decreases with a decrease in heading range.

Table A-1: Explanation of the two-dimensional model

Model Parameter	Value	Unit
E	Expected number of conflicts	—
N	Instantaneous number of aircraft	—
k	Parameter to match the model and the simulation results	—
d_{sep_h}	Horizontal separation criterium	m
v	Speed	m/s
t	Look-ahead time	sec
A	Experiment area	m^2
α	heading range	rad

Table A-2: Model parameters for validation simulations of two-dimensional scenarios

Model Parameter	Value	Unit
d_{sep_h}	5.0	nm
v	500.0	kts
t	300.0	sec
A	$57.6e^3$	nm^2

**Figure A-1:** Model validation with a heading range of 360 degrees.**Figure A-2:** Model validation with a heading range of 180 degrees.

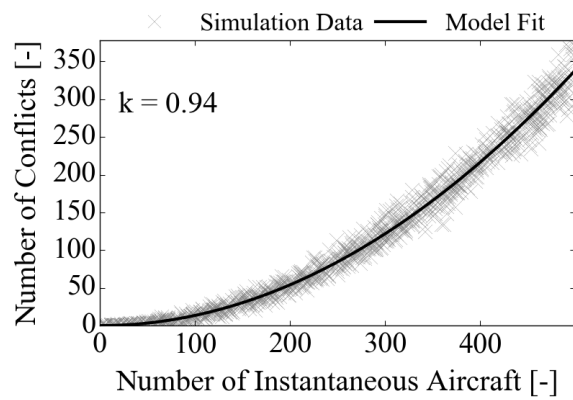


Figure A-3: Model validation with a heading range of 90 degrees.

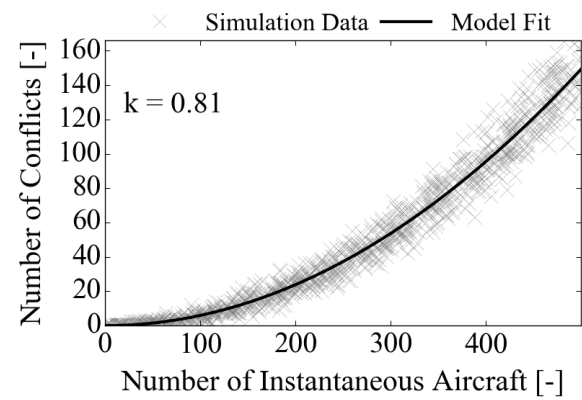


Figure A-4: Model validation with a heading range of 45 degrees.

Appendix B

Graphs of Thesis Results for All Airspace Concepts

In this appendix, the results are visualized using graphs for all airspace concept. First, the results for the validation of the conflict probability model will be elaborated on. Second, the results regarding the effect of airspace design on capacity is elaborated on. Finally, results that are not directly used for the validation and capacity analysis are presented.

B-1 Validation of Conflict Probability Model

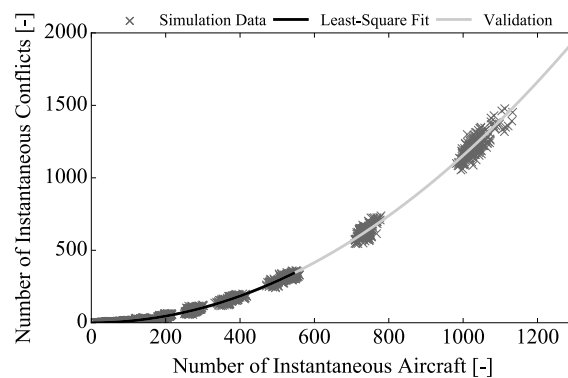


Figure B-1: Free Flight: model fitted at low densities with a k -value of 0.92.

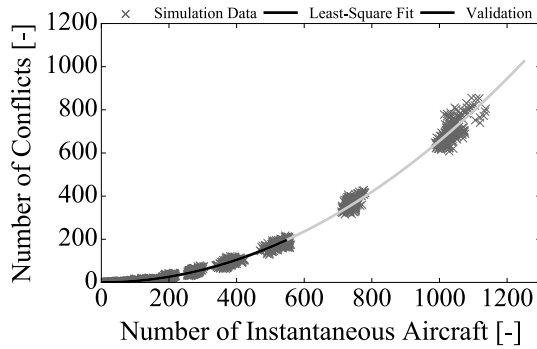


Figure B-2: Layers 360: model fitted at low densities with a k_1 of 1.15, k_2 of 1.65 and k_3 of 1.05.

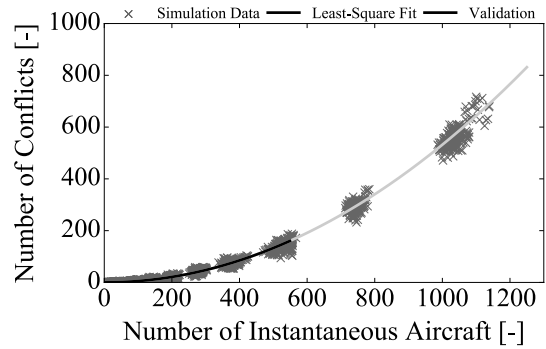


Figure B-3: Layers 180: model fitted at low densities with a k_1 of 0.99, k_2 of 1.61 and k_3 of 1.09.

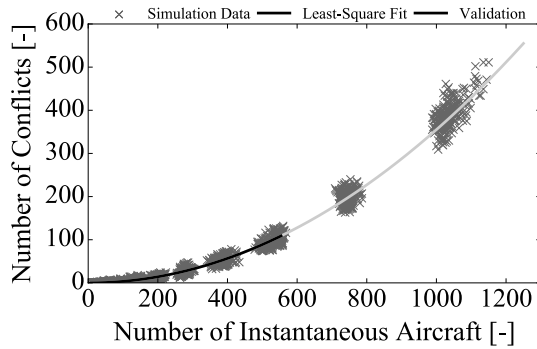


Figure B-4: Layers 90: model fitted at low densities with a k_1 of 0.93, k_2 of 1.34 and k_3 of 0.82.

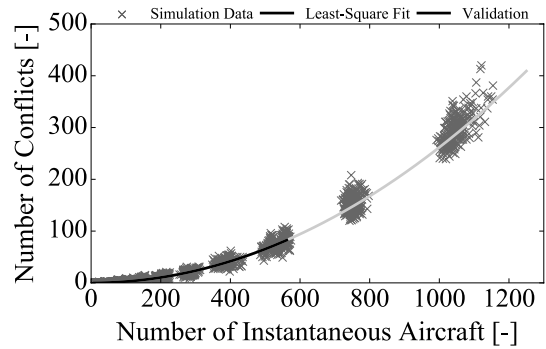


Figure B-5: Layers 45: model fitted at low densities with a k_1 of 0.93, k_2 of 1.12 and k_3 of 0.64.

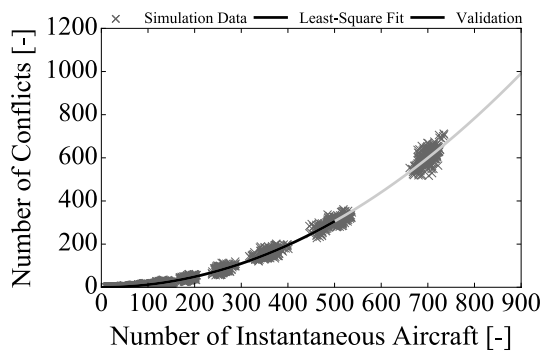


Figure B-6: Variation in vertical speed for the Free Flight concept: model fitted at low densities with a k value of 1.07.

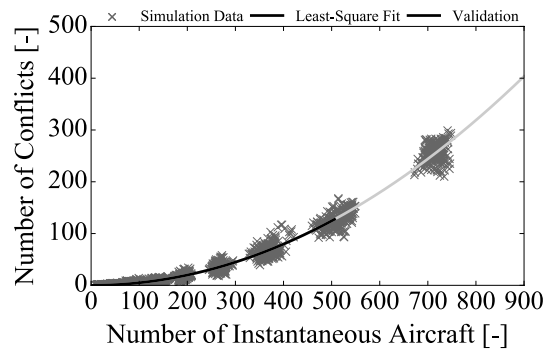


Figure B-7: Variation in vertical speed for the Layers 45 concept: model fitted at low densities with a k_1 of 1.01, k_2 of 1.23 and k_3 of 1.48.

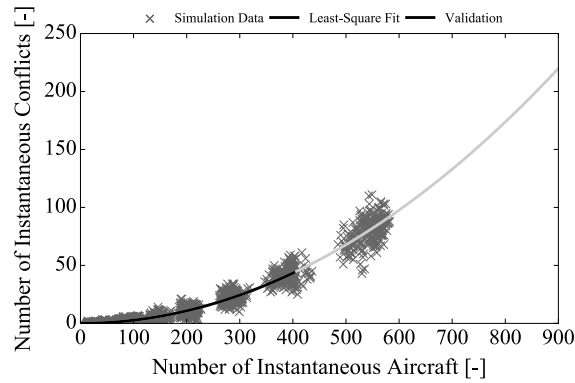


Figure B-8: Variation in speed settings for the Layers 45 concept: A uniform speed distribution between 450 kts and 550 kts. Model fitted at low densities with a k_1 of 0.99, k_2 of 1.24 and k_3 of 0.94.

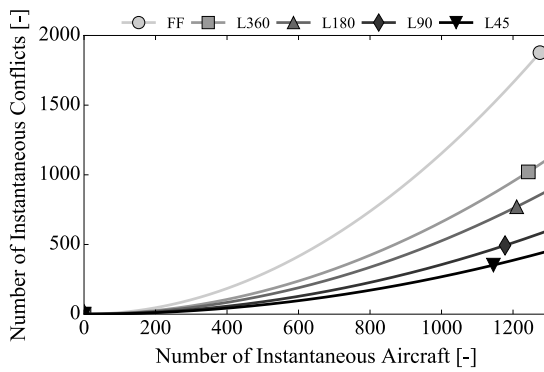


Figure B-9: Comparison of all concepts: all conflict types.

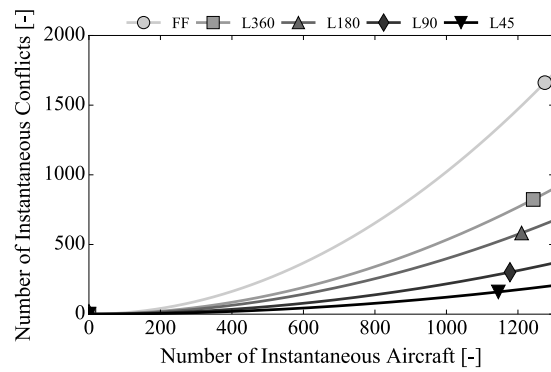


Figure B-10: Comparison of all concepts: cruise - cruise conflicts.

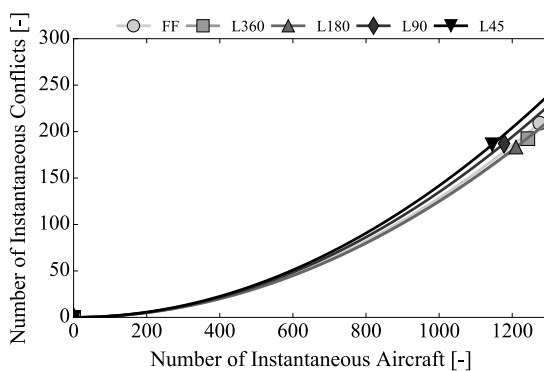


Figure B-11: Comparison of all concepts: cruise - climbing/descending conflicts.

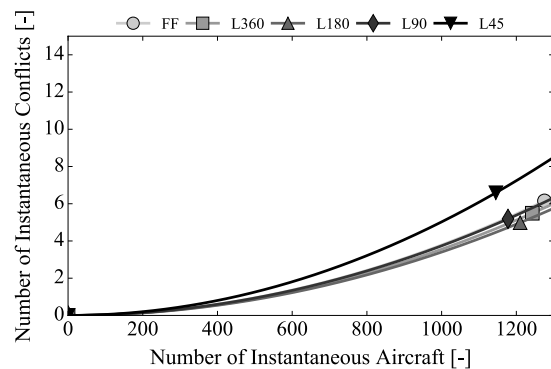


Figure B-12: Comparison of all concepts: climbing/descending - climbing/descending conflicts.

In addition to the validation of the conflict probability, as described in the scientific paper, the instantaneous conflict probability, p_2 , is provided for the five different airspace concepts. This is obtained using the probabilistic model in Equation B-1, and the values are presented in Table B-1:

$$E = \frac{N(N-1)}{2} \cdot p_2 \quad (\text{B-1})$$

Table B-1: Instantaneous Conflict Probability, p_2 (filtered on t_{cpa})

Airspace Concept	p_2
Free Flight	0.0023
Layers 360	0.0013
Layers 180	0.0011
Layers 90	0.00071
Layers 45	0.00052

Table B-2: Overview of the average instantaneous number of conflicts [filtered / non-filtered], for simulations without conflict resolution. Filtering is based on t_{cpa} , as discussed in the scientific paper.

Number of aircraft per 10,000 nm^2 , for complete vertical airspace	Free Flight	Layers 360	Layers 180	Layers 90	Layers 45
2.0	0.4 / 0.7	0.3 / 0.5	0.2 / 0.5	0.1 / 0.5	0.1 / 0.3
2.7	0.8 / 1.7	0.6 / 1.2	0.4 / 1.1	0.3 / 1.0	0.2 / 0.7
3.8	1.5 / 3.8	1.0 / 2.6	0.6 / 1.7	0.4 / 1.0	0.3 / 0.7
5.4	3.6 / 6.8	2.3 / 4.6	1.6 / 3.7	1.6 / 3.3	0.3 / 0.9
7.6	6.5 / 13.0	3.4 / 7.2	3.3 / 6.7	1.9 / 4.3	0.8 / 2.1
10.6	11.3 / 23.8	6.8 / 14.3	5.6 / 12.7	3.1 / 8.9	1.5 / 3.5
14.8	21.9 / 44.8	13.1 / 28.2	10.5 / 23.8	7.2 / 18.0	2.8 / 7.7
20.7	44.2 / 88.9	26.0 / 54.2	21.0 / 45.7	14.0 / 33.8	5.8 / 14.9
29.0	86.3 / 176.4	50.6 / 105.9	41.5 / 90.0	27.1 / 68.7	10.9 / 28.5
40.6	163.3 / 332.6	93.7 / 200.9	77.2 / 168.7	53.0 / 129.1	20.3 / 55.6
56.9	309.5 / 649.7	176.5 / 388.4	142.3 / 319.7	98.0 / 251.1	39.8 / 106.6
79.6	630.6 / 1291.6	365.6 / 774.5	291.6 / 633.1	198.9 / 489.1	76.1 / 206.4
111.5	1220.1 / 2502.4	698.6 / 1493.4	563.1 / 1234.9	389.9 / 966.9	297.1 / 795.1

B-2 Effect of Airspace Design on Capacity

B-2-1 Safety

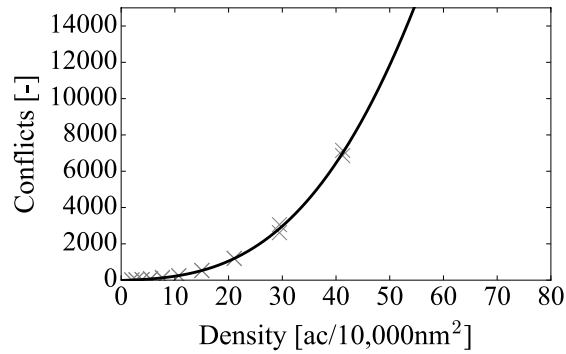


Figure B-13: Free Flight: Total number of conflicts during the experiment time. Simulation results fitted to the model $f(x) = -4.3e^{-6} \cdot x^5 + 2.9e^{-4} \cdot x^4 + 7.6e^{-2} \cdot x^3 + 5.9e^{-1} \cdot x^2 + 9.7 \cdot x - 17.1$, where x is the number of aircraft.

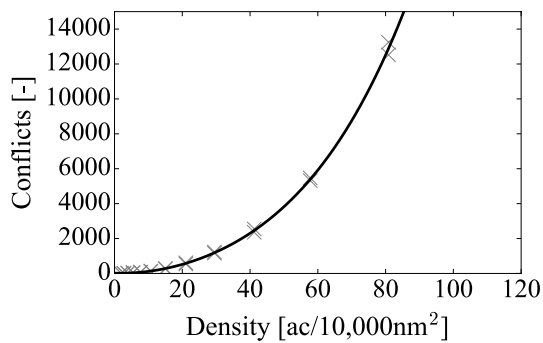


Figure B-14: Layers 360: Total number of conflicts during the experiment time. Simulation results fitted to the model $f(x) = -1.6e^{-7} \cdot x^5 + 1.8e^{-4} \cdot x^4 - 8.7e^{-3} \cdot x^3 + 1.6 \cdot x^2 - 5.3 \cdot x + 15.4$, where x is the number of aircraft.

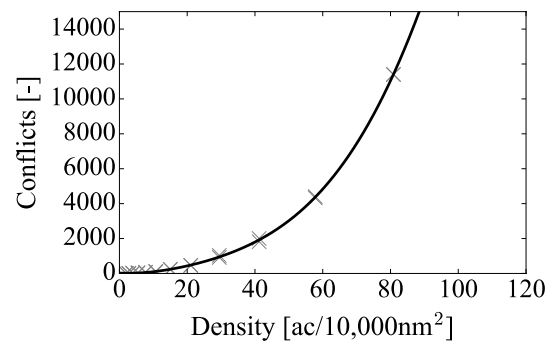


Figure B-15: Layers 180: Total number of conflicts during the experiment time. Simulation results fitted to the model $f(x) = -2.3e^{-6} \cdot x^5 + 6.6e^{-4} \cdot x^4 - 4.2e^{-2} \cdot x^3 + 2.1e \cdot x^2 - 10.3 \cdot x + 24.0$, where x is the number of aircraft.

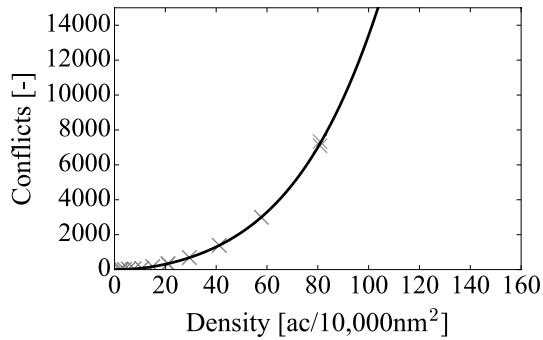


Figure B-16: Layers 90: Total number of conflicts during the experiment time. Simulation results fitted to the model $f(x) = -3.8e^{-7} \cdot x^5 + 1.9e^{-4} \cdot x^4 - 1.2e^{-2} \cdot x^3 + 1.1 \cdot x^2 - 4.2 \cdot x + 10.49$, where x is the number of aircraft.

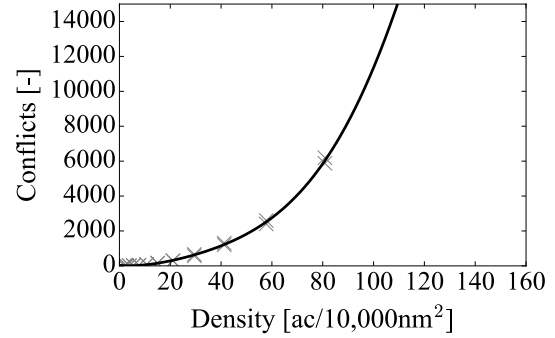


Figure B-17: Layers 45: Total number of conflicts during the experiment time. Simulation results fitted to the model $f(x) = -1.1e^{-6} \cdot x^5 + 3.8e^{-4} \cdot x^4 - 3.1e^{-2} \cdot x^3 + 1.7 \cdot x^2 - 12.0 \cdot x + 31.3$, where x is the number of aircraft.

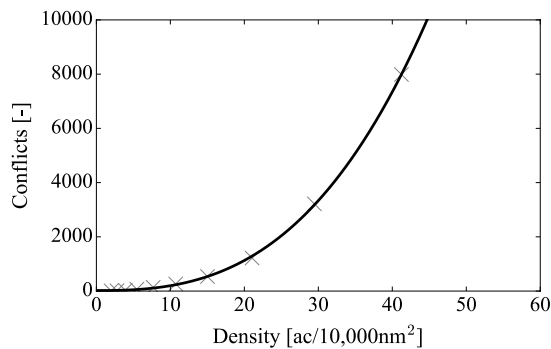


Figure B-18: Free Flight with secondary priority settings: Total number of conflicts during the experiment time. Simulation results fitted to the model $f(x) = 8.7e^{-2} \cdot x^3 + 1.2 \cdot x^2 - 2.6 \cdot x + 22.1$, where x is the number of aircraft.

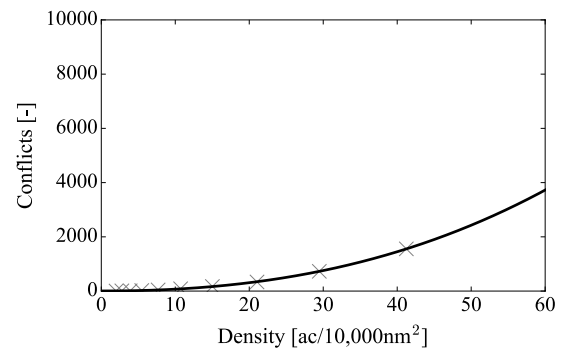


Figure B-19: Layers 45 with secondary priority settings: Total number of conflicts during the experiment time. Simulation results fitted to the model $f(x) = 6.2e^{-3} \cdot x^3 + 6.8e^{-1} \cdot x^2 - 7.8e^{-1} \cdot x + 4.0$, where x is the number of aircraft.

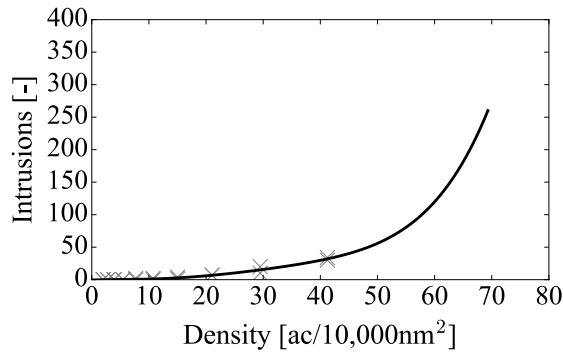


Figure B-20: Free Flight: Total number of intrusions during the experiment time. Simulation results fitted to the model $f(x) = 8.1e6-7 \cdot x^5 - 8.8e^{-5} \cdot x^4 + 3.4e^{-3} \cdot x^2 - 3.5e^{-2} \cdot x + 2.2e^{-1} \cdot x - 0.4$, where x is the number of aircraft.

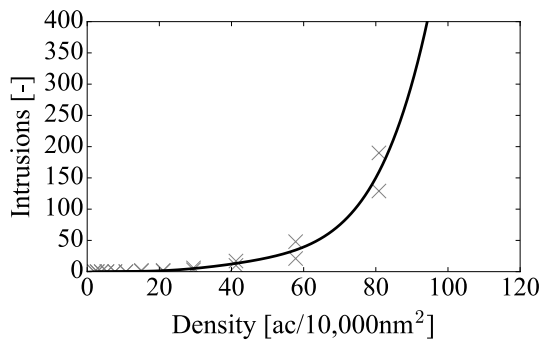


Figure B-21: Layers 360: Total number of intrusions during the experiment time. Simulation results fitted to the model $f(x) = 2.8e^{-7} \cdot x^5 - 4.1e^{-5} \cdot x^4 + 2.3e^{-3} \cdot x^3 - 4.4e^{-2} \cdot x^2 + 3.7e^{-1} \cdot x - 0.8$, where x is the number of aircraft.

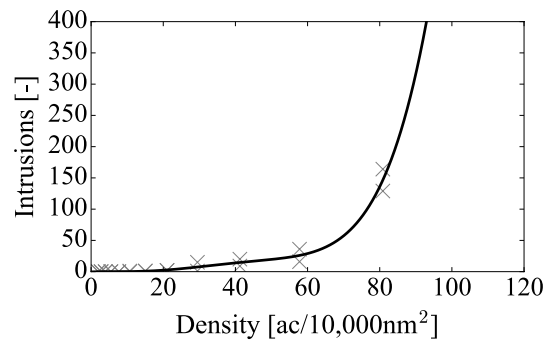


Figure B-22: Layers 180: Total number of intrusions during the experiment time. Simulation results fitted to the model $f(x) = 4.1e^{-7} \cdot x^5 - 5.8e^{-5} \cdot x^4 + 2.7e^{-3} \cdot x^3 - 3.9e^{-2} \cdot x^2 + 2.2e^{-1} \cdot x - 0.4$, where x is the number of aircraft.

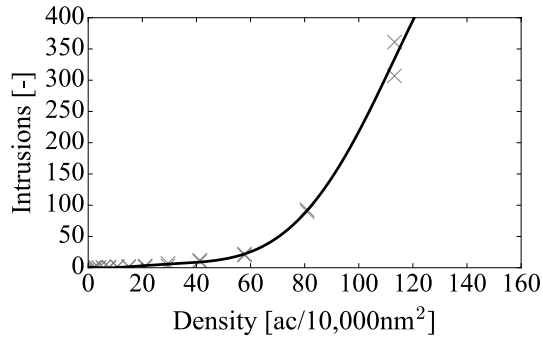


Figure B-23: Layers 90: Total number of intrusions during the experiment time. Simulation results fitted to the model $f(x) = -9.3e^{-8} \cdot x^5 + 2.5e^{-5} \cdot x^4 - 2.0e^{-3} \cdot x^3 + 6.2e^{-2} \cdot x^2 - 5.6e^{-1} \cdot x + 1.4$, where x is the number of aircraft.

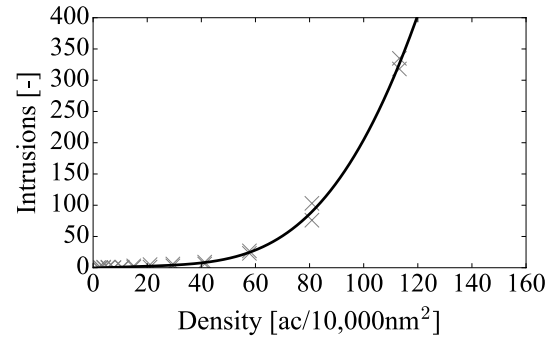


Figure B-24: Layers 45: Total number of intrusions during the experiment time. Simulation results fitted to the model $f(x) = -1.8e^{-8} \cdot x^5 + 6.0e^{-6} \cdot x^4 - 2.8e^{-4} \cdot x^3 + 5.3e^{-3} \cdot x^2 + 9.4e^{-2} \cdot x - 0.3$, where x is the number of aircraft.

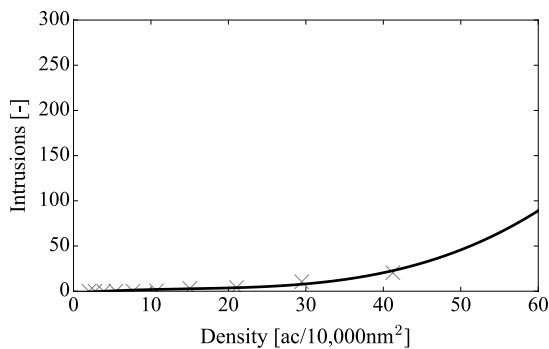


Figure B-25: Free Flight with secondary priority settings: Total number of intrusions during the experiment time. Simulation results fitted to the model $f(x) = 0.0008516 \cdot x^3 - 3.7e^{-2} \cdot x^2 + 7.0e^{-1} \cdot x - 2.3$, where x is the number of aircraft.

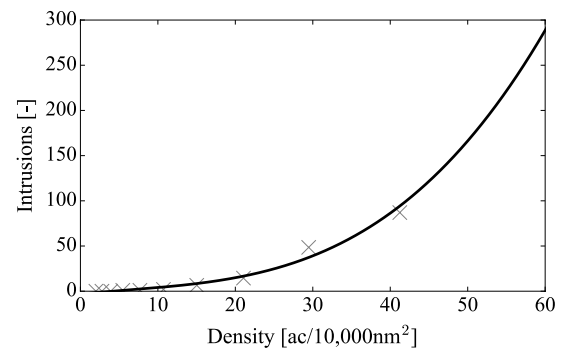


Figure B-26: Layers 45 with secondary priority settings: Total number of intrusions during the experiment time. Simulation results fitted to the model $f(x) = 1.6e^{-3} \cdot x^3 - 3.1e^{-2} \cdot x^2 + 8.7e^{-1} \cdot x - 3.2$, where x is the number of aircraft.

B-2-2 Stability

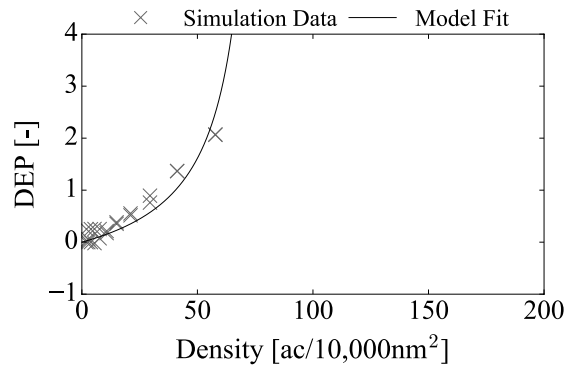


Figure B-27: Free Flight: Domino Effect Parameter, with a ρ_{max} of 81 aircraft per 10,000 nm^2 .

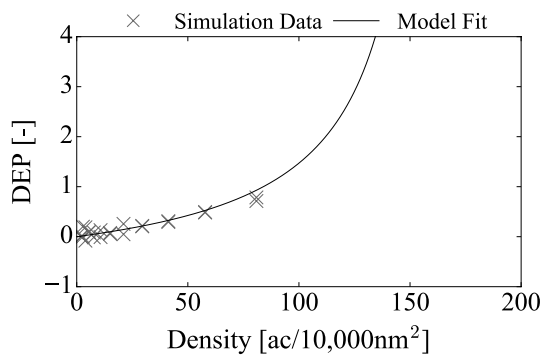


Figure B-28: Layers 360: Domino Effect Parameter, with a ρ_{max} of 168 aircraft per 10,000 nm^2 .

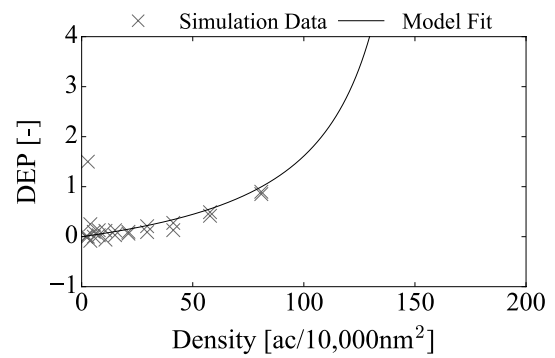


Figure B-29: Layers 180: Domino Effect Parameter, with a ρ_{max} of 162 aircraft per 10,000 nm^2 .

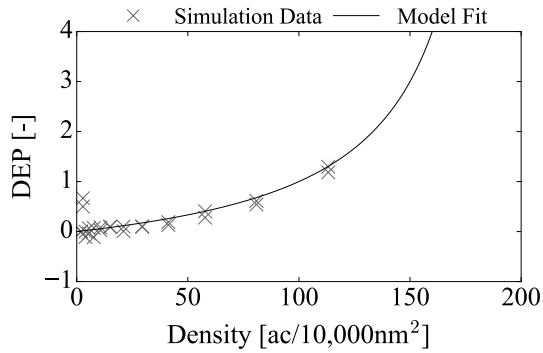


Figure B-30: Layers 90: Domino Effect Parameter, with a ρ_{max} of 200 aircraft per 10,000 nm^2 .

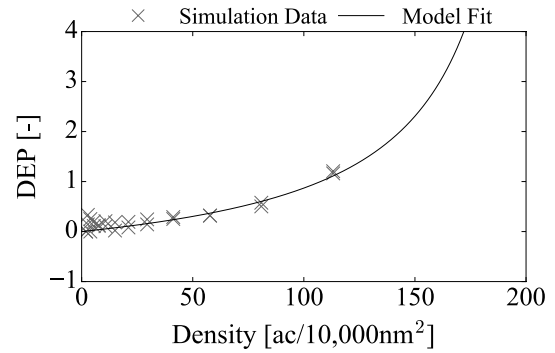


Figure B-31: Layers 45: Domino Effect Parameter, with a ρ_{max} of 215 aircraft per 10,000 nm^2 .

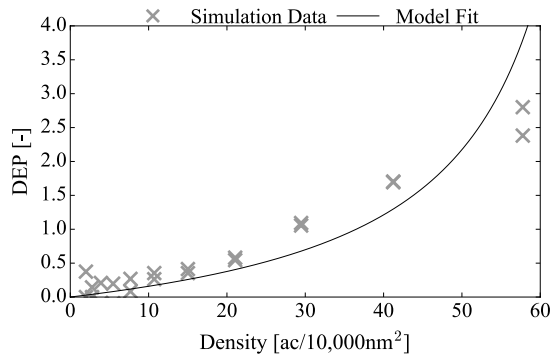


Figure B-32: Free Flight with secondary priority settings: Domino Effect Parameter, with a ρ_{max} of 73 aircraft per 10,000 nm^2 .

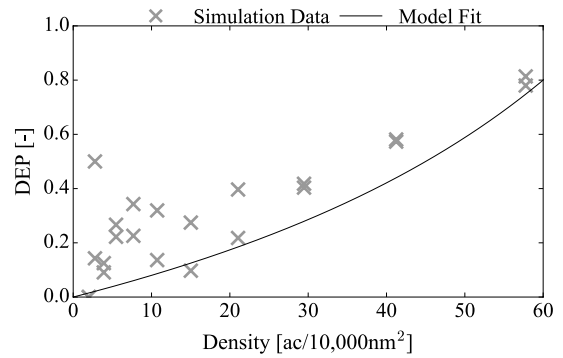


Figure B-33: Layers 45 with secondary priority settings: Domino Effect Parameter, with a ρ_{max} of 135 aircraft per 10,000 nm^2 .

B-2-3 Efficiency

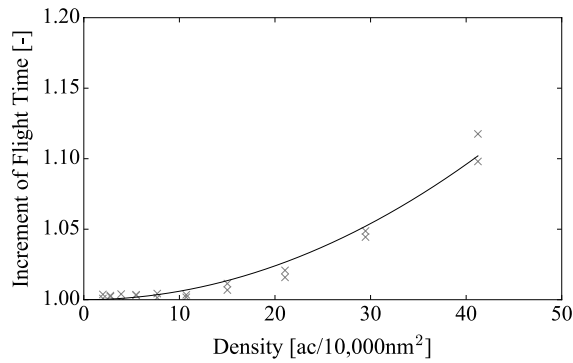


Figure B-34: Free Flight: The increment of the flight time for simulations with CR compared to simulations without CR. Simulation results fitted to the model $f(x) = 6.00e^{-5} \cdot x^2 + 1.0$, where x is the number of aircraft.

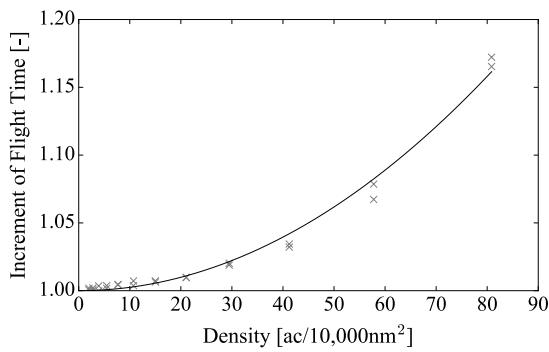


Figure B-35: Layers 360: The increment of the flight time for simulations with CR compared to simulations without CR. Simulation results fitted to the model $f(x) = 2.47e^{-5} \cdot x^2 + 1.0$, where x is the number of aircraft.

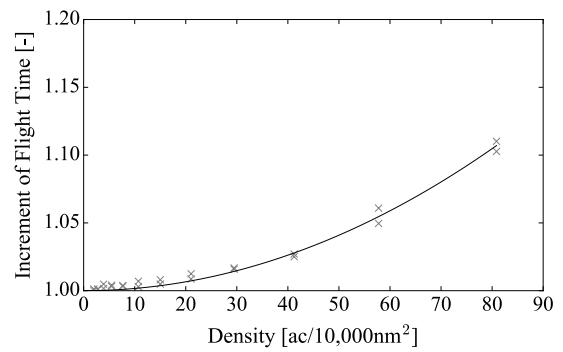


Figure B-36: Layers 180: The increment of the flight time for simulations with CR compared to simulations without CR. Simulation results fitted to the model $f(x) = 1.64e^{-5} \cdot x^2 + 1.0$, where x is the number of aircraft.

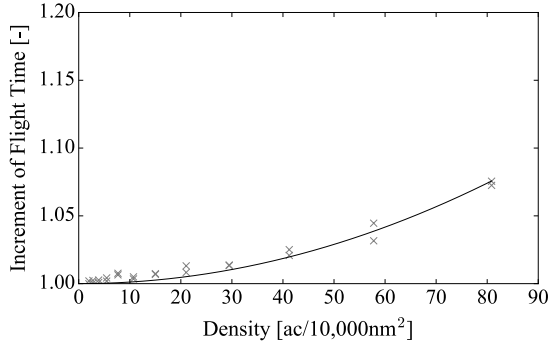


Figure B-37: Layers 90: The increment of the flight time for simulations with CR compared to simulations without CR. Simulation results fitted to the model $f(x) = 1.16e^{-5} \cdot x^2 + 1.0$, where x is the number of aircraft.

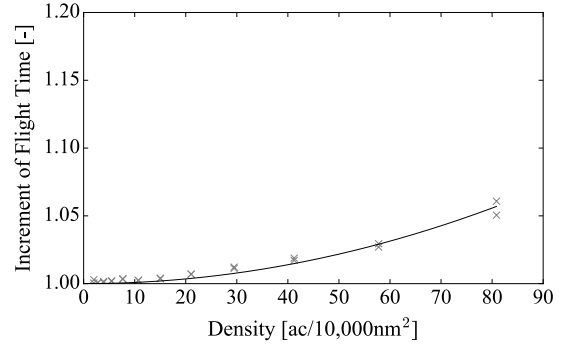


Figure B-38: Layers 45: The increment of the flight time for simulations with CR compared to simulations without CR. Simulation results fitted to the model $f(x) = 8.71e^{-6} \cdot x^2 + 1.0$, where x is the number of aircraft.

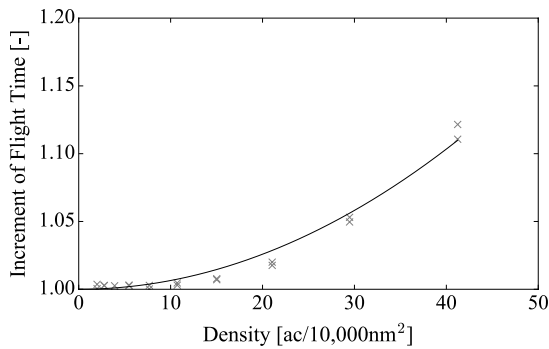


Figure B-39: Free Flight with secondary priority settings: The increment of the flight time for simulations with CR compared to simulations without CR. Simulation results fitted to the model $f(x) = 6.46e^{-5} \cdot x^2 + 1.0$, where x is the number of aircraft.

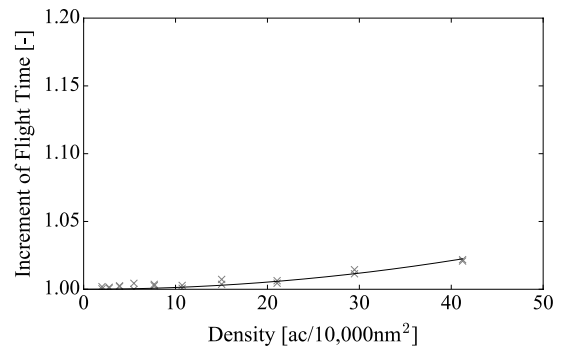


Figure B-40: Layers 45 with secondary priority settings: The increment of the flight time for simulations with CR compared to simulations without CR. Simulation results fitted to the model $f(x) = 1.32e^{-5} \cdot x^2 + 1.0$, where x is the number of aircraft.

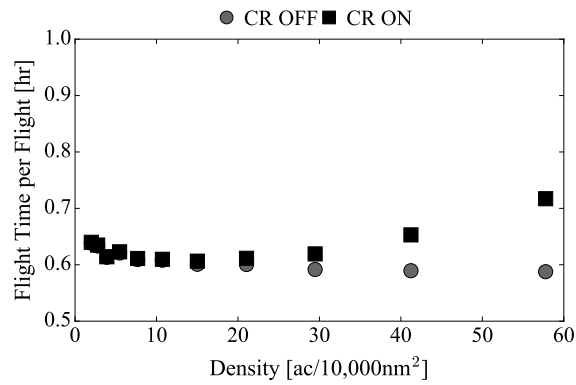


Figure B-41: Free Flight: The average flight time for simulations with and without CR.

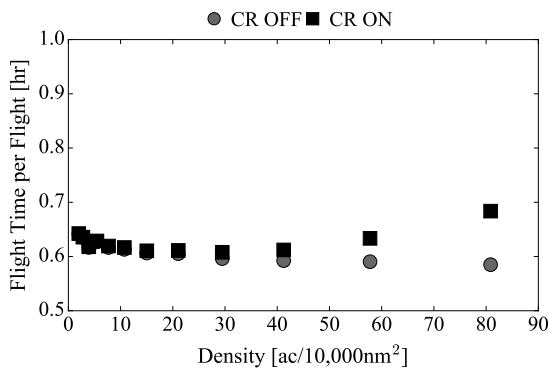


Figure B-42: Layers 360: The average flight time for simulations with and without CR.

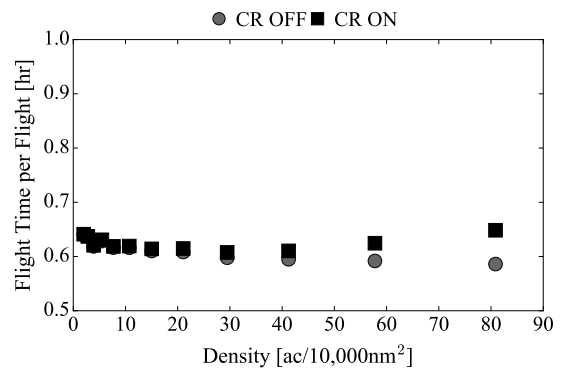


Figure B-43: Layers 180: The average flight time for simulations with and without CR.

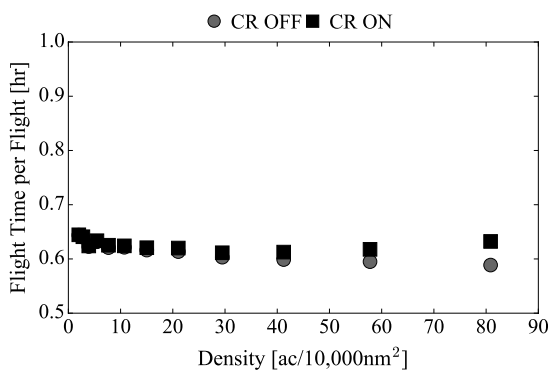


Figure B-44: Layers 90: The average flight time for simulations with and without CR.

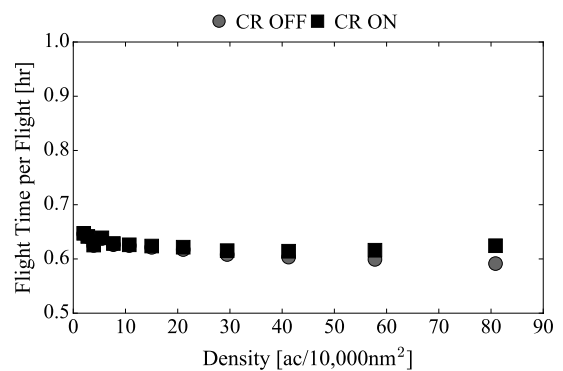


Figure B-45: Layers 45: The average flight time for simulations with and without CR.

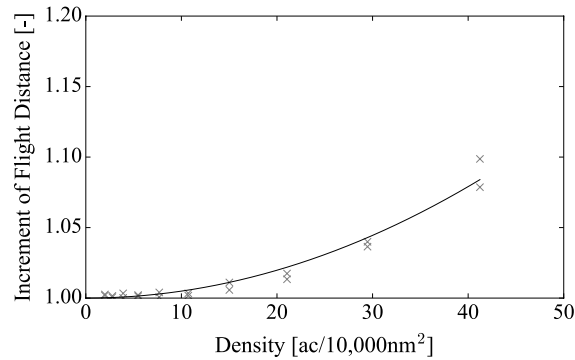


Figure B-46: Free Flight: The increment of the flight distance for simulations with CR compared to simulations without CR. Simulation results fitted to the model $f(x) = 4.94e^{-5} \cdot x^2 + 1.0$, where x is the number of aircraft.

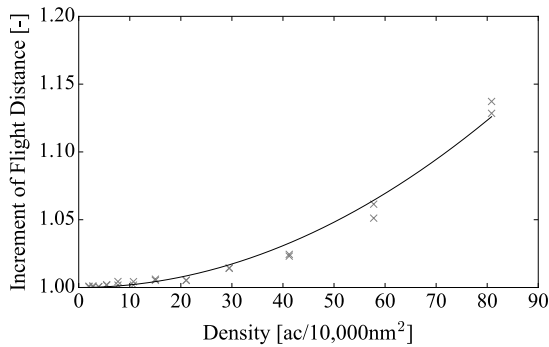


Figure B-47: Layers 360: The increment of the flight distance for simulations with CR compared to simulations without CR. Simulation results fitted to the model $f(x) = 1.93e^{-5} \cdot x^2 + 1.0$, where x is the number of aircraft.

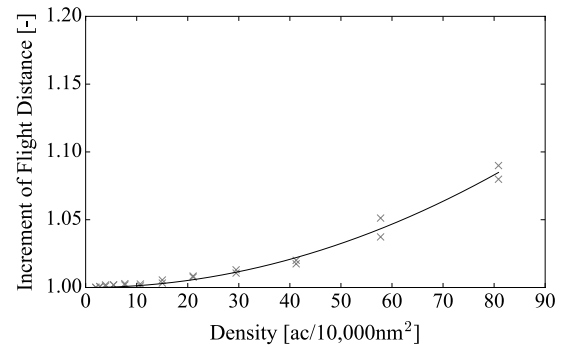


Figure B-48: Layers 180: The increment of the flight distance for simulations with CR compared to simulations without CR. Simulation results fitted to the model $f(x) = 1.30e^{-5} \cdot x^2 + 1.0$, where x is the number of aircraft.

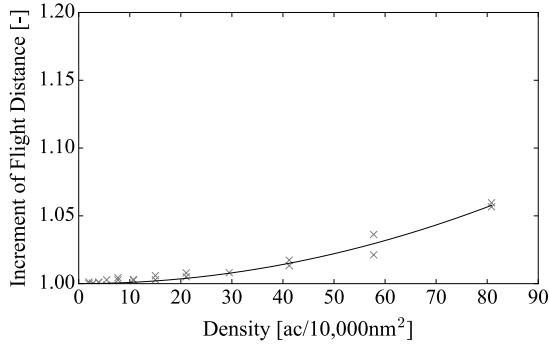


Figure B-49: Layers 90: The increment of the flight distance for simulations with CR compared to simulations without CR. Simulation results fitted to the model $f(x) = 8.83e^{-6} \cdot x^2 + 1.0$, where x is the number of aircraft.

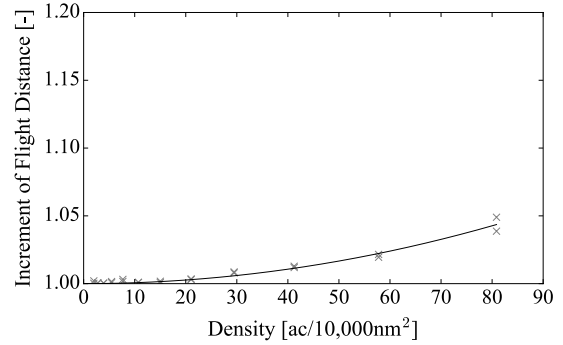


Figure B-50: Layers 45: The increment of the flight distance for simulations with CR compared to simulations without CR. Simulation results fitted to the model $f(x) = 6.67e^{-6} \cdot x^2 + 1.0$, where x is the number of aircraft.

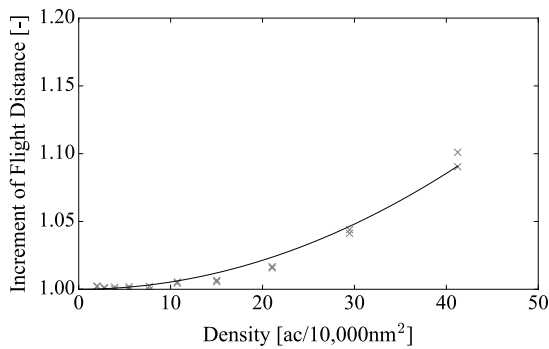


Figure B-51: Free Flight with secondary priority settings: The increment of the flight distance for simulations with CR compared to simulations without CR. Simulation results fitted to the model $f(x) = 5.34e^{-5} \cdot x^2 + 1.0$, where x is the number of aircraft.

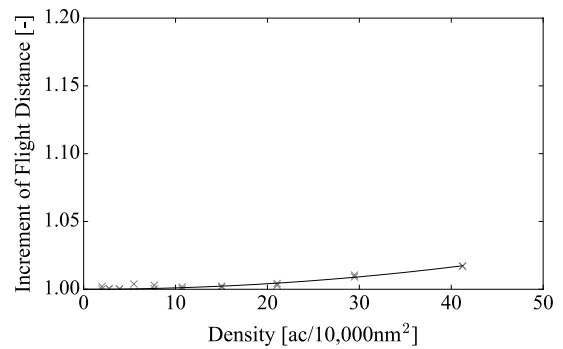


Figure B-52: Layers 45 with secondary priority settings: The increment of the flight distance for simulations with CR compared to simulations without CR. Simulation results fitted to the model $f(x) = 1.02e^{-5} \cdot x^2 + 1.0$, where x is the number of aircraft.

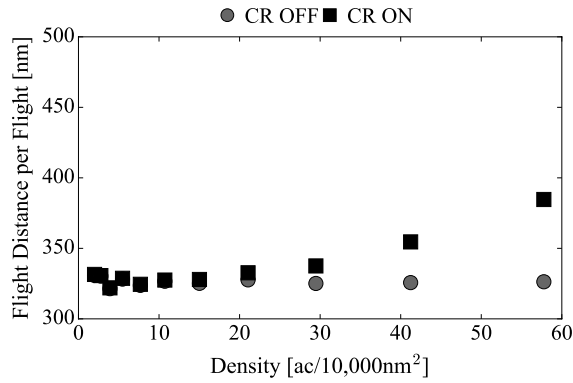


Figure B-53: Free Flight: The average flight distance for simulations with and without CR.

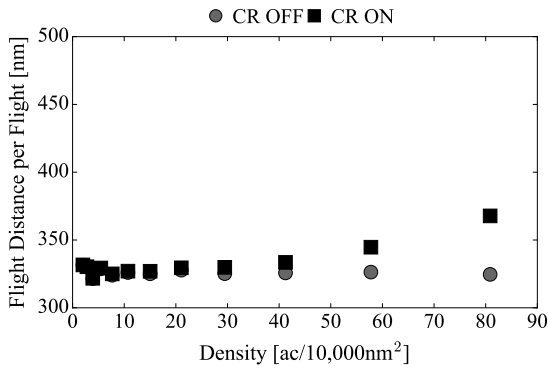


Figure B-54: Layers 360: The average flight distance for simulations with and without CR.

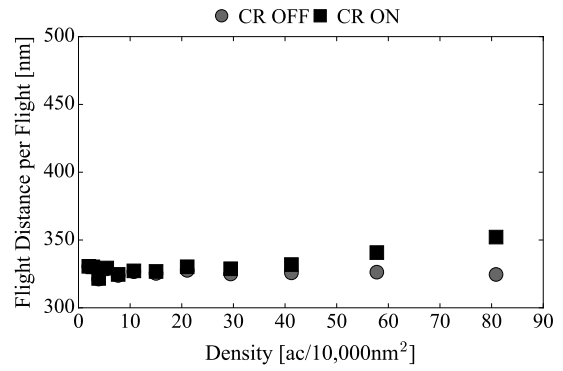


Figure B-55: Layers 180: The average flight distance for simulations with and without CR.

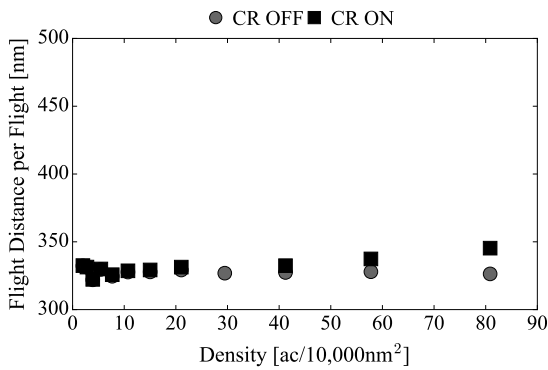


Figure B-56: Layers 90: The average flight distance for simulations with and without CR.

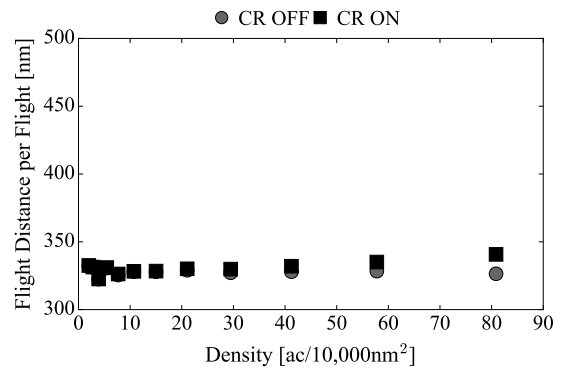


Figure B-57: Layers 45: The average flight distance for simulations with and without CR.

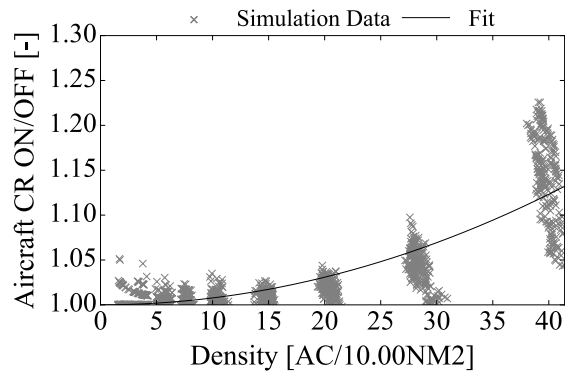


Figure B-58: Free Flight: Ratio of aircraft in the simulation with and without CR. Simulation results fitted to the model $f(x) = 1.45e^{-7} \cdot x^2 + 1$, where x is the number of aircraft without CR.

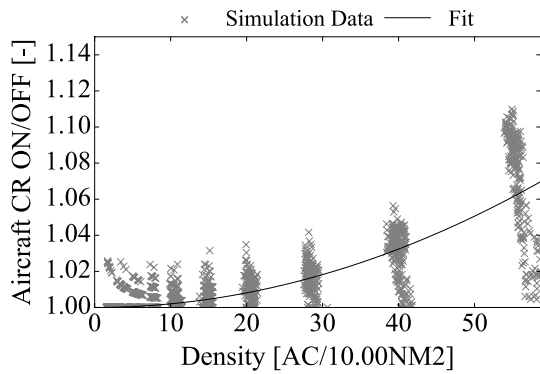


Figure B-59: Layers 360: Ratio of aircraft in the simulation with and without CR. Simulation results fitted to the model $f(x) = 3.81e^{-8} \cdot x^2 + 1$, where x is the number of aircraft without CR.

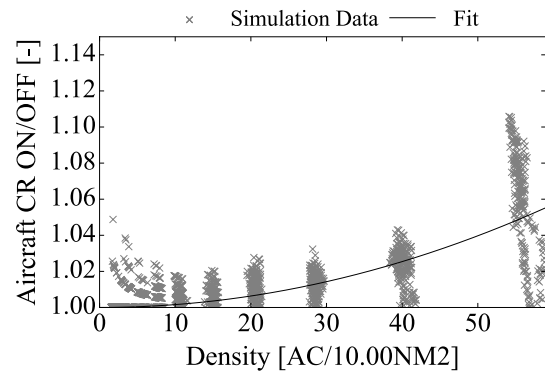


Figure B-60: Layers 180: Ratio of aircraft in the simulation with and without CR. Simulation results fitted to the model $f(x) = 2.99e^{-8} \cdot x^2 + 1$, where x is the number of aircraft without CR.

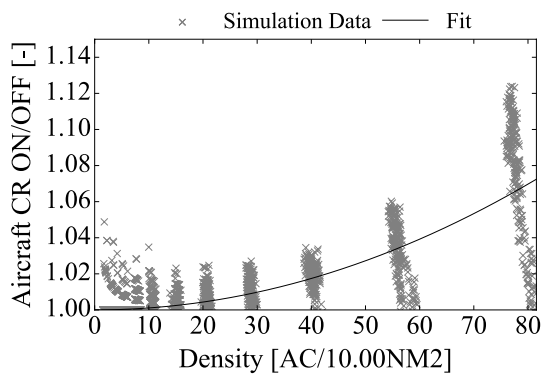


Figure B-61: Layers 90: Ratio of aircraft in the simulation with and without CR. Simulation results fitted to the model $f(x) = 2.05e^{-8} \cdot x^2 + 1$, where x is the number of aircraft without CR.

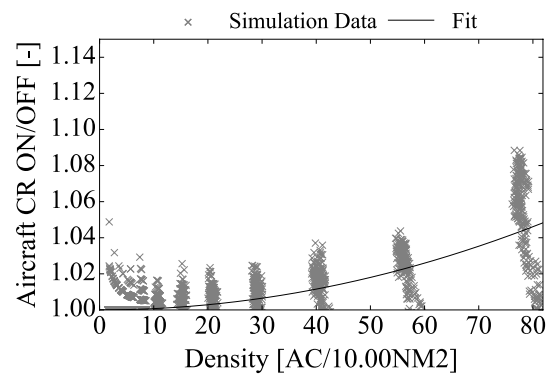


Figure B-62: Layers 45: Ratio of aircraft in the simulation with and without CR. Simulation results fitted to the model $f(x) = 1.36e^{-8} \cdot x^2 + 1$, where x is the number of aircraft without CR.

B-3 Miscellaneous

B-3-1 Density Distribution in Experiment Area

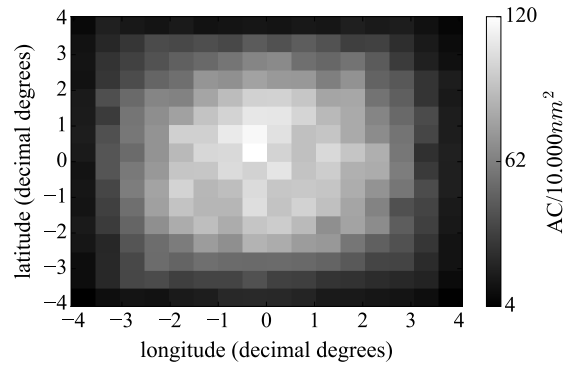


Figure B-63: Free Flight: The average density distribution in the experiment area, with 1331 instantaneous aircraft.

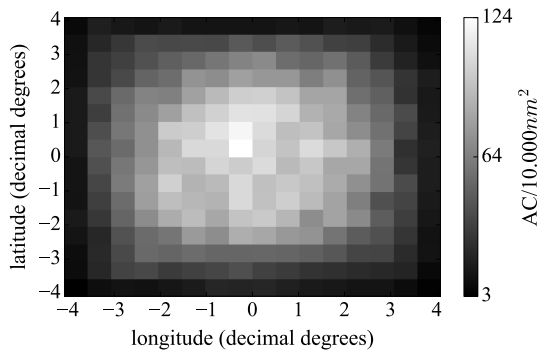


Figure B-64: Layers 360: The average density distribution in the experiment area, with 1331 instantaneous aircraft.

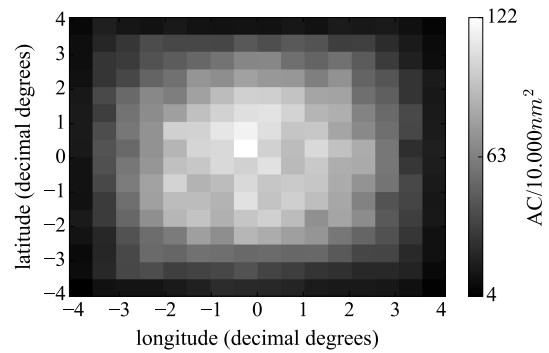


Figure B-65: Layers 180: The average density distribution in the experiment area, with 1331 instantaneous aircraft.

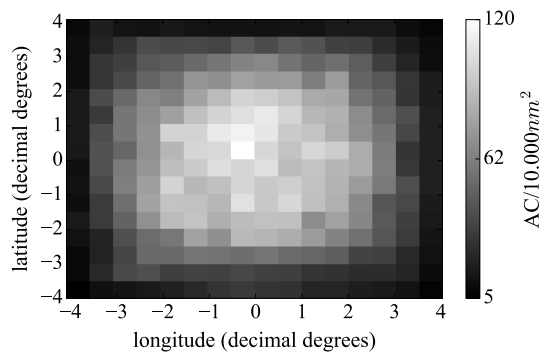


Figure B-66: Layers 90: The average density distribution in the experiment area, with 1331 instantaneous aircraft.

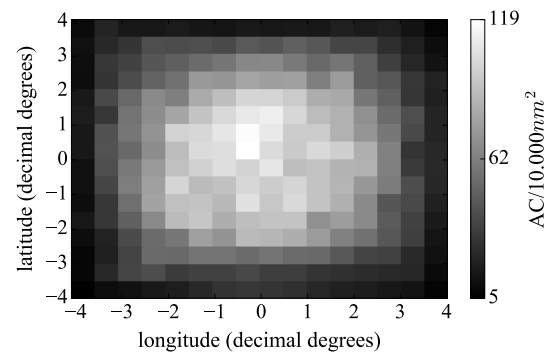


Figure B-67: Layers 45: The average density distribution in the experiment area, with 1331 instantaneous aircraft.

B-3-2 Average Conflict Angle

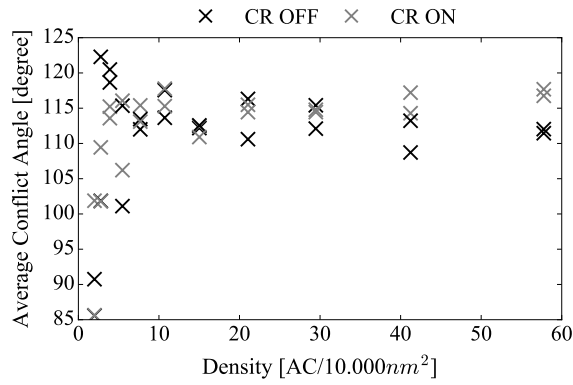


Figure B-68: Free Flight: The average conflict angle per simulation run. Only conflicts between cruising aircraft are considered.

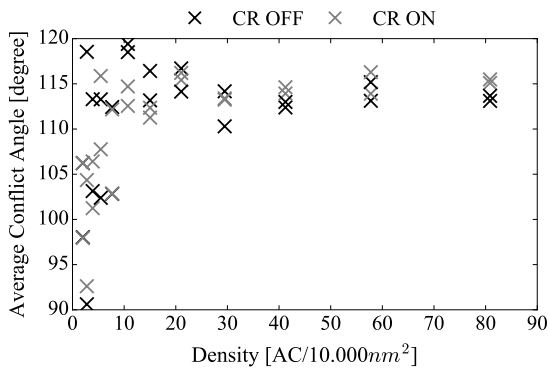


Figure B-69: Layers 360: The average conflict angle per simulation run. Only conflicts between cruising aircraft are considered.

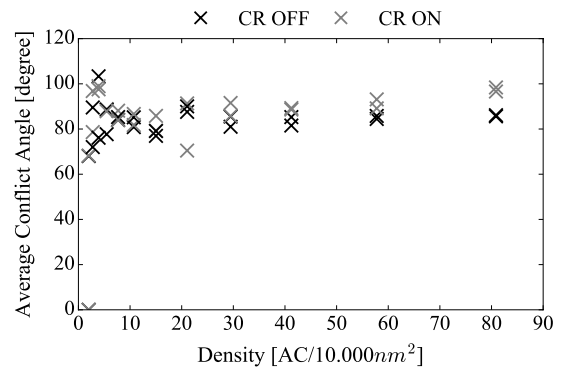


Figure B-70: Layers 180: The average conflict angle per simulation run. Only conflicts between cruising aircraft are considered.

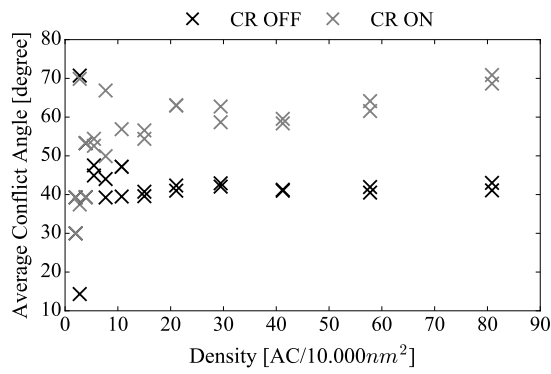


Figure B-71: Layers 90: The average conflict angle per simulation run. Only conflicts between cruising aircraft are considered.

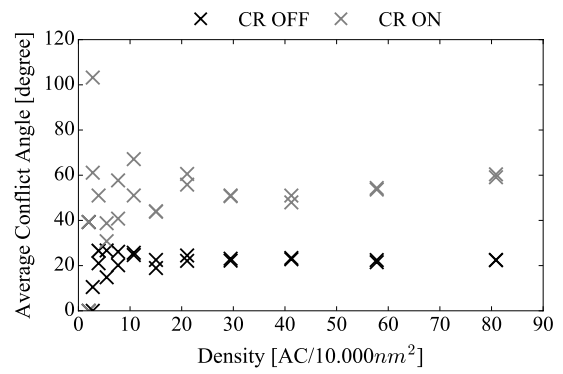


Figure B-72: Layers 45: The average conflict angle per simulation run. Only conflicts between cruising aircraft are considered.

B-3-3 Ratio of Cruising Aircraft

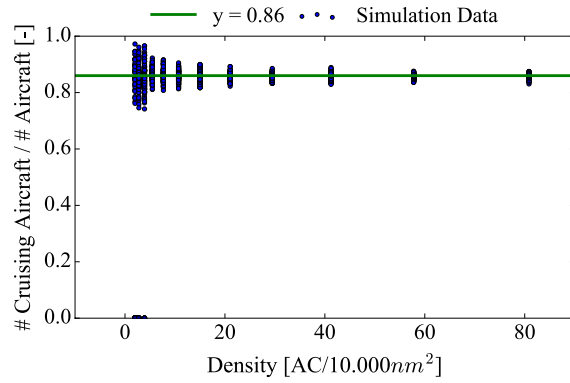


Figure B-73: Free Flight: The ratio of cruising aircraft in the experiment area during the simulations.

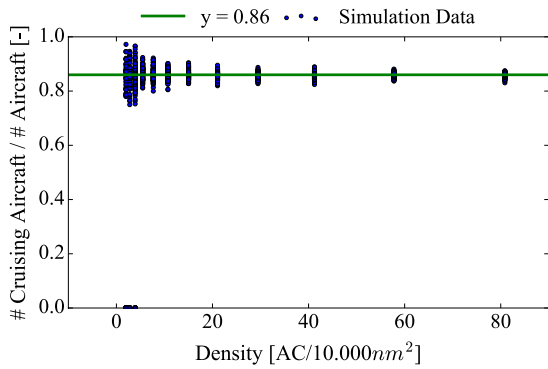


Figure B-74: Layers 360: The ratio of cruising aircraft in the experiment area during the simulations.

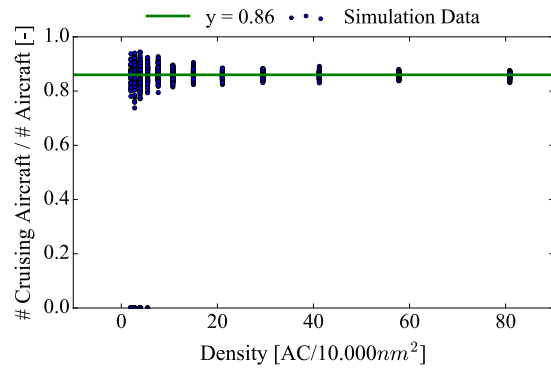


Figure B-75: Layers 180: The ratio of cruising aircraft in the experiment area during the simulations.

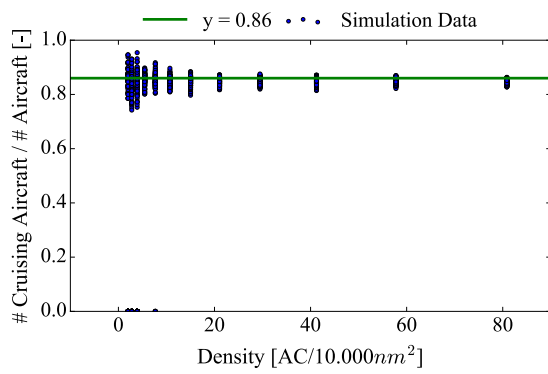


Figure B-76: Layers 90: The ratio of cruising aircraft in the experiment area during the simulations.

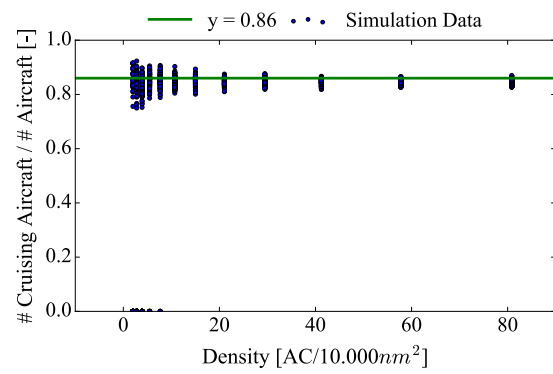


Figure B-77: Layers 45: The ratio of cruising aircraft in the experiment area during the simulations.

Simulation Scenarios Generation

The simulation scenarios are generated using four modules, as displayed in Figure C-1. This Appendix contains the scripts of the four different modules: *Airport Generation*, *Origin-Destination Pairs Generation*, *Scenario Generation* and *Scenario Writing*. The final output is a simulation scenario, according to the BlueSky command stack.

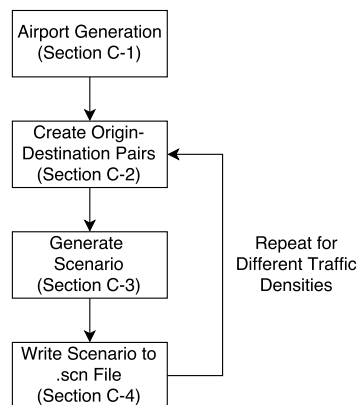


Figure C-1: Graphic overview of the interaction between the four different modules in the scenario generation.

C-1 Airport Generation

```

1  # -*- coding: utf-8 -*-
2  """
3  Created on Tue Jan 26 14:50:07 2016
4
5  Airport Generation:
6
7  This script is used to create a grid of airports, based on: area, spacing
   between airports, minimum and maximum flight distance
8  The outputs are: locations of airports (with 0,0 as center point),
   histogram of fkght distances between possible origin and destination
   pairs
9
10 @author: MTra
11
12
13 """
14
15 import matplotlib.pyplot as plt
16 import numpy as np
17 from scipy.stats import nanmean
18 import math
19 import pickle
20
21 plt.close("all")
22
23 filename = 'Airports_480'
24 def SaveLoad(opt):
25     # Defining the saving function
26     global airports, distance, average_flight, min_distance, max_distance
27     if opt == "save":
28         # Save the 'global' variables to a text file
29         with open(filename, 'w') as f:
30             pickle.dump([airports, distance, average_flight, min_distance
31                          , max_distance], f)
32             f.close
33         # Save the airports to .dat file that can be used in BlueSky
34         file = open('airportsTra.text', 'w')
35         for i in range(len(airports)):
36             file.write("%s, %s , %s , %s, Large , 0, BS\n" % (hex(i)[2:].
37                     upper(),airports[i][0],airports[i][1]/60,airports[i
38                     ][2]/60))
39             file.write("\n")
40         file.close()
41         print 'data saved'
42     else:
43         print 'Invalid saveLoad option'
44
45 ## Set the area parameters
46 area = 480. #nm
47 airports_spacing = 30. #nm

```

```

45
46 ## Set limitations on flight distance
47 min_distance = 0.5 * area #nm
48 max_distance = 450 #nm
49
50 ## Set aircraft performance parameters
51 speed = 500. # [knots]
52
53 ## Define the location of the airports
54 def airports():
55     num = int((area/airports_spacing)+1) # Number of airports along one
        axis
56     airports = [[0,airports_spacing*x, airports_spacing*y] for x in range
        (num) for y in range(num)]
57     for i in range(len(airports)):
58         airports[i][0]= i
59         airports[i][1]-= area/2
60         airports[i][2]-= area/2
61     return airports
62
63 # Create the airports
64 airports = airports()
65
66 ## Make a plot of the airport locations
67 plt.figure()
68 for i in range(len(airports)):
69     plt.plot(airports[i][1],airports[i][2] , 'bo')
70
71 ## Calculate the distance between the airports: Boundary (outer) - Area (
        inner) couples
72 distance = np.zeros((len(airports), len(airports)))
73 for i in range(len(airports)):
74     for j in range(len(airports)):
75         distance[i][j] = math.hypot(airports[j][1]-airports[i][1],
            airports[j][2]-airports[i][2])
76
77 ## Apply restrictions on flight distance and calculate the average flight
        distance
78 #print np.average(distance) # before filtering
79 distance[distance<min_distance] = np.nan
80 distance[distance>max_distance] = np.nan
81 average_flight = nanmean(nanmean(distance)) #nm
82
83 plt.figure()
84 num_bins = 10
85 plt.hist(distance[~np.isnan(distance)],num_bins)
86 plt.title("Distance Histogram")
87 plt.xlabel("Distance [nm]")
88 plt.ylabel("Frequency")
89
90 ## Print the settings and results
91 print 'Number of Airports: %s ' % len(airports)
92 print ''

```

```

93 print 'Minimum Flight Distance is %s [nm]' % min_distance
94 print 'Maximum Flight Distance is %s [nm]' % max_distance
95 print 'Average Flight Distance is %s [nm]' % average_flight
96
97 distance[np.isnan(distance)] = 0
98 distance[distance!=0] = 1
99
100 SaveLoad("save")

```

C-2 Origin-Destination Pairs Generation

```

1  # -*- coding: utf-8 -*-
2  """
3  Created on Thu Jan 21 14:28:47 2016
4
5  Origin - Destination Pairs Generation:
6
7  This script is used to create randomly generated origin-destination (O-D)
8  pairs, based on: the available airports (from the Airport Generation)
9  , the desired instantaneous number of aircraft, their speed and the
10 simulation time.
11 The output is: a list of origin-destination pairs
12
13 @author: MTra
14 """
15
16 import matplotlib.pyplot as plt
17 import numpy as np
18 import math
19 import random
20 import pickle
21
22 repetition = raw_input("Please enter repetition setting (1/2): ")
23 # Based on the repetition setting, a seed is selected
24 if repetition == 1:
25     random.seed(1)
26 elif repetition == 2:
27     random.seed(2)
28 plt.close("all")
29
30 def SaveLoad(opt):
31     #Defining the save/load function
32     global airports, distance, average_flight, number_intervals, pairs,
33     tau, min_dist, max_dist, desired_density, repetition
34     if opt == "save":
35         with open(filename, 'w') as f:
36             pickle.dump([airports, average_flight, min_dist, max_dist,
37                 number_intervals, pairs, tau, desired_density, repetition
38                 ], f)
39         f.close
40     print 'data saved'

```

```

36     elif opt == "load":
37         average_flight = []
38         airports = []
39         with open(filename) as f:
40             airports, distance, average_flight, min_dist, max_dist =
                 pickle.load(f)
41     else:
42         print 'Invalid saveLoad option'
43
44     # Set the name of the input file for the airports, and load the data
45     filename = 'Airports_480'
46     SaveLoad("load")
47
48     # Experiment time
49     experimenttime = 3.*60.*60. #[sec]
50
51     # Set aircraft performance parameters
52     speed = 535. # [knots]
53
54     # Desired number of instantaneous aircraft
55     desired_density = 46.
56
57     # Calculate the spawn rate 'tau'
58     tau = ((average_flight/speed)*3600.)*(len(airports)/desired_density)
59
60     # Select OD-pairs
61     number_intervals = int(math.ceil(experimenttime/tau))
62     pairs = np.zeros((number_intervals, len(distance), 2))
63
64     for k in range(number_intervals):
65         for i in range(len(distance)):
66             henk = sum(distance[i])
67             number = random.randint(0, henk-1)
68             idx = np.where(distance[i]==1)[0]
69             pairs[k][i][0]=i
70             pairs[k][i][1]=idx[number]
71
72
73     # Save the OD-pairs
74     filename = 'OD_%sac_%s' % (int(desired_density), repetition)
75     SaveLoad("save")

```

C-3 Scenario Generation

```

1 # -*- coding: utf-8 -*-
2 """
3 Created on Tue Jan 26 16:30:18 2016
4
5 Scenario Generation:
6
7 This script is used to generate the scenario, based on: the Origin-
    Destination pairs (from the Origin-Destination Pair Generation module)

```

```

8 The output is: A list with Origin-Destination pairs, including a time
  stamp for the generation of an aircraft at the origin.
9
10 @author: MTra
11 """
12
13 import matplotlib.pyplot as plt
14 import numpy as np
15 import math
16 import random
17 import pickle
18
19 plt.close("all")
20
21 def SaveLoad(opt):
22     #Defining the save/load function
23     global airports, distance, average_flight, number_intervals, pairs,
24         tau, spawns_total_sorted, min_dist, max_dist, desired_density,
25         repetition
26     if opt == "save":
27         with open(filename, 'w') as f:
28             pickle.dump([spawns_sorted, average_flight, min_dist,
29                 max_dist, desired_density, repetition], f)
30         f.close
31         print 'data saved'
32     elif opt == "load":
33         airports = []
34         average_flight = []
35         min_dist = []
36         max_dist = []
37         number_intervals = []
38         pairs = []
39         tau = []
40         desired_density = []
41         repetition = []
42         with open(filename) as f:
43             airports, average_flight, min_dist, max_dist,
44                 number_intervals, pairs, tau, desired_density, repetition
45                 = pickle.load(f)
46     else:
47         print 'Invalid saveLoad option'
48
49 # Set the name of the input file for the origin-destination pairs, and
50 load the data
51 filename = 'OD_46ac_1'
52 SaveLoad("load")
53
54 # Based on the repetition setting, a seed is selected
55 if repetition == '1':
56     np.random.seed(1)
57     random.seed(1)
58 elif repetition == '2':
59     np.random.seed(2)

```

```

54     random.seed(2)
55
56     ## Generate a list for the spawning of the airports
57     #spawns: time,code_orig, lat_orig, lon_orig, code_dest, lat_dest,
        lon_dest)
58     spawns = np.zeros((len(pairs)*len(pairs[0]),7))
59
60     k = 0
61     for i in range(len(pairs)):
62         for j in range(len(pairs[0])):
63             spawns[k][0] = round(((i*tau)+tau*np.random.rand()),1)
64             spawns[k][1] = j
65             spawns[k][2] = round(airports[j][1]/60.,4)
66             spawns[k][3] = round(airports[j][2]/60.,4)
67             spawns[k][4] = int(pairs[i][j][1])
68             spawns[k][5] = round(airports[int(pairs[i][j][1])][1]/60.,4) #
                Converted to decimal degrees
69             spawns[k][6] = round(airports[int(pairs[i][j][1])][2]/60.,4) #
                Converted to decimal degrees
70             k+=1
71
72     # Sort the list based on the time stamp
73     spawns_sorted=spawns[spawns[:, 0].argsort()]
74
75     # Save the data
76     filename = 'Scenario_%sac_%s' % (int(desired_density), repetition)
77     SaveLoad("save")

```

C-4 Scenario Writing

```

1     # -*- coding: utf-8 -*-
2     """
3     Spyder Editor
4
5     Scenario Writing:
6
7     This script is used to write the scenario to a BlueSky format, based on:
        the output of the Scenario Generation module.
8     The output is: a .scn file containing the BlueSky simulation scenario
9
10    @author: MTra
11    """
12    import numpy as np
13    import pickle
14    from math import *
15
16    # Set the seed
17    np.random.seed(1)
18
19    def SaveLoad(opt):
20        # Defining the save/load function

```

```

21     global spawns, average_flight, min_dist, max_dist, desired_density,
        repetition
22     if opt == "save":
23         #         with open(filename, 'w') as f:
24             #             pickle.dump([spawns_total_sorted], f)
25         #         f.close
26         print 'data saved'
27     elif opt == "load":
28         spawns = []
29         average_flight = []
30         min_dist = []
31         max_dist = []
32         desired_density = []
33         repetition = []
34         with open(filename) as f:
35             spawns, average_flight, min_dist, max_dist, desired_density,
                repetition = pickle.load(f)
36     else:
37         print 'Invalid saveLoad option'
38
39 def AispaceConcept(concept, average_flight, min_dist, max_dist, hdg_route
, dist):
40     # This function is used to determine the cruise altitude, based on
        the selected airspace concept
41     wpalt = []
42     layers = [5000. + 1100*x for x in range(8)] # The predefined
        Layers Flight Levels
43     if concept == 'LAY360': # Layers 360
44         d_dist = (max_dist - min_dist)/8.
45         if dist <= (min_dist + d_dist):
46             wpalt = layers[0]
47         elif dist <= (min_dist + 2*d_dist):
48             wpalt = layers[1]
49         elif dist <= (min_dist + 3*d_dist):
50             wpalt = layers[2]
51         elif dist <= (min_dist + 4*d_dist):
52             wpalt = layers[3]
53         elif dist <= (min_dist + 5*d_dist):
54             wpalt = layers[4]
55         elif dist <= (min_dist + 6*d_dist):
56             wpalt = layers[5]
57         elif dist <= (min_dist + 7*d_dist):
58             wpalt = layers[6]
59         elif dist > (min_dist + 7*d_dist):
60             wpalt = layers[7]
61     return wpalt
62     elif concept == 'LAY180': # Layers 180
63         d_dist = (max_dist - min_dist)/4.
64         if hdg_route < 0.:
65             if dist <= (min_dist + d_dist):
66                 wpalt = layers[0]
67             elif dist <= (min_dist + 2*d_dist):
68                 wpalt = layers[2]

```

```
69         elif dist <= (min_dist + 3*d_dist):
70             wpalt = layers[4]
71         elif dist > (min_dist + 3*d_dist):
72             wpalt = layers[6]
73     elif hdg_route >= 0.:
74         if dist <= (min_dist + d_dist):
75             wpalt = layers[1]
76         elif dist <= (min_dist + 2*d_dist):
77             wpalt = layers[3]
78         elif dist <= (min_dist + 3*d_dist):
79             wpalt = layers[5]
80         elif dist > (min_dist + 3*d_dist):
81             wpalt = layers[7]
82     return wpalt
83 elif concept == 'LAY90': # Layers 90
84     if hdg_route < -90.:
85         if dist <= average_flight:
86             wpalt = layers[0]
87         elif dist > average_flight:
88             wpalt = layers[4]
89     elif hdg_route >= -90. and hdg_route < 0.:
90         if dist <= average_flight:
91             wpalt = layers[1]
92         elif dist > average_flight:
93             wpalt = layers[5]
94     elif hdg_route >= 0. and hdg_route < 90.:
95         if dist <= average_flight:
96             wpalt = layers[2]
97         elif dist > average_flight:
98             wpalt = layers[6]
99     elif hdg_route >= 90.:
100         if dist <= average_flight:
101             wpalt = layers[3]
102         elif dist > average_flight:
103             wpalt = layers[7]
104     return wpalt
105 elif concept == 'LAY45': # Layers 45
106     if hdg_route >= -180. and hdg_route < -135.:
107         wpalt = layers[0]
108     elif hdg_route >= -135. and hdg_route < -90.:
109         wpalt = layers[1]
110     elif hdg_route >= -90. and hdg_route < -45.:
111         wpalt = layers[2]
112     elif hdg_route >= -45. and hdg_route < 0.:
113         wpalt = layers[3]
114     elif hdg_route >= 0. and hdg_route < 45.:
115         wpalt = layers[4]
116     elif hdg_route >= 45. and hdg_route < 90.:
117         wpalt = layers[5]
118     elif hdg_route >= 90. and hdg_route < 135.:
119         wpalt = layers[6]
120     elif hdg_route >= 135.:
121         wpalt = layers[7]
```

```

122     return wpalt
123 elif concept == 'FM': # Free Flight
124     wpalt = round((layers[0] + (layers[-1]-layers[0])/(max_dist-
125         min_dist))*(dist-min_dist)),0)
126     return wpalt
127 else:
128     print 'Airspace Concept unknown!'
129
130 def create_route(lat_begin,lon_begin,lat_end,lon_end,AC_ID,concept,
131     average_flight, min_dist, max_dist):
132     # Creating the necessary waypoints to define the route
133     qdr, dist = qdrdist(lat_begin, lon_begin, lat_end, lon_end)
134     hdg_route = qdr
135     cruise_alt = AispaceConcept(concept, average_flight, min_dist,
136         max_dist, hdg_route, dist)
137     toc_tod = 100. #cruise_alt/2000. * 500./60.
138     lat_toc = lat_begin*60 + toc_tod*np.cos(qdr/180*np.pi)
139     lon_toc = lon_begin*60 + toc_tod*np.sin(qdr/180*np.pi)
140     lat_tod = lat_end*60 - toc_tod*np.cos(qdr/180*np.pi)
141     lon_tod = lon_end*60 - toc_tod*np.sin(qdr/180*np.pi)
142     n_toc + (waypoint_spacing*x)*np.sin(qdr/180*np.pi) for x in
143         num_waypoints]
144     wplat = [lat_toc, lat_tod]
145     wplon = [lon_toc, lon_tod]
146     wpalt = [cruise_alt, cruise_alt]
147     alt_m = cruise_alt* 0.3048
148     tas = 500.#np.random.uniform(450.,550.)
149     spd = tas2cas(tas, alt_m)
150     wptype = [0,0]
151
152     wplat = np.divide(wplat,60)
153     wplon = np.divide(wplon,60)
154     return hdg_route, wplat, wplon, wpalt, spd, wptype
155
156 def rwgs84(latd):
157     # Function to calculate the local radius of the earth
158     lat = np.radians(latd)
159     a = 6378137.0 # [m] Major semi-axis WGS-84
160     b = 6356752.314245 # [m] Minor semi-axis WGS-84
161     coslat = np.cos(lat)
162     sinlat = np.sin(lat)
163
164     an = a*a*coslat
165     bn = b*b*sinlat
166     ad = a*coslat
167     bd = b*sinlat
168
169     # Calculate radius in meters
170     r = np.sqrt((an*an+bn*bn)/(ad*ad+bd*bd))
171
172     return r

```

```

171 def qdrdist(latd1,lond1,latd2,lond2):
172     # Function to determine the distance and bearing between 2
        coordinates
173     # Using WGS'84 calculate (input in degrees!)
174     # qdr [deg] = heading from 1 to 2
175     # d [nm]     = distance from 1 to 2 in nm
176
177     # Haversine with average radius
178     # Calculate average local earth radius
179     if latd1 == 0:
180         latd1 = 0.0001
181     if latd2 == 0:
182         latd2 = 0.0001
183     if latd1*latd1>0.: # same hemisphere
184         R = rwgs84(0.5*(latd1+latd2))
185
186     else:             # different hemisphere
187         a = 6378137.0         # [m] Major semi-axis WGS-84
188         r1 = rwgs84(latd1)
189         r2 = rwgs84(latd2)
190         R = 0.5*(abs(latd1)*(r1+a) + abs(latd2)*(r2+a))/ \
191             (abs(latd1)+abs(latd2))
192     dLat = radians(latd2-latd1)
193     dLon = radians(lond2-lond1)
194     lat1 = radians(latd1)
195     lat2 = radians(latd2)
196
197     a = sin(dLat/2.) * sin(dLat/2.) + \
198         sin(dLon/2.) * sin(dLon/2) * cos(lat1) * cos(lat2);
199     c = 2. * atan2(sqrt(a), sqrt(1.-a));
200     nm = 1852.
201     dist = R * c / nm # nm
202
203     # Bearing
204     y = sin(dLon) * cos(lat2)
205     x = cos(lat1)*sin(lat2) - sin(lat1)*cos(lat2)*cos(dLon)
206     qdr = degrees(atan2(y, x))
207
208
209     return qdr,dist
210
211 def sec2time(sec, n_msec=2):
212     # Convert seconds to 'D days, HH:MM:SS.FFF'
213     if hasattr(sec, '__len__'):
214         return [sec2time(s) for s in sec]
215     m, s = divmod(sec, 60)
216     h, m = divmod(m, 60)
217     d, h = divmod(h, 24)
218     if n_msec > 0:
219         pattern = '%02d:%02d:%00d.%df' % (n_msec+3, n_msec)
220     else:
221         pattern = r'%02d:%02d:%02d'
222     if d == 0:

```

```

223     return pattern % (h, m, s)
224     return ('%d days, ' + pattern) % (d, h, m, s)
225
226 def tas2cas(tas,h):
227     # tas2cas conversion both m/s
228     p0 = 101325. # Pa      Sea level pressure ISA
229     rho0 = 1.225 # kg/m3  Sea level density ISA
230     p,rho,T = atmos(h)
231     qdyn    = p*((1.+rho*tas*tas/(7.*p))**3.5-1.)
232     cas     = np.sqrt(7.*p0/rho0*((qdyn/p0+1.)**(2./7.)-1.))
233     return cas
234
235 def atmos(hinput):
236     # Base values and gradient in table from hand-out
237     # (but corrected to avoid small discontinuities at borders of layers)
238     g0 = 9.80665 # m/s2   Sea level gravity constant
239     R  = 287.05287 # Used in wikipedia table: checked with 11000 m
240     p0 = 101325. # Pa     Sea level pressure ISA
241     T0  = 288.15 # K     Sea level temperature ISA
242
243     h0 = [0.0, 11000., 20000., 32000., 47000., 51000., 71000., 86852.]
244
245     p0 = [101325.,           # Sea level
246          22631.7009099,     # 11 km
247          5474.71768857,    # 20 km
248          867.974468302,    # 32 km
249          110.898214043,    # 47 km
250          66.939,           # 51 km
251          3.9564 ]          # 71 km
252
253     T0 = [288.15, # Sea level
254          216.65, # 11 km
255          216.65, # 20 km
256          228.65, # 32 km
257          270.65, # 47 km
258          270.65, # 51 km
259          214.65] # 71 km
260
261     # a = lapse rate (temp gradient)
262     # integer 0 indicates isothermic layer!
263
264     a = [-0.0065, # 0-11 km
265          0,      # 11-20 km
266          0.001,  # 20-32 km
267          0.0028, # 32-47 km
268          0,      # 47-51 km
269          -0.0028, # 51-71 km
270          -0.002] # 71- km
271
272     # Clip altitude to maximum!
273     h = max(0.0,min(float(hinput),h0[-1]))
274
275     # Find correct layer

```

```

276     i = 0
277     while h>h0[i+1] and i<len(h0)-2:
278         i = i+1
279
280     # Calculate if sothermic layer
281     if a[i]==0:
282         T = T0[i]
283         p = p0[i]*exp(-g0/(R*T)*(h-h0[i]))
284         rho = p/(R*T)
285
286     # Calculate for temperature gradient
287     else:
288         T = T0[i] + a[i]*(h-h0[i])
289         p = p0[i]*((T/T0[i])**(-g0/(a[i]*R)))
290         rho = p/(R*T)
291
292     return p,rho,T
293
294 # Load the data from the scenario generation
295 filename = 'Scenario_1863ac_1'
296 SaveLoad("load")
297
298 # Simulation settings
299 reso_setting = raw_input("Please enter resolution setting (CR_OFF/CR_ON):
    ") #'nr': No resolution, 'wr': With resolution
300 concept = raw_input("Please enter concept (FM/LAY360/LAY180/LAY90/LAY45):
    ") #FullMix, Layers
301 if reso_setting == 'CR_ON':
302     if concept[:3] == 'LAY':
303         reso_method = 'MVP_LAY' #'MVP': Modified Voltage Potential
304     else:
305         reso_method = 'MVP'
306 file = open('%s_%sAC_%s_%s.scn' % (concept, int(desired_density),
    reso_setting, repetition), 'w')
307
308 ## PAN to 0,0
309 file.write("00:00:00.00>PAN 0,0\n")
310 ## Print Area Settings
311 file.write("00:00:00.00>AREA 6 6 -6 -6 4000\n")
312 ## Turn the symbol on
313 file.write("00:00:00.00>SYMBOL\n")
314
315 ## Print Resolution settings
316 if reso_setting == 'CR_OFF':
317     file.write("00:00:00.00>ASA_ASAS OFF\n")
318     file.write("00:00:00.00>ASA_PASAS OFF\n")
319     file.write("00:00:00.00>ASA_RESO OFF\n")
320 elif reso_setting == 'CR_ON':
321     file.write("00:00:00.00>ASA_ASAS ON\n")
322     file.write("00:00:00.00>ASA_PASAS ON\n")
323     file.write("00:00:00.00>ASA_RESO %s\n" % reso_method)
324     file.write("00:00:00.00>ASA_PRI0 ON\n")
325     if concept[:3] == 'LAY':

```

```

326         file.write("00:00:00.00>LAYER ON\n")
327         file.write("00:00:00.00>LAYER %s\n" % concept[3:])
328     else:
329         print 'Error in the ASAS settings'
330
331     file.write("00:00:00.00>ASA_ZONER 5.0\n")
332     file.write("00:00:00.00>ASA_ZONEDH 1000.\n")
333     file.write("00:00:00.00>FIXDT ON\n")
334     file.write("00:00:00.00>DT 0.1\n")
335     file.write("00:00:00.00>FLSTLOG ON\n")
336     file.write("00:00:00.00>ASA_DTNOLOOK 4\n")
337
338
339     ## Empty line
340     file.write("\n")
341
342     ## Print the Aircraft creation and routes
343     asas = 0
344     dt = 0
345     log = 0
346     snapoff = 0
347     for i in range(len(spawns)):
348         AC_ID = 'AC%04d' % (i+1)
349         speed = 500 #kts
350         hdg_route, wplat, wplon, wpalt, spd, wptype = create_route(spawns[i][2],
351             spawns[i][3], spawns[i][5], spawns[i][6], AC_ID, concept,
352             average_flight, min_dist, max_dist)
353         time = sec2time(spawns[i][0])
354         if time > sec2time(1800) and dt == 0:
355             file.write("00:30:00.00>ASA_DTNOLOOK 2\n")
356             file.write("\n")
357             print dt
358             dt += 1
359         if time > sec2time(2700) and dt == 1:
360             file.write("00:45:00.00>ASA_DTNOLOOK 1\n")
361             file.write("\n")
362             print dt
363             dt += 1
364         if time > sec2time(3600) and log == 0:
365             file.write("01:00:00.00>DATALOG ON\n")
366             file.write("01:00:00.00>CFLLOG ON\n")
367             file.write("01:00:00.00>INTLOG ON\n")
368             file.write("01:00:00.00>SNAPLOG ON\n")
369             file.write("01:00:00.00>INSTLOG ON\n")
370             file.write("01:00:00.00>TRAJLOG ON\n")
371             file.write("\n")
372             print log
373             log += 1
374         if time > sec2time(7200) and snapoff == 0:
375             file.write("02:00:00.00>SNAPLOG OFF\n")
376             file.write("02:00:00.00>DATALOG OFF\n")
377             file.write("02:00:00.00>CFLLOG OFF\n")
378             file.write("02:00:00.00>INTLOG OFF\n")

```

```
377     file.write("02:00:00.00>INSTLOG OFF\n")
378     file.write("02:00:00.00>TRAJLOG OFF\n")
379     file.write("\n")
380     print snapoff
381     snapoff += 1
382     if reso_setting == 'CR_OFF':
383         if time > sec2time(2700) and asas == 0:
384             file.write("00:45:00.00>ASA_ASAS ON\n")
385             file.write("\n")
386             print asas
387             asas = asas + 1
388
389     file.write("%s>CRE %s B744 %s %s %s 0 %s\n" % (time,AC_ID, spawns[i
390         ][2], spawns[i][3],hdg_route,spd))
391     file.write("\n")
392     # Add Origin and Destination
393     file.write("%s>ORIG %s %s \n" % (time,AC_ID, hex(int(spawns[i][1])
394         [2:])))
395     file.write("%s>DEST %s %s \n" % (time,AC_ID, hex(int(spawns[i][4])
396         [2:])))
397     file.write("\n")
398     # Add Waypoints
399     k = 0
400     file.write("%s>ADDWPT %s %s %s %s\n" % (time,AC_ID, round((wplat[k]
401         ),4), round((wplon[k]),4),wpalt[k]))
402     file.write("\n")
403     file.write("%s>%s LNAV ON\n" % (time,AC_ID))
404     file.write("%s>%s VNAV ON\n" % (time,AC_ID))
405     file.write("\n")
406     file.write("05:00:00.00>FLSTLOG OFF\n")
407     file.write("\n")
408     file.close()
```

Bibliography

- [1] J. M. Hoekstra and J. Ellerbroek, *AE4321 Air Traffic Management - Navigation*. Faculty of Aerospace Engineering, Delft University of Technology, 2015.
- [2] Eurocontrol, “Challenges for Growth 2013 - Task 7: European Air Traffic in 2050,” 2013.
- [3] E. Sunil, J. Hoekstra, J. Ellerbroek, F. Bussink, D. Nieuwenhuisen, A. Vidosavljevic, and S. Kern, “Metropolis: Relating Airspace Structure and Capacity for Extreme Traffic Densities,” in *ATM seminar 2015, 11th USA/EUROPE Air Traffic Management R&D Seminar*, 2015.
- [4] J. Krozel, M. Peters, K. D. Bilimoria, C. Lee, and J. S. Mitchell, “System performance characteristics of centralized and decentralized air traffic separation strategies,” in *Fourth USA/Europe air traffic management research and development seminar*, 2001.
- [5] “FIR/UIR charts | Eurocontrol.” <http://www.eurocontrol.int/articles/firuir-charts>. Accessed: 2015-12-15.
- [6] J. M. Hoekstra, R. C. J. Ruigrok, and R. Van Gent, “Free flight in a crowded airspace?,” *Progress in Astronautics and Aeronautics*, vol. 193, p. 9, 2000.
- [7] M. R. Jardin, “Analytical relationships between conflict counts and air-traffic density,” *Journal of Guidance, Control, and Dynamics*, vol. 28, no. 6, pp. 1150–1156, 2005.
- [8] J. M. Hoekstra and J. Maas, “Analysis of the effect of a layered airspace structure on safety and capacity.” unpublished, 2015.
- [9] W. Feller, *An Introduction to Probability Theory and Its Application*, vol. Volume 1. New York: John Wiley & Sons, third edition ed., 1970.
- [10] P. J. G. Teunissen, D. G. Simons, C. C. J. M. Tiberius, and S. Verhagen, “Probability and Statistics for Aerospace Engineering (AE2107),” Aug. 2015.
- [11] M. S. Nolan, *Fundamentals of Air Traffic Control*. Belmont, California: Wadsworth Publishing Company, second edition ed., 1994.

- [12] M. Janic and V. Tasic, "En route sector capacity model," *Transportation Science*, vol. 25, no. 4, pp. 299–307, 1991.
- [13] F. J. van Schaik, *Introduction to Air Traffic Management (AE4428)*. Faculty of Aerospace Engineering, Delft University of Technology, Sept. 2010.
- [14] International Civil Aviation Organization, "Procedures for Air Navigation Services - Doc 4444," 2001.
- [15] J. M. Histon, R. J. Hansman, B. Gottlieb, H. Kleinwaks, S. Yenson, D. Delahaye, and S. Puechmorel, "Structural considerations and cognitive complexity in air traffic control," in *Digital Avionics Systems Conference, 2002. Proceedings. The 21st*, vol. 1, IEEE, 2002.
- [16] M. L. Cummings, C. G. Tsonis, and D. C. Cunha, "Complexity mitigation through airspace structure," in *13th International Symposium on Aviation Psychology, Oklahoma City, Oklahoma*, Citeseer, 2005.
- [17] European Commission, "Single European Sky - Transport." http://ec.europa.eu/transport/modes/air/single_european_sky/. Accessed: 2015-11-29.
- [18] P. Brooker, "Controller workload, airspace capacity and future systems.," *Human Factors and Aerospace Safety*, vol. 3, no. 1, pp. 1 – 23, 2003.
- [19] SESAR Consortium, "SESAR Concept of Operations," tech. rep., SESAR Consortium, July 2007.
- [20] NextGen Joint Planning and Development Office, "Concept of Operations for the Next Generation Air Transportation System," tech. rep., Federal Aviation Administration, June 2007.
- [21] K. D. Bilimoria and H. Q. Lee, "Properties of Air Traffic Conflicts for Free and Structured Routing," *AIAA Guidance, Navigation, and Control Conference and Exhibit*, Aug. 2001.
- [22] J. M. Hoekstra, R. N. van Gent, and R. C. Ruigrok, "Designing for safety: the 'free flight' air traffic management concept," *Reliability Engineering & System Safety*, vol. 75, no. 2, p. 18, 2002.
- [23] RTCA Inc., "Final report of the RTCA task force 3: Free Flight Implementation," tech. rep., Radio Technical Commission for Aeronautics, Washington DC, Oct. 1995.
- [24] R. L. Ford, "On the use of height rules in off-route airspace," *Journal of Navigation*, vol. 36, no. 02, pp. 269–287, 1983.
- [25] M. S. Eby, "A Self-Organizational Approach for Resolving Air Traffic Conflicts.," *Lincoln Laboratory Journal*, 1994.
- [26] K. Leiden, S. Peters, and S. Quesada, "Flight level-based dynamic airspace configuration," in *Proceedings of the 9th AIAA Aviation Technology, Integration and Operations (ATIO) Forum. American Institute of Aeronautics and Astronautics*, 2009.
- [27] R. Irvine and C. Shaw, "Layers of parallel tracks: a speculative approach to the prevention of crossing conflicts between cruising aircraft," Sept. 2004.

-
- [28] R. Irvine and H. Hering, "Towards Systematic Air Traffic Management in a Regular Lattice," in *7th AIAA ATIO Conf, 2nd CEIAT Int'l Conf on Innov and Integr in Aero Sciences, 17th LTA Systems Tech Conf; followed by 2nd TEOS Forum*, p. 7780, 2007.
- [29] R. A. Paielli, "A Linear Altitude Rule for Safer and More Efficient Enroute Air Traffic," *Air Traffic Control Quarterly*, vol. Vol. 8, 2000.
- [30] International Civil Aviation Organization, "Annex 2 - Rules of the Air," July 2005.
- [31] R. Hoffman and J. Prete, "Principles of airspace tube design for dynamic airspace configuration," in *AIAA-ATIO Conference, Anchorage Alaska*, 2008.
- [32] K. D. Bilimoria, K. S. Sheth, H. Q. Lee, and S. R. Grabbe, "Performance evaluation of airborne separation assurance for free flight," *Air Traffic Control Quarterly*, vol. 11, no. 2, pp. 85–102, 2000.
- [33] S. Ratcliffe and R. L. Ford, "Conflicts between random flights in a given area," *Journal of Air Navigation*, vol. 35, pp. 47–71, 1982.
- [34] "ProfHoekstra/bluesky." <https://github.com/ProfHoekstra/bluesky>. Accessed: 2015-11-29.
- [35] J. Maas, "A Quantitative Comparison of Conflict Resolution Strategies for Free Flight," MSc Thesis, Faculty of Aerospace Engineering, Delft University of Technology, June 2015.
- [36] Eurocontrol, "High-Density 2015 European Traffic Distributions for Simulation," Mar. 2000.

